Rheology and application of thermoreversible polymer networks based on the Diels-Alder cycloaddition

by

Richard James Sheridan

B.S., Illinois Institute of Technology, 2007

M.S., University of Colorado, 2009

A thesis submitted to the

Faculty of the Graduate School of the

University of Colorado in partial fulfillment

of the requirements for the degree of

Doctor of Philosophy

Department of Chemical and Biological Engineering

2012

This thesis entitled:

Rheology and application of thermoreversible polymer networks

based on the Diels-Alder Cycloaddition

written by Richard James Sheridan

has been approved for the Department of Chemical and Biological Engineering

_____

Committee Chair: Professor Christopher N. Bowman

_____

Professor Daniel K. Schwartz

Date: _____

The final copy of this thesis has been examined by the signatories, and we

find that both the content and the form meet acceptable presentation standards

of scholarly work in the above mentioned discipline.

Abstract

Sheridan, Richard James (Ph.D., Dept. of Chem. and Biol. Engineering)

Rheology and application of thermoreversible polymer networks based on the Diels-Alder cycloaddition

Thesis directed by Professor Christopher N. Bowman

A model thermoreversible network based on the Diels-Alder cycloaddition reaction was synthesized. These materials exhibit extreme changes in material properties near a critical temperature. The model network was used to test theoretical predictions of viscoelasticity near this critical temperature. The resulting data supported the theory and allowed for the description of the complex process of stress relaxation in transient networks to be written in terms of a simple linear scaling relationship.

To use the scaling relationship, we revisited earlier work on externally triggered healing, in which the thermal reactivity of the material could be activated by self-limited RF hysteresis heating. This composite of chromium(IV) dioxide particles suspended in the model Diels-Alder material was used to demonstrate their ability to be readily tailored to applications that are constrained by factors not related directly to the polymer, such as the Curie temperature of CrO_2. We demonstrated the effect of composition on fracture healing, showing that more highly crosslinked materials take longer to recover strength after fracture.

To bring some of the temporal and spatial control of optical curing techniques to thermally activated systems, we developed a robust custom nanoparticle to serve as a durable photothermal chromophore. The particle was designed to efficiently convert laser light into heat while maintaining surface plasmon resonance and colloidal behavior even in the high temperature, poor solubility environment of a Diels-Alder network. We observed a unique reaction to laser irradiation, in the formation of bumps at the location of exposure. We demonstrated substantial control over the height of these features by varying the time and intensity of the laser exposure, and investigated the cause of feature formation.

Dedication

This thesis is dedicated to my parents

James J Sheridan and Diane M Sheridan

For always believing in me

Even when I didn't

Acknowledgements

Over the years, a staggering number of people have donated their time, effort, and expertise to the work presented here, in both small and large capacities. Although each contribution may have been minor, the sum total represents the difference between the progress I've made, and the rut that I could have been stuck in. I'd like to thank my advisor, Chris Bowman, for taking a chance on me, and accepting the challenge of molding me into a presentable scientist. I'd like to thank my committee members, Charles Musgrave, Daniel Schwartz, Robert McLeod, and Mark Stoykovich, for helping me to refine my ideas, and for being willing to donate their time and equipment so freely. I'd like to thank all my colleagues in the Bowman group for their help and many invaluable discussions – especially former members such as Chris Kloxin, Brian Adzima, and Kathleen Schreck, who showed me the ropes and put up with my relentless questioning. I would also like to thank a number of other graduate students, postdocs, and researchers who helped me in various capacities: Katherine Rice, Parag Shah, Devatha Nair, Troy Gould, Ian Campbell, Mark Tibbitt, Benjamin Fairbanks, Sarah Gould, Josh McCall, April Kloxin, Tom Giddings, Robert Walder, Nathan Nelson, Adam Urness, and Martha Bodine.

This project was supported by NSF grant 0933828, the ARRA, and a GAANN fellowship.

CONTENTS

Chapter 1: Introduction

Polymers and Polymer Networks

Polymeric materials have traditionally been classified into two categories: those that flow when heated (thermoplastics) and those that do not (thermosets.)[1] Thermoplastics dissolve and flow due to being composed of linear polymers. Thermosets are typically insoluble, but can have superior material properties (modulus, toughness, hardness) in comparison to thermoplastics due to being composed of a covalently crosslinked polymer macromolecule (i.e. a gel or network). A linear polymer may be a rigid semicrystalline thermoplastic, a thermoplastic elastomer, or an amorphous glass. Yet, upon heating all of these materials form polymer melts where liquid-like behavior predominates. The mechanisms responsible for these behaviors allow thermoplastics to undergo fracture healing[2], welding[3] and molding[4] lending to their ubiquitous use in everyday life (e.g., as fibers, rubbers, structural materials, and paints).[5] Some thermoplastics with properties similar to thermosets exist, e.g. Lexan and other polycarbonates, Kevlar and other aramids; however, to mix-and-match properties of thermosets and thermoplastics in one class of materials requires novel approaches.

More recently, non-covalent polymer networks formed by weak intermolecular interactions – like microphase separation[6], pi-pi stacking[7], and hydrogen bonding[6, 8] – have been shown to exhibit behavior and properties similar to those of thermoplastics. These types of "weak" networks often behave as viscoelastic liquids, as defined by having a finite steady shear viscosity. Yet, under

certain conditions they also exhibit solid-like behavior.[9] The liquid-like properties of weak networks are due to the transient nature of their intermolecular interactions[10]. Therefore, covalent polymer networks should also behave as liquids, if the covalent connections between crosslinks have the ability to reversibly break and rearrange on the appropriate timescale. That is, despite the "strength" of the covalent bond type, a network held together by reversible bonds should have the properties of a "weak" network, i.e. plasticity, when examined under appropriate conditions.

Covalent Adaptable Networks

Polymer networks composed of reversibly labile crosslinks – including non-covalent interactions such as hydrogen bonds[11] or pi stacking,[7] or reversible covalent reactions like the Diels-Alder,[10] boronate-diol,[12] and most recently transesterification[13] reactions – are becoming popular as mendable,[14] recyclable,[15] and smart[16] materials. The ability of these various materials to respond to an external stimulus such as exposure to light, changes in pH, or an increase in temperature with a change in material properties[16-17] makes them potentially valuable in many fields, from biomaterials to photolithography. As these materials are unified, at least in part, by common attributes of their chemical mechanism, a common structure-property relationship should be applicable to both the overall class of materials as well as being individually applicable to each one of these network types.

When the reversibility of these bonds is triggerable via an external stimulus, these networks can be classified as covalent adaptable networks (CANs).[16] CANs generally have the ability to: relieve stress, including polymerization-shrinkage-induced stress;[18] incorporate new chemical functionality post-cure[19]; chemically bridge interfaces, including fractures;[14] undergo recycling;[20] control the diffusivity of particles via an adjustable mesh size;[21] and actuate mechanical motion.[22] Because all these CANs and applications rely on a common mechanism (i.e., the reversible scission and recombination of all crosslinking bonds in the network) there should be commonalities in the viscoelastic properties of the materials in their activated state. Furthermore, there should be fundamental structure-property relationships that govern the mechanical and relaxation behavior of CANs. By using a model polymer network , we should be able to evaluate these structure-property relationships.

Diels-Alder Reaction and Crosslinking

The Diels-Alder[23] cycloaddition reaction, often occurring between maleimide and furan functional groups (Scheme 1.1), has become a common feature of the thermoreversible networks literature, thanks to its relatively ideal and orthogonal character as an addition reaction. The idea of polymers featuring the Diels-Alder reaction is fairly old, with a patent by Craven[20] appearing in 1969. However, thanks to work done by Wudl's group,[14] the field has seen a revitalization, with different groups demonstrating different polymer architectures and Diels-Alder pairs.[10, 24]

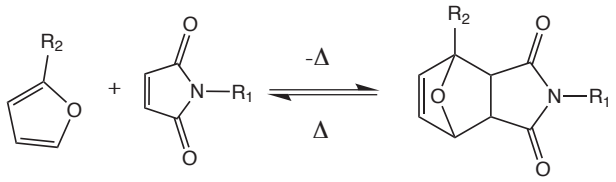

Scheme 1.1: The Diels-Alder reaction between a maleimide and a furan. The [4+2] tricyclic adduct structure on the right generally forms at high yield at ambient temperature. At increased temperature, the adduct reversibly decouples to reform the reactants at a rate and quantity which is determined by standard chemical equilibrium and kinetics. Multifunctional furans and maleimides can thus be reacted to form thermoreversibly crosslinked polymer networks at ambient conditions.

Arising from an exothermic thermoreversible reaction, the equilibrium conversion of Diels-Alder functional groups is a strong function of temperature. At low temperatures, the equilibrium is shifted towards the adduct state, while at elevated temperatures adducts tend to break apart into the original furan and maleimide moieties. Multifunctional furan and maleimide monomers have been used in a number[20, 24a-d, 25] of applications to form thermoreversibly crosslinked polymers. This reaction generally follows standard chemical equilibrium behavior as in equation 1.1, which has previously been reported.[10]

$$K_C(T) = \frac{x}{[L]_0(1-x)(r^{-1}-x)} = e^{\left(-\frac{\Delta H^\circ - T\Delta S^\circ}{RT}\right)} \qquad (1.1)$$

Here, x is the conversion of a limiting reagent, $[L]_0$ is the initial concentration of that limiting reagent, r is the ratio of limiting to excess reagent, ΔH^0 is the molar heat of reaction and ΔS^0 is the molar entropy of the reaction. This approach describes the equilibrium constant K_C as a function of absolute temperature T with the ideal gas constant, R. Following this equilibrium, the degree of polymerization and therefore

the crosslink density of a gel containing this kind of bond becomes directly a function of temperature. Therefore, the mechanical properties of such a material become a function of temperature as well.

In Figure 1.1, the important temperature regimes of a crosslinked Diels-Alder covalent adaptable network are presented in terms of the solid modulus, G'. At ambient temperature, the material is a glass with a high modulus. As temperature increases, the material goes through the glass transition and reaches it's equivalent of the rubbery state, with a storage modulus dominated by the behavior of a transient network. The forward and reverse Diels-Alder reactions are able to proceed to equilibrium, which shifts ever further towards the reactants with increasing temperature and a concomitant decrease in the crosslink density. Eventually, the conversion of reactive groups and the associated crosslink density in the network become less than the critical level necessary to sustain a gel, i.e., the gel point conversion which correlates to what is here referred to as the gel temperature, T_{gel}. Above this temperature, G' falls off dramatically as the material becomes increasingly liquid-like. Near the gel temperature, the viscosity is a strong function of temperature rapidly becoming a typical Newtonian fluid at temperatures sufficiently above the gel temperature.

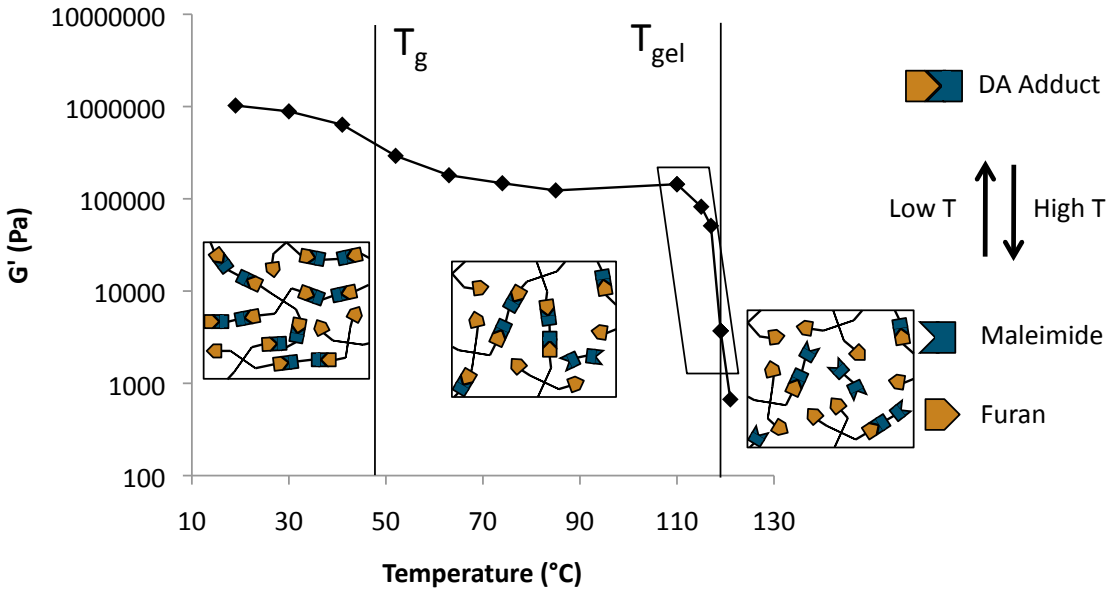

Figure 1.1: Solid modulus as a function of temperature for a model Diels-Alder polymer network, demonstrating the three major material states in transient networks: glass, transient rubber, and liquid. This study focuses on the immediate gelation and post-gelation region indicated by the parallelogram. Data are illustrative of a mixture of the furan and maleimide monomers used here (SRF and DPBM at a stoichiometric ratio of 10:6 or r=0.6). For T<90°C, G' was measured by a tensile test, whereas for T>90°C, G' was measured via shear.

For this work we use a commercially available bismaleimide and a low molecular weight, but flexible multifuran crosslinker (schemes 1.2 and 1.3). We synthesize the multifuran via the Michael addition of furfuryl mercaptan to a simple commercial tetra-acrylate. The synthesis is straightforward and scalable, and requires only limited equipment and knowledge to perform. By limiting the reaction with a less-than-stoichiometric amount of furfuryl mercaptan, reduced functionality analogues are readily produced simply by eliminating residual acrylate groups in a second Michael addition step, using a thiol inert to the Diels-Alder reaction, such as octanethiol.

The crosslink density of such networks is high enough in the fully functionalized case to form a stiff polymer at ambient temperature; however, its functionality is low enough that a modest inequality of stoichiometry (in our case r=0.36 to 0.5) is sufficient to prevent gelation, even at the equilibrium conversion of the limiting reactant at all temperatures studied. By combining the effects of these two capabilities for controlling the system, a gel point conversion and its corresponding gel temperature can be targeted during the formulation step, without any additional synthesis. We took advantage of this effect to test theory with analogous materials at several different conditions.

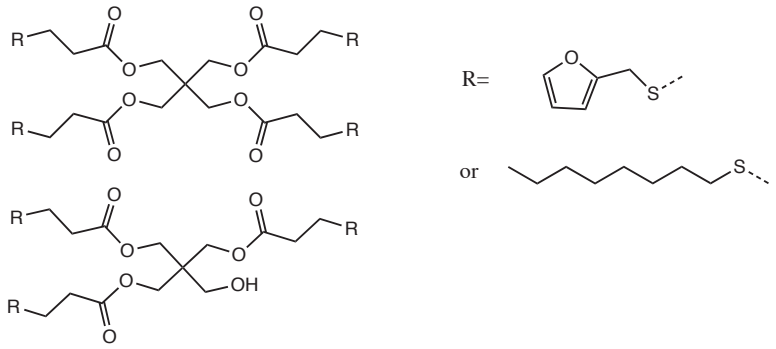

Scheme 1.2: Multifuran monomer SRF used in this study, a pentaerythritol tri-/tetraacrylate (SR295) substituted via Michael addition with furfuryl mercaptan and octanethiol. Functionality is adjusted by varying the ratio of furan to octane moieties in the reaction step. These compositions are distinguished by displaying the resultant effective functionality in parentheses, e.g. SRF(3.0).

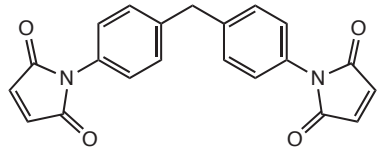

Scheme 1.3: Bismaleimide monomer DPBM used in this study (1,1′-(methylenedi-4,1-phenylene) bismaleimide). Whenever a composition's stoichiometric ratio is indicated, as in SRF(3.8) r=0.6, the ratio indicates the amount of maleimide used, as a fraction of the furan moieties used.

Theory

The theoretical foundations for the behavior of "transient",[8b] "thermoreversible",[26] "dynamic",[24e] or "adaptable"[16] networks have been derived, most recently and completely by Semenov and Rubinstein.[27] Their theory of linear dynamics for associating polymers is suitable for many aspects and details specific to their associative network of interest; however, the derivation begins with polymer scaling theory that should be applicable to most thermoreversible networks. The crucial insight they provide is that by considering only "typical" (characteristic percolation cutoff size)[28] clusters and network chains and "backbone"[29] transient bonds within those clusters (Figure 1.2), a scaling relationship between bond lifetime and relaxation in the sol and gel states near the gel point can be derived.

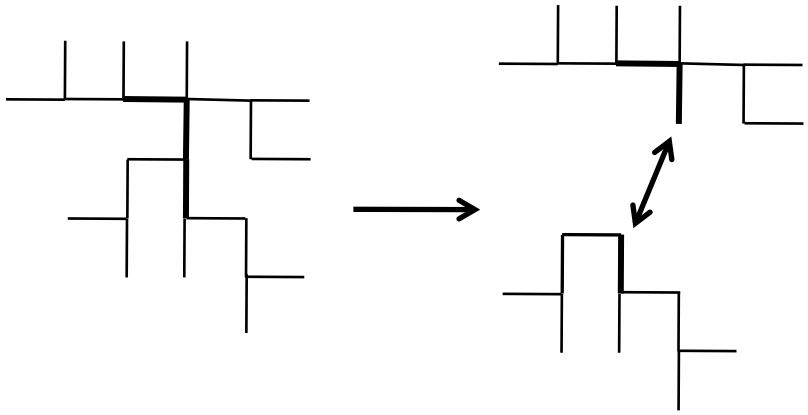

Figure 1.2: Visualization of transient cluster relaxation via backbone breakage. Bolded bonds represent critical connections which, when split, transform one transient cluster into two roughly equal parts.

$$\tau_l \propto \tau_b |\varepsilon| \tag{1.2}$$

In equation (1.2), the bond lifetime τ_b is the decay constant or the inverse of the kinetic rate constant for the thermoreversible links in the cluster, and τ_l is the rheological lifetime of the cluster as a whole. In their paper, Semenov and Rubinstein make the argument that the two timescales can be related through $\varepsilon=p-p_{gel}$, the distance from the Flory[30] gel point in terms of conversion, in the post-gel regime. If a thermoreversible network is considered as a generalized Maxwell material,[1] the longest relaxation time, τ_{max}, represents the transition timescale between viscoelastic and purely viscous behavior, and should correspond to τ_l. If we rewrite the scaling relationship as an explicit proportionality, with a material-dependent constant, C, we can algebraically rearrange it to obtain a simple equation in terms of the most important material parameters: conversion (p), bond lifetime (τ_b), gel point conversion (p_{gel}), and the longest relaxation time in the network (τ_{max}).

$$p = C\frac{\tau_{max}}{\tau_b} + p_{gel} \tag{1.3}$$

In circumstances where a material is far above its gel point conversion, and the lifetime of a bond is orders of magnitude longer than the timeframe of interest, the viscoelastic spectrum is well predicted by classical crosslink calculations without consideration of the reversible bonds. To calculate elasticity based on conversion and the distribution of multifunctional monomers, we can employ the Miller and Macosko[31] recursive method, solving for the crosslink density, υ, numerically. This value may be converted into a "plateau" modulus via the relationship $G_p=\upsilon RT$, disregarding other potential contributions to the modulus as a

first order approximation.[32] At lower temperatures, deviations are seen as the glass transition begins to interfere with measurement of the purely rubbery behavior.[10]

Similarly, the main property of interest in the regime far away from the gel point, i.e., the viscosity, is not substantially determined by the bond breakage rate. Rather, the viscosity is largely determined by the properties of the unreacted monomers. Nearer to the gel point, a simple scaling exponent adequately[10] describes viscosity until very close to the gel point ($|p-p_{gel}| < \varepsilon_{min}$),[27b] where the largest molecular clusters are big enough that bond breakage begins to have an effect.

Remote Activation and Network Triggers

CANs have the ability to respond to an external stimulus, and it is this triggerable change in properties or behavior that motivates this research for the purpose of making smart and responsive materials tuned to a given event. As this work is focused on thermally reversible network behavior, our trigger is inevitably "heat", however the method of heating can have a drastic effect. Application of interfacial heat by radiative, conductive, or convective sources like heat lamps, hot plates, or ovens is typically a limiting factor due to the interplay of heat transfer time, activation depth, and thermal gradients. Therefore, various remote triggers could be worthwhile to explore.

A promising trigger for purely thermally activated reversible bonds is the use of self-limited hysteresis heating. By suspending a ferromagnetic particle in a reversible network matrix, a magnetically sensitized composite is formed which

heats up when exposed to a radio-frequency, high-strength, oscillating magnetic field. Depending on particle composition and geometry, Néel relaxation is the dominant contribution to the heating mechanism; so, as the Curie temperature of the material is approached and the magnetic susceptibility decreases, the amount of power the particles can extract from the RF magnetic field drops until the material reaches a steady temperature.

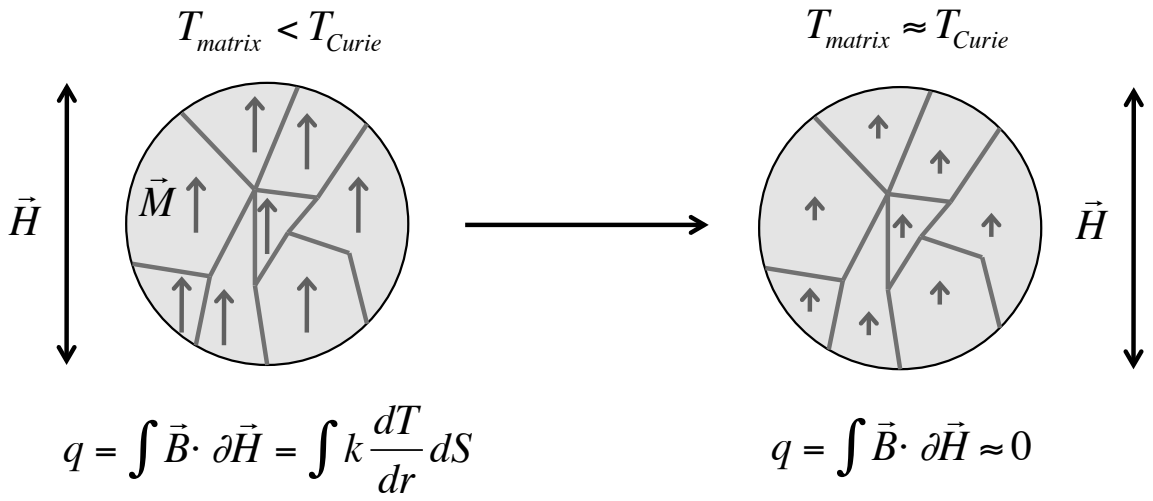

Figure 1.3: The process of hysteresis heating. When the magnetic particle such as CrO_2 is in a matrix below the Curie temperature of the material, the particle itself must be less than the Curie temperature as well due to heat transfer, so the material is coerced to a magnetization $\vec{M}$ due to the oscillating magnetic field $|\vec{H}| = H_0 \sin(2\pi ft + \omega)$. The heat added to the matrix is equal to the hysteresis work. When the matrix approaches the Curie temperature, by the same argument, the particle must be near the Curie temperature, so the hysteresis work per cycle drops, and the heating rate approaches zero, producing a self-limiting steady final temperature.

Chromium(IV) dioxide particles were chosen for this study, as CrO_2 has the lowest Curie temperature (113°C) of any common ferromagnetic material. Alternative particles suffer from large contributions by additional heating mechanisms, such as inductive resistance and excessively high Curie temperatures.

(The next lowest Curie temperature amongst common materials is 358°C for Nickel – easily hot enough to irreversibly decompose the material.) Clearly, the Curie temperature of the particles is a double-edged sword, as it provides a neatly self-limited heating mechanism, but at a pre-defined temperature that is not, in principle, adjustable. Compositions must therefore be tuned to behave appropriately at the steady state temperature of the hysteresis heating process.

Our group has previously reported[33] the use of a thermoreversible Diels-Alder resin with appropriate properties to achieve, within 5 minutes, total reshaping or fracture healing, over the course of as many as 15 individual heating cycles. This outcome was achieved because the resin studied essentially totally depolymerized into oligomeric species and completely relaxed/flowed on the timescale of the experiment. However, it would be desireable to vary this performance using methods suggested by a structure-property relationship valid in the material. Fracture healing performance is generally understood to be related to the mechanical relaxation processes, and so by varying the factors responsible for relaxation, it should be possible to understand the variability in various thermoreversible CANs subjected to identical healing or reshaping processes.

One of the most promising classes of CANs is the photoreversible network, wherein crosslink scission is triggered via reversible addition fragmentation chain-transfer (RAFT) of radicals generated by photoinitiation. Photo-CANs have been used in stress relaxation,[34] patterned texturing,[35] and photoactuated shape memory motion.[22] Generally, the effects observed are the result of the strong spatial and

temporal control of stress relaxation afforded by the light-activated nature of the process. However, despite the name, the RAFT process is not perfectly reversible, as it is highly coupled to the typically irreversible processes of radical initiation and termination. Furthermore, the radicals themselves are subject to a wide variety of potential side reactions that limit reversibility.

Thermoreversible CANs represent an adaptable network architecture that is in principle totally reversible. Among the possible thermoreversible covalent addition reactions that can be used in a network polymerization, the Diels-Alder (DA) reaction between maleimide and furan represents one of the most ideal and orthogonal options. Because the DA equilibrium conversion is strongly temperature dependent over a modest temperature range, one has substantial control over the material properties, especially viscosity, despite the lack (in principle) of any thermodynamic phase changes.

However, the fundamental roles of temperature and heat transfer are also natural limitations of thermoreversible networks. Typically, thermally activated polymers are heated by ovens or hot plates, and involve using high temperatures at the external interface to drive heat into the material via thermal gradients. Using these methods, there will be an inevitable tradeoff between the desired speed, uniformity, and depth of activation. Our group has already considered one alternative heating method, the pseudo-bulk heating provided by hysteresis loss of ferromagnetic composites in an RF magnetic field. This method provides fast, relatively uniform heating at all depths, but lacks the spatial control afforded by the

photo-activated techniques. To move in the opposite direction, a technique with total spatial and temporal control of temperature in a thermally activated CAN could be very useful.

Generating heat with a high intensity light source is a straightforward method of achieving this goal. However, some sort of chromophore is necessary to capture the light and efficiently convert it to heat. Chemical dyes are not suitable in this application as they are subject to photochemical effects, including photobleaching. Metal oxide dyes offer high stability, but a limited set of absorbance spectra. Other highly stable absorbers, such as carbon black, have a broad absorption that would limit application. An ideal dye would have tunable absorption, thermal and chemical stability, and efficiently convert light to heat.

The photothermal effect[36] observed when metal nanoparticles absorb light due to localized surface plasmon resonance (LSPR) has found use in applications that demand localized, switchable heating, such as microfluidic switching,[37] cancer treatment,[38] and drug release.[39] Noble metal nanoparticles themselves are generally stable, until extreme temperatures or light intensities are reached. However, chemisorbed capping ligands, which must approach equilibrium with the population dissolved in the surrounding matrix, are necessarily somewhat temperature sensitive. To prevent irreversible aggregation and loss of the LSPR, a covalently bound shell of silica can be added to the surface of the particles to form what has been termed Au@SiO_2 core/shell nanoparticles. Additionally, silica surfaces are amenable to further functionalization to enhance compatability with the matrix.

Suspending such $Au@SiO_2$ nanoparticles in a Diels-Alder network could produce a photothermally sensitized CAN that can be manipulated on small size scales using laser light.

Summary

In this chapter, we have introduced some of the basic concepts and motivations for the projects and experiments in the forthcoming chapters. Chapter 2 defines concretely the overarching objectives of our work and what impact we expect them to have in the broader polymeric materials community. Chapter 3 introduces our model covalent adaptable network material and examines its viscoelasticity from empirical and theoretical standpoints. Chapter 4 explicitly tests the predictions of transient network theory using the model network and attempts to clarify how the theory may be practically applied in real situations. Chapter 5 records our evaluation of single-fluorophore microrheology as a tool for testing the assumptions of the theory on a more fundamental level. Chapter 6 investigates applying the knowledge developed towards understanding fracture healing in TR-CANs triggered by hysteresis heating, both empirically and in context of theoretical predictions of viscoelasticity. Chapter 7 investigates the nature of the spatial and temporal control of TR-CANs afforded by photothermal laser heating. We conclude with chapter 8, where we revisit the specific aims, how we achieved them, and their wider repercussions, and discuss directions that future research on the topic could take.

References

1. Ferry, J. D., *Viscoelastic properties of polymers*. 3rd ed. ed.; Wiley: New York, 1980; p 641.

2. Wool, R. P.; O'Connor, K. M., A theory crack healing in polymers. *J Appl Phys* **1981,** *52* (10), 5953-5963.
3. Jud, K.; Kausch, H. H.; Williams, J. G., Fracture mechanics studies of crack healing and welding of polymers. *J Mater Sci* **1981,** *16* (1), 204-210-210.
4. Macht, M. L.; Rahm, W. E.; Paine, H. W., Injection Molding. *Industrial & Engineering Chemistry* **1941,** *33* (5), 563-567.
5. Olabisi, O., *Handbook of thermoplastics*. Marcel Dekker: New York, 1997; p xvi, 1053 p.
6. Winter, H.; Mours, M., Rheology of Polymers Near Liquid-Solid Transitions. In *Neutron Spin Echo Spectroscopy Viscoelasticity Rheology*, Springer Berlin / Heidelberg: 1997; Vol. 134, pp 165-234-234.
7. Cordier, P.; Tournilhac, F.; Soulie-Ziakovic, C.; Leibler, L., Self-healing and thermoreversible rubber from supramolecular assembly. *Nature* **2008,** *451* (7181), 977-80.
8. (a) Feldman, K. E.; Kade, M. J.; Meijer, E. W.; Hawker, C. J.; Kramer, E. J., Model Transient Networks from Strongly Hydrogen-Bonded Polymers. *Macromolecules* **2009,** *42* (22), 9072-9081; (b) Stadler, R., Transient networks by hydrogen bond interactions in polybutadiene-melts. In *Permanent and Transient Networks*, Springer Berlin / Heidelberg: 1987; Vol. 75, pp 140-145-145.
9. Brunsveld, L.; Folmer, B. J. B.; Meijer, E. W.; Sijbesma, R. P., Supramolecular Polymers. *Chemical Reviews* **2001,** *101* (12), 4071-4098.
10. Adzima, B. J.; Aguirre, H. A.; Kloxin, C. J.; Scott, T. F.; Bowman, C. N., Rheological and chemical analysis of reverse gelation in a covalently crosslinked Diels-Alder polymer network. *Macromolecules* **2008,** *41* (23), 9112-9117.
11. van Beek, D. J. M.; Spiering, A. J. H.; Peters, G. W. M.; te Nijenhuis, K.; Sijbesma, R. P., Unidirectional Dimerization and Stacking of Ureidopyrimidinone End Groups in Polycaprolactone Supramolecular Polymers. *Macromolecules* **2007,** *40* (23), 8464-8475.
12. Jay, J. I.; Langheinrich, K.; Hanson, M. C.; Mahalingam, A.; Kiser, P. F., Unequal stoichiometry between crosslinking moieties affects the properties of transient networks formed by dynamic covalent crosslinks. *Soft Matter* **2011,** *7* (12), 5826-5835.
13. Montarnal, D.; Capelot, M.; Tournilhac, F. o.; Leibler, L., Silica-Like Malleable Materials from Permanent Organic Networks. *Science* **2011,** *334* (6058), 965-968.
14. Chen, X.; Dam, M. A.; Ono, K.; Mal, A.; Shen, H.; Nutt, S. R.; Sheran, K.; Wudl, F., A Thermally Re-mendable Cross-Linked Polymeric Material. *Science* **2002,** *295* (5560), 1698-1702.
15. Zhang, Y.; Broekhuis, A. A.; Picchioni, F., Thermally Self-Healing Polymeric Materials: The Next Step to Recycling Thermoset Polymers? *Macromolecules* **2009,** *42* (6), 1906-1912.
16. Kloxin, C. J.; Scott, T. F.; Adzima, B. J.; Bowman, C. N., Covalent Adaptable Networks (CANs): A Unique Paradigm in Cross-Linked Polymers. *Macromolecules* **2010,** *43* (6), 2643-2653.
17. Bowman, C. N.; Kloxin, C. J., Covalent Adaptable Networks: Reversible Bond Structures Incorporated in Polymer Networks. *Angewandte Chemie International Edition* **2012,** *51* (18), 4272-4274.

18. (a) Park, H. Y.; Kloxin, C. J.; Scott, T. F.; Bowman, C. N., Stress Relaxation by Addition-Fragmentation Chain Transfer in Highly Cross-Linked Thiol-Yne Networks. *Macromolecules* **2010,** *43* (24), 10188-10190; (b) Kloxin, C. J.; Scott, T. F.; Bowman, C. N., Stress Relaxation via Addition-Fragmentation Chain Transfer in a Thiol-ene Photopolymerization. *Macromolecules* **2009,** *42* (7), 2551-2556.
19. Amamoto, Y.; Kikuchi, M.; Masunaga, H.; Sasaki, S.; Otsuka, H.; Takahara, A., Reorganizable Chemical Polymer Gels Based on Dynamic Covalent Exchange and Controlled Monomer Insertion. *Macromolecules* **2009,** *42* (22), 8733-8738.
20. Craven, J. M. Cross-Linked Thermally Reversible Polymers Produced from Condensation Polymers with Pendant Furan Groups Cross-Linked with Maleimides. 3435003, 1969.
21. Roberts, M. C.; Mahalingam, A.; Hanson, M. C.; Kiser, P. F., Chemorheology of Phenylboronate-Salicylhydroxamate Cross-Linked Hydrogel Networks with a Sulfonated Polymer Backbone. *Macromolecules* **2008,** *41* (22), 8832-8840.
22. Scott, T. F.; Draughon, R. B.; Bowman, C. N., Actuation in Crosslinked Polymers via Photoinduced Stress Relaxation. *Advanced Materials* **2006,** *18* (16), 2128-2132.
23. Diels, O.; Alder, K., Synthesen in der hydroaromatischen Reihe. *Justus Liebigs Annalen der Chemie* **1928,** *460* (1), 98-122.
24. (a) Goiti, E.; Heatley, F.; Huglin, M. B.; Rego, J. M., Kinetic aspects of the Diels-Alder reaction between poly(styrene-co-furfuryl methacrylate) and bismaleimide. *European Polymer Journal* **2004,** *40* (7), 1451-1460; (b) Goiti, E.; Huglin, M. B.; Rego, J. M., Some properties of networks produced by the Diels-Alder reaction between poly(styrene-co-furfuryl methacrylate) and bismaleimide. *European Polymer Journal* **2004,** *40* (2), 219-226; (c) Costanzo, P. J.; Beyer, F. L., Thermoresponsive, Optically Active Films Based On Diels-Alder Chemistry. *Chemistry of Materials* **2007,** *19* (25), 6168-6173; (d) Peterson, A. M.; Jensen, R. E.; Palmese, G. R., Reversibly cross-linked polymer gels as healing agents for epoxy-amine thermosets. *ACS Appl Mater Interfaces* **2009,** *1* (5), 992-5; (e) Reutenauer, P.; Buhler, E.; Boul, P. J.; Candau, S. J.; Lehn, J. M., Room temperature dynamic polymers based on Diels-Alder chemistry. *Chemistry* **2009,** *15* (8), 1893-900; (f) Inglis, A. J.; Nebhani, L.; Altintas, O.; Schmidt, F. G.; Barner-Kowollik, C., Rapid Bonding/Debonding on Demand: Reversibly Cross-Linked Functional Polymers via Diels,àíAlder Chemistry. *Macromolecules* **2010,** *43* (13), 5515-5520; (g) Peterson, A. M.; Jensen, R. E.; Palmese, G. R., Room-Temperature Healing of a Thermosetting Polymer Using the Diels-Alder Reaction. *ACS Appl Mater Interfaces* **2010,** *2* (4), 1141-1149.
25. (a) Jones, J. R.; Liotta, C. L.; Collard, D. M.; Schiraldi, D. A., Cross-Linking and Modification of Poly(ethylene terephthalate-co-2,6-anthracenedicarboxylate) by Diels,àíAlder Reactions with Maleimides. *Macromolecules* **1999,** *32* (18), 5786-5792; (b) Swanson, J. P.; Rozvadovsky, S.; Seppala, J. E.; Mackay, M. E.; Jensen, R. E.; Costanzo, P. J., Development of Polymeric Phase Change Materials On the basis of Diels-Alder Chemistry. *Macromolecules* **2010,** *43* (14), 6135-6141; (c) Goussé, C.; Gandini, A., Diels–Alder polymerization of difurans with bismaleimides. *Polym Int* **1999,** *48* (8), 723-731; (d) McElhanon, J. R.; Russick, E. M.; Wheeler, D. R.; Loy, D. A.; Aubert, J. H., Removable foams based on an epoxy resin incorporating reversible Diels-Alder adducts. *Journal of Applied Polymer Science* **2002,** *85* (7), 1496-1502.

26. te Nijenhuis, K., Calculation of network parameters in thermoreversible gels. *Polymer Gels and Networks* **1996,** *4* (5-6), 415-433.
27. (a) Semenov, A. N.; Rubinstein, M., Thermoreversible Gelation in Solutions of Associative Polymers. 1. Statics. *Macromolecules* **1998,** *31* (4), 1373-1385; (b) Rubinstein, M.; Semenov, A. N., Thermoreversible Gelation in Solutions of Associating Polymers. 2. Linear Dynamics. *Macromolecules* **1998,** *31* (4), 1386-1397.
28. Stauffer, D., Scaling theory of percolation clusters. *Physics Reports* **1979,** *54* (1), 1-74.
29. Herrmann, H. J., Geometrical cluster growth models and kinetic gelation. *Physics Reports* **1986,** *136* (3), 153-224.
30. Flory, P. J., Molecular Size Distribution in Three Dimensional Polymers. I. Gelation1. *Journal of the American Chemical Society* **1941,** *63* (11), 3083-3090.
31. Miller, D. R.; Macosko, C. W., A New Derivation of Post Gel Properties of Network Polymers. *Macromolecules* **1976,** *9* (2), 206-211.
32. Dotson, N. A.; Galvan, R.; Laurence, R. L.; Tirrell, M., *Polymerization Process Modeling*. Wiley-VCH: New York, 1995.
33. Adzima, B. J.; Kloxin, C. J.; Bowman, C. N., Externally Triggered Healing of a Thermoreversible Covalent Network via Self-Limited Hysteresis Heating. *Advanced Materials* **2010,** *22* (25), 2784-2787.
34. Scott, T. F.; Schneider, A. D.; Cook, W. D.; Bowman, C. N., Photoinduced Plasticity in Cross-Linked Polymers. *Science* **2005,** *308* (5728), 1615-1617.
35. Kloxin, C. J.; Scott, T. F.; Park, H. Y.; Bowman, C. N., Mechanophotopatterning on a Photoresponsive Elastomer. *Advanced Materials* **2011,** *23* (17), 1977-1981.
36. Govorov, A.; Richardson, H., Generating heat with metal nanoparticles. *Nano Today* **2007,** *2* (1), 30-38.
37. Sershen, S. R.; Mensing, G. A.; Ng, M.; Halas, N. J.; Beebe, D. J.; West, J. L., Independent Optical Control of Microfluidic Valves Formed from Optomechanically Responsive Nanocomposite Hydrogels. *Advanced Materials* **2005,** *17* (11), 1366-1368.
38. (a) Huang, X.; El-Sayed, I. H.; Qian, W.; El-Sayed, M. A., Cancer cell imaging and photothermal therapy in the near-infrared region by using gold nanorods. *Journal of the American Chemical Society* **2006,** *128* (6), 2115-20; (b) El-Sayed, I. H.; Huang, X.; El-Sayed, M. A., Selective laser photo-thermal therapy of epithelial carcinoma using anti-EGFR antibody conjugated gold nanoparticles. *Cancer Lett* **2006,** *239* (1), 129-35.
39. Skirtach, A. G.; Dejugnat, C.; Braun, D.; Susha, A. S.; Rogach, A. L.; Parak, W. J.; M√∂hwald, H.; Sukhorukov, G. B., The Role of Metal Nanoparticles in Remote Release of Encapsulated Materials. *Nano Lett* **2005,** *5* (7), 1371-1377.

Chapter 2: Objectives

Covalent adaptable networks (CANs) are polymer networks (crosslinked macromolecular materials) in which the connections between monomers in the network can be reversibly cleaved by an external stimulus.[1] CANs have the ability to relieve stress, including polymerization-shrinkage-induced stress;[2] incorporate chemical functionality post-cure;[3] chemically bridge interfaces, including fractures;[4] undergo recycling;[5] control the diffusivity of particles via adjustable mesh size;[6] and actuate mechanical motion.[7] These different effects are due to varying underlying chemical mechanisms; however, the fundamental nature of the phenomenon in each case is the cleavage and recombination of crosslinks. Therefore, the fundamental viscoelastic behavior should be analogous for each of the cases. Several studies have been published which present effective structure-property relationships for specific CANs or for particular applications; however, no successful attempt has been made to find relationships between the models or to arrive at a more universal model for CAN behavior and performance.

In particular, Chen and Wudl published an account of a "re-mendable" Diels-Alder material in which they demonstrated reversibility of the DA bond in the material, as well as recovery of fracture toughness ranging from 50% to 85%, depending on the specific monomers and processes implemented.[4] However, except for the fracture healing properties, they primarily examined ambient temperature material properties, without focusing on the rheology of the material at elevated

temperature. Zhang, Broekhuis, and Picchioni created a recyclable Diels-Alder material using the Paal-Knorr polyketone grafting-to technique as a less-costly alternative to other published DA crosslinking strategies.[8] However, they used elevated temperatures to achieve their reprocessing ability, which often leads to significant, irreversible side reactions.[9] Furthermore, the monomer system, while inexpensive, was also polydisperse and ill defined for determining and analyzing specific rheological behavior. Goiti *et al.* studied a number of properties of polymerizing poly(styrene-co-furfuryl acrylate)/bis-maleimide/toluene organogels, including swelling ratio, viscosity, and shear modulus though they stopped attempting to characterize the material under conditions (such as low stoichiometric ratio or high temperature) that caused the material to behave as a transient network.[10]

Reversible bonding strategies other than the Diels-Alder reactions, such as hydrogen bonding[11] or π-π stacking[12], have also been shown to have promising attributes, despite the lack of a complete understanding of how the monomer structure relates to those same attributes. Söntjens[11b] was one of the few authors to simultaneously examine temperature and frequency dependence of features in the complex modulus of a hydrogen bonded system; however, the analysis was empirical in nature, lacking any specific comparison to theoretical predictions. Furthermore, observations were confounded by crystallinity-induced properties. Burattini's self-healing π-π stacking[12] polymer has the ability to mend fractures and fuse interfaces repeatedly, without additional heat input. However, the polymer is more accurately characterized as an elastomer with additional reversible crosslinks.

No attempt has been made, to our knowledge, to characterize the material's viscoelastic properties. As these materials are unified, at least in part, by common attributes of their chemical mechanism, a common structure-property relationship should be applicable to each of them.

With such a body of work surrounding thermoreversible covalent adaptable networks, treating each material -- to the greatest extent possible -- as a member of one class of materials, bound by the same underlying mechanism and theory, represents an opportunity to make a valuable contribution to the field. This approach presents the chance to enhance fundamental understanding of the current, practical materials, while simultaneously providing a framework through which future materials can be characterized and evaluated. The overarching goal of this project is to describe the behavior of thermoreversible CANs explicitly in terms of bond kinetics and thermodynamics, relating the chemistry of the system to the time and temperature-dependent material properties. It is an aim of this project to use the knowledge gained from analyzing these model materials to improve the state of materials research based on reversible networks. Rather than showing, for example, that a material containing reversible bonds can flow at elevated temperatures, we will show that there is a material of maximum crosslink density that can be liquefied and reshaped on a reasonable timescale via radio frequency (RF) heating of suspended ferromagnetic CrO_2 particles. The ability to produce localized heating and therefore localized activation of thermoreversible CANs is desirable, so an optically sensitized Diels-Alder composite is to be designed capable

of activation by laser light using a robust chromophore such as Au@SiO_2. To that purpose, specific aims of this project are therefore twofold:

(1) **To evaluate structure-property relationships for reversible networks** – in this case, using a model Diels-Alder network.

(2) **To design and manipulate materials through understanding of these structure-property relationships** – specifically, by compositing the model network with CrO_2 and Au@SiO_2 particles.

Results of research performed in the pursuit of achieving these aims will provide a resource to the transient network community for an enhanced fundamental understanding of the material dynamics, as well as a basis for comparing various reversible materials. By demonstrating the importance of the structure property relationships in the context of real applications, other researchers will be able to see how the knowledge is applied and may find it a more straightforward task to implement them in their own experiments and analyses.

References

1. Kloxin, C. J.; Scott, T. F.; Adzima, B. J.; Bowman, C. N., Covalent Adaptable Networks (CANs): A Unique Paradigm in Cross-Linked Polymers. *Macromolecules* **2010,** *43* (6), 2643-2653.
2. (a) Park, H. Y.; Kloxin, C. J.; Scott, T. F.; Bowman, C. N., Stress Relaxation by Addition-Fragmentation Chain Transfer in Highly Cross-Linked Thiol-Yne Networks. *Macromolecules* **2010,** *43* (24), 10188-10190; (b) Kloxin, C. J.; Scott, T. F.; Bowman, C. N., Stress Relaxation via Addition-Fragmentation Chain Transfer in a Thiol-ene Photopolymerization. *Macromolecules* **2009,** *42* (7), 2551-2556.
3. Amamoto, Y.; Kikuchi, M.; Masunaga, H.; Sasaki, S.; Otsuka, H.; Takahara, A., Reorganizable Chemical Polymer Gels Based on Dynamic Covalent Exchange and Controlled Monomer Insertion. *Macromolecules* **2009,** *42* (22), 8733-8738.
4. (a) Chen, X.; Dam, M. A.; Ono, K.; Mal, A.; Shen, H.; Nutt, S. R.; Sheran, K.; Wudl, F., A Thermally Re-mendable Cross-Linked Polymeric Material. *Science* **2002,** *295*

(5560), 1698-1702; (b) Chen, X.; Wudl, F.; Mal, A. K.; Shen, H.; Nutt, S. R., New Thermally Remendable Highly Cross-Linked Polymeric Materials. *Macromolecules* **2003,** *36* (6), 1802-1807.
5. Craven, J. M. Cross-linked Thermally Reversible Polymers Produced from Condensation Polymers with Pendant Furan Groups Cross-linked with Maleimides. 3435003, 1969.
6. Roberts, M. C.; Mahalingam, A.; Hanson, M. C.; Kiser, P. F., Chemorheology of Phenylboronate-Salicylhydroxamate Cross-Linked Hydrogel Networks with a Sulfonated Polymer Backbone. *Macromolecules* **2008,** *41* (22), 8832-8840.
7. Scott, T. F.; Draughon, R. B.; Bowman, C. N., Actuation in Crosslinked Polymers via Photoinduced Stress Relaxation. *Advanced Materials* **2006,** *18* (16), 2128-2132.
8. Zhang, Y.; Broekhuis, A. A.; Picchioni, F., Thermally Self-Healing Polymeric Materials: The Next Step to Recycling Thermoset Polymers? *Macromolecules* **2009,** *42* (6), 1906-1912.
9. Hopewell, J. L.; Hill, D. J. T.; Pomery, P. J., Electron spin resonance study of the homopolymerization of aromatic bismaleimides. *Polymer* **1998,** *39* (23), 5601-5607.
10. (a) Goiti, E.; Heatley, F.; Huglin, M. B.; Rego, J. M., Kinetic aspects of the Diels-Alder reaction between poly(styrene-co-furfuryl methacrylate) and bismaleimide. *European Polymer Journal* **2004,** *40* (7), 1451-1460; (b) Goiti, E.; Huglin, M. B.; Rego, J. M., Some properties of networks produced by the Diels-Alder reaction between poly(styrene-co-furfuryl methacrylate) and bismaleimide. *European Polymer Journal* **2004,** *40* (2), 219-226.
11. (a) Bosman, A. W.; Sijbesma, R. P.; Meijer, E. W., Supramolecular polymers at work. *Materials Today* **2004,** *7* (4), 34-39; (b) Soentjens, S. H. M.; Renken, R. A. E.; van Gemert, G. M. L.; Engels, T. A. P.; Bosman, A. W.; Janssen, H. M.; Govaert, L. E.; Baaijens, F. P. T., Thermoplastic Elastomers Based on Strong and Well-Defined Hydrogen-Bonding Interactions. *Macromolecules* **2008,** *41* (15), 5703-5708.
12. Burattini, S.; Colquhoun, H. M.; Greenland, B. W.; Hayes, W., A novel self-healing supramolecular polymer system. *Faraday Discussions* **2009,** *143*, 251-264.

Chapter 3: Temperature Dependent Stress Relaxation in a Model Diels-Alder Network

Abstract

The effect of temperature on the complex shear modulus ($G^*(\omega)$) of a model reversible covalent network formed by the Diels–Alder reaction was studied. The gel temperature of 119°C and the functional group conversion at this temperature were determined by the Winter–Chambon criterion. The complex modulus of the crosslinked network was measured from 110°C to 121°C, near the gel temperature, to determine the frequency ranges over which stress relaxation could occur. The crossover time was found to have a strong dependence on temperature ($E_a \sim 260$ kJ/mol) – greater than would be expected from a typical thermally activated retro-Diels-Alder process. Low frequency scaling of $G^*(\omega)$ over the experimental frequency and temperature range was interpreted to be a result of the existence of a distribution of transient clusters in these thermoreversible covalent gels.

Introduction

Few materials behave either as ideal Hookean solids or Newtonian liquids. Indeed, polymeric materials often show dramatic time and temperature dependent behavior due to their molecular structure[1]. A linear polymer may be a rigid semicrystalline thermoplastic, a thermoplastic elastomer, or an amorphous glass. Yet, upon heating all of these materials form polymer melts where liquid-like behavior predominates. The mechanisms responsible for these behaviors allow

thermoplastics to undergo fracture healing[2], welding[3] and molding[4] lending to their ubiquitous use in everyday life (e.g. fibers, rubbers, structural materials, and paints).[5] More recently, non-covalent polymer networks formed by weak intermolecular interactions – like microphase separation[6], pi-pi stacking[7], and hydrogen bonding[6, 8] – have been shown to exhibit behavior and properties similar to those of thermoplastics. These types of "weak" networks often behave as viscoelastic liquids, as defined by having a finite steady shear viscosity, yet under certain conditions they also exhibit solid-like behavior.[9]

The liquid-like properties of weak networks are due to the transient nature of their intermolecular interactions[10]. Therefore, covalent polymer networks should also behave as liquids, if the covalent connections between crosslinks have the ability to reversibly break and rearrange on the appropriate timescale. That is, despite the "strength" of the covalent bond type, a network held together by reversible bonds should have the properties of a "weak" network, i.e. plasticity, when examined under appropriate conditions.

When the reversibility of these bonds is triggerable via an external stimulus, these networks can be classified as covalent adaptable networks (CANs).[11] CANs generally have the ability to: relieve stress, including polymerization-shrinkage-induced stress[12]; incorporate new chemical functionality post-cure[13]; chemically bridge interfaces, including fractures[14]; undergo recycling[15]; control the diffusivity of particles via adjustable mesh size[16]; and actuate mechanical motion[17]. Because all these CANs and applications rely on a common mechanism (i.e. the reversible

scission and recombination of all crosslinking bonds in the network,) there should be commonalities in the viscoelastic properties of the materials in their activated state. Furthermore, there should be fundamental structure-property relationships that govern the mechanical and relaxation behavior of CANs. Several studies have been published which present effective structure-property relationships for specific CANs in particular studies or for particular applications; however, to our knowledge no successful attempt has been made to find relationships between the models or to arrive at a more universal model.

In Figure 3.1, the important regimes of the solid modulus behavior of a Diels-Alder covalent adaptable network are presented. At ambient temperature, the material is a glass with a high modulus. As temperature increases, the material goes through the glass transition and reaches it's equivalent of the rubbery state, with a storage modulus dominated by the behavior of a transient network. The forward and reverse Diels-Alder reactions are able to proceed to equilibrium, which shifts ever further towards the reactants with increasing temperature with a concomitant decrease in the crosslink density. Eventually, the conversion of reactive groups and the associated crosslink density in the network become less than the critical level necessary to sustain a gel, i.e., the gel point conversion which correlates to what is here referred to as the "gel temperature." Above this temperature, G' falls off dramatically as the material becomes evermore liquid-like. Near the gel temperature, the viscosity is a strong function of temperature rapidly becoming typical Newtonian behavior at temperatures sufficiently above the gel temperature.

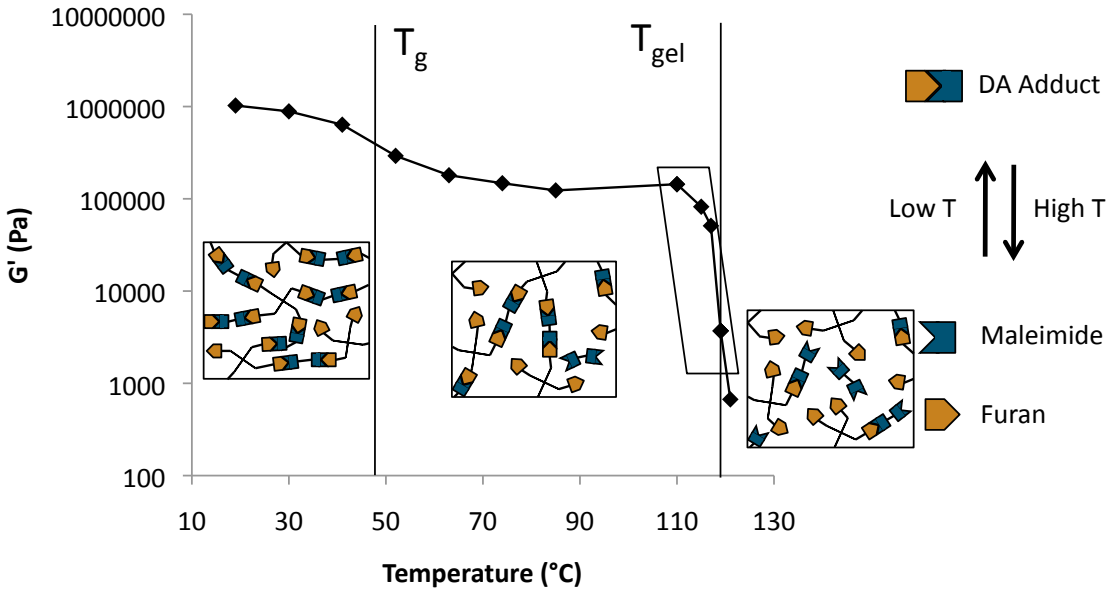

Figure 3.1: Solid modulus as a function of temperature for a model Diels-Alder polymer network, demonstrating the three major material states in transient networks: glass, transient rubber, and liquid. This study focuses on the immediate post-gelation region indicated by the parallelogram. Data are illustrative of a mixture of the furan and maleimide monomers used here (SRF and DPBM at a stoichiometric ratio of 10:6). For T<90°C, G' was measured by a tensile test, whereas for T>90°C, G' was measured via shear.

In this work, we synthesized a well-defined covalent adaptable network comprised of thermoreversible Diels-Alder linkages to probe the transient nature of this covalent network near the gel point and within the post-gelation regime, highlighted with a parallelogram Figure 3.1. This behavior is in contrast to other studies in which thermoreversible moieties are grafted to high-molecular weight pre-polymers,[18] or are polymerized together in an uncontrolled radical chain-growth polymerization,[19] thus obfuscating the relationships between macromolecular structure and material properties. We used dynamic mechanical analysis to demonstrate the presence of a covalent network via the complex shear

modulus, G*(ω), and to demonstrate that the timescale over which the network behaves as a solid is adjustable and a strong function of the temperature.

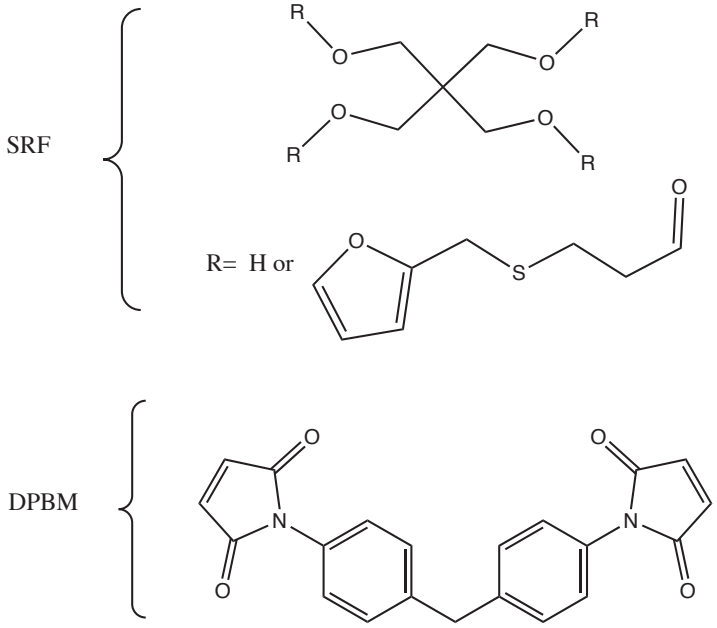

Figure 3.2: Monomers SRF and DPBM used for the experiments in this work. SRF is a mixture of 19% trifunctional and 81% tetrafunctional units leading to a functionality-weighted average functionality of 3.8.

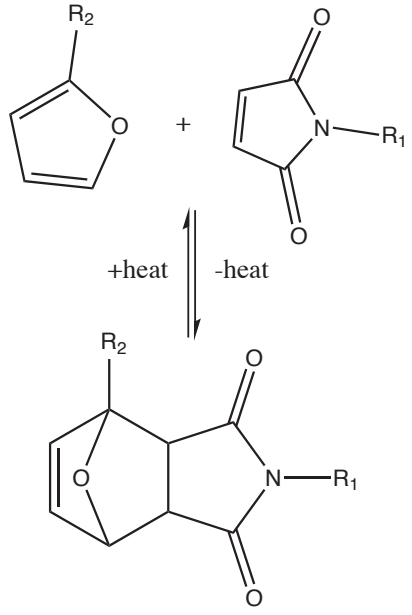

Figure 3.3: The thermoreversible Diels-Alder reaction between furan (left) and maleimide (right) moieties. These moieties tend to form adducts at low temperature, where the adducts are subsequently thermoreversible with constant formation and cleavage of the adduct structure dictated by the temperature dependent kinetics and equilibrium reaction extent.

Results and Discussion

To demonstrate the dichotomy in the nature of transient covalent networks, we synthesized a thermally responsive Diels–Alder network and evaluated its mechanical and reaction behavior for a number of temperatures at which the material is above, near, or below its gel point conversion. The Diels–Alder network was formed from a bifunctional maleimide monomer and a multifunctional furan crosslinker with an effective functionality of 3.8 furans per monomer (see Figures 3.2 and 3.3). The gel temperature was lowered to an appropriate experimental range for analysis by utilizing an off-stoichiometric mixture of furan and maleimide formed in a ratio of 6 maleimides to 10 furans (r=0.6). (The experimental T_{gel} for r=1.0 was above the upper limit of the operating temperature range for the rheometer, 160°C, so that the gel temperature could not be experimentally verified for the stoichiometric mixture.) As well as permitting the present study to be performed, lowering of the gel temperature by altering the stoichiometric ratio of the reactants also demonstrates the relative ease with which this critical point can be altered in gels of this nature. For the bifunctional furan and 3.8 functional maleimide with r=0.6, the Flory–Stockmayer (F-S) equation, $x_{gel} = [r(f_a - 1)(f_b - 1)]^{-1/2}$ predicts a gel point conversion of 76.4% maleimide moieties reacted. Qualitatively, the prepared resin at its equilibrium reacted state is glassy at room temperature, tacky at about 80°C, and flows readily at 130°C, due to the

equilibrium reversion of the Diels-Alder adduct to maleimide and furan groups at high temperatures.

Fourier transform infrared (FTIR) spectroscopy was used to determine the equilibrium conversion of the maleimide as a function of temperature by monitoring the absorption peak of an asymmetric maleimide ring-deformation mode[20] at 690 cm^{-1}. The equilibrium constant at each temperature was calculated using Equation 3.1, where x is the conversion of the limiting reagent (maleimide), $[L]_0$ is the initial concentration of the limiting reagent, and r represents the stoichiometric ratio of the limiting reagent to the excess reagent.

$$K_{eq} = \frac{x}{[L]_0(1-x)(r^{-1}-x)} \tag{3.1}$$

Because $[L]_0$ is unknown and assumed not to be a function of temperature, we grouped the concentration and equilibrium constant together to form a van't Hoff equation (Equation 3.2)

$$\ln(K_{eq}[L]_0) = -\frac{\Delta H}{RT} + \frac{\Delta S}{R} \tag{3.2}$$

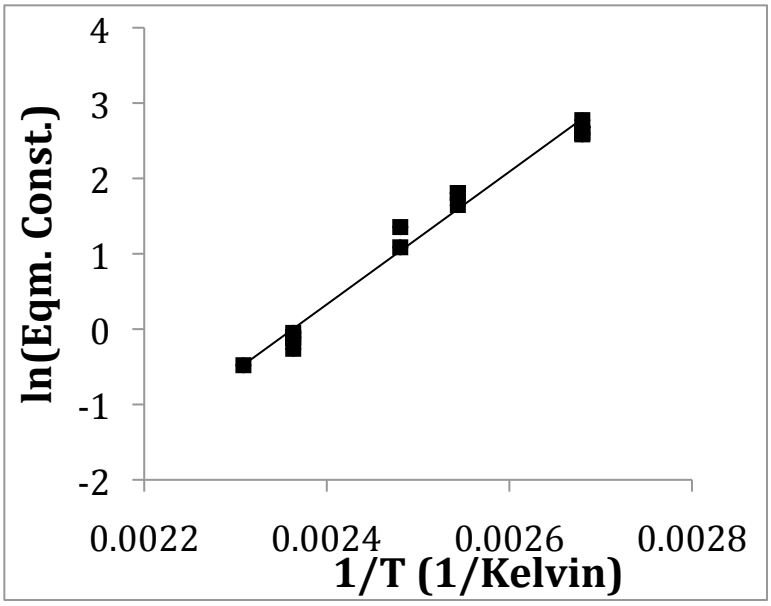

Figure 3.4: Van't Hoff plot for the Diels–Alder reaction from 110°C to 160°C. Monomers SRF and DPBM were mixed in a 10:6 furan:maleimide ratio (r=0.6) and conversion was monitored based on the maleimide peak at 690 cm^{-1}. The heat of reaction for this reaction was found to be ΔH=-73±8 kJ/mol.

A van't Hoff plot (Figure 3.4) of the logarithm of the equilibrium constant times the initial concentration as a function of the inverse temperature enables the molar heat of reaction, ΔH, to be determined from the equilibrium conversion measurements over a range of temperatures. At -73±8 kJ/mol, this heat of reaction is somewhat greater than previously reported.[10] We attribute this to the difference in temperature range studied as well as chemical differences in the materials used. According to the equilibrium conversion measurements and the Flory-Stockmayer equation, the gel point conversion of 76.4% should occur at 125±8°C.

To determine the experimental gel temperature, the frequency dependence of the complex shear modulus G*(ω) was recorded at several temperatures near the gel point, and the storage and loss components, G' and G'' are plotted in Figure 3.5.

Above 120°C, G'' is greater than G' for the entire frequency range, which is a characteristic of liquid-like materials. At temperatures below 118°C, G' is greater than G'' for high shear frequencies, but as the frequency decreases, the moduli cross over one another and the liquid modulus is greater than the solid modulus thereafter.

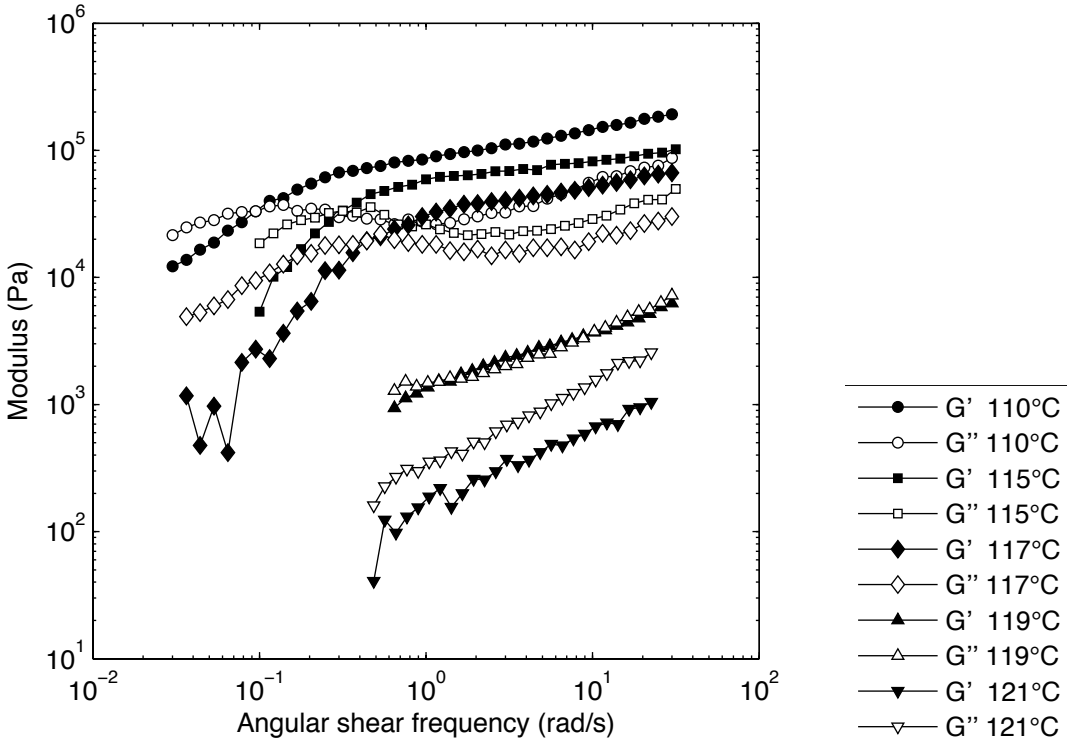

Figure 3.5: The loss and storage moduli for a Diels-Alder crosslinked network at temperatures near the gel point of 119°C. Samples are comprised of a 10:6 ratio of furan:maleimide from the SRF and DPBM monomers, respectively.

According to the Winter–Chambon (W–C) criterion, both components of the modulus of a material at its gel point scale with frequency according to the same power law. This relationship can also be represented as frequency independence of the loss tangent, tan(δ), at the gel point conversion or temperature for these Diels-Alder networks.

It has been shown that, for physical networks, the W–C criterion still applies[6] for timescales much shorter than the average cluster lifetime,

$$\lambda_{pg} = \frac{\lambda_b}{N_{avg,eqm}} \tag{3.3}$$

where λ_b is the bond lifetime. In the case of the Diels-Alder networks evaluated here, this value is precisely the reciprocal of the retro-Diels-Alder reaction rate constant. $N_{avg,eqm}$ is the instantaneous number of adducts in an average cluster of connected monomers in the sol fraction at equilibrium. In practice, this analysis implies that at the gel point of a material, the loss tangent becomes frequency-independent only over a range of frequencies between a high frequency threshold associated with the mobility of individual segments, and a low frequency threshold associated with the kinetics of the bond cleavage. Figure 3.6 illustrates this physical network-like liquid-solid transition occurring in the Diels–Alder network at ~119°C, when the equilibrium polymer network is essentially at its true gel point conversion. Although this temperature is slightly different than the F-S prediction, 119°C (81% conversion) is within the 95% confidence prediction interval for the temperature indicated by the van't Hoff plot fit at the F-S gel point conversion (125±8°C.) It has been shown[21] that thermal history can become an important factor in the final material properties of a Diels-Alder network where irreversible side reactions are present. This characteristic may account for some of the deviation observed between the W-C and F-S gelation criteria.

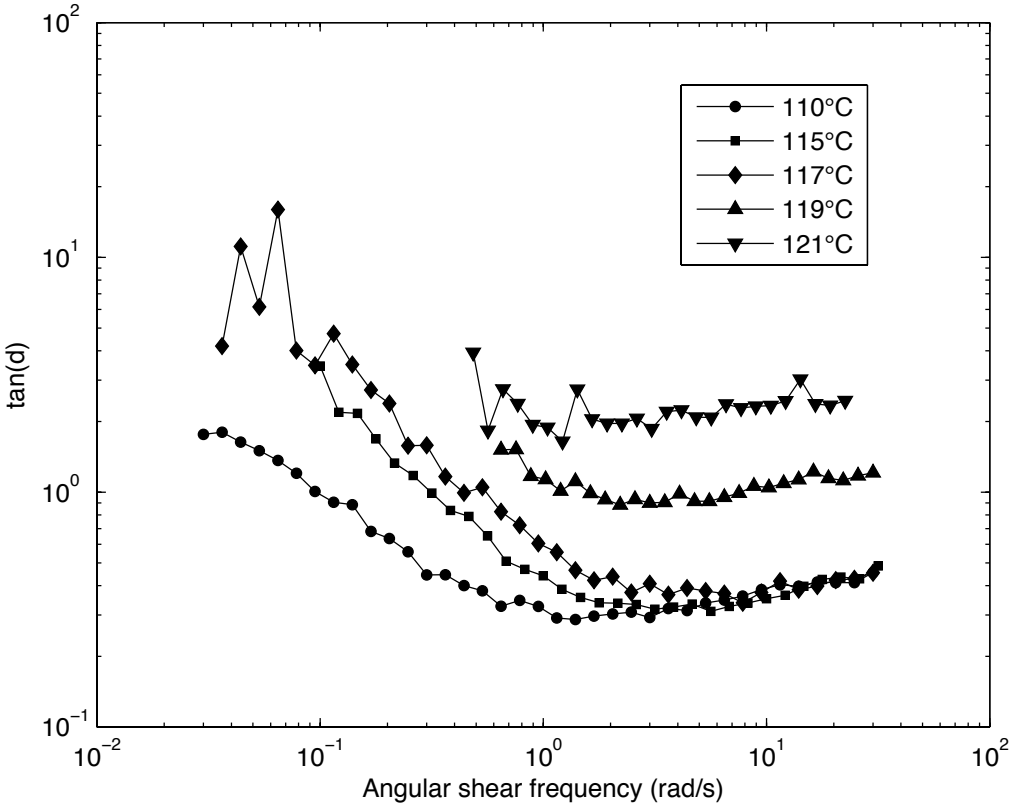

Figure 3.6: The loss tangent, tan(δ), of the Diels-Alder network as a function of frequency at temperatures near the gel point for Diels-Alder networks formed from SRF and DPBM in a 10:6 ratio of furan to maleimide functional groups.

The crossover frequency for the material was found to decrease substantially with decreasing temperature, which is consistent with the picture of elastically effective chains in the network breaking due to the retro-Diels–Alder reaction, as well as decreased crosslink density due to the temperature dependence of the equilibrium conversion of the Diels–Alder reaction. However, the crossover time is not directly related to the retro-Diels–Alder characteristic time, because the temperature dependence of the crossover time indicates an Arrhenius activation

energy of nearly 260 kJ/mol, whereas the rDA activation energy has been measured[10] at 88 kJ/mol.

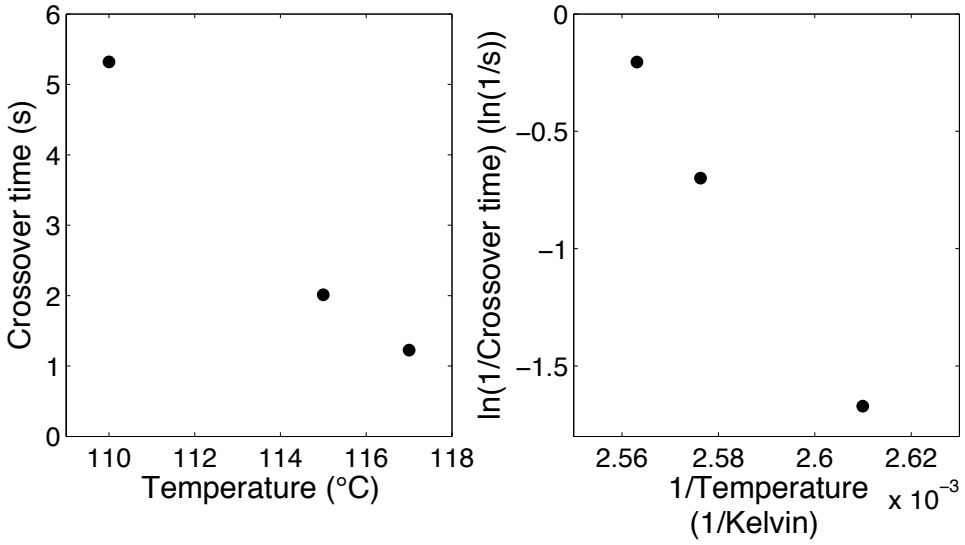

Figure 3.7: G* crossover time versus temperature, plotted (left) linearly and (right) as an Arrhenius plot.

In the low frequency limit of any viscoelastic liquid, tan(δ) must[22] scale as $G''/G' \sim \omega^1/\omega^2 = \omega^{-1}$; however, the tan(δ) for the Diels–Alder material at (e.g.) 115°C scales to the power of -0.8 below the crossover frequency. We take this value to mean that the clusters of connected monomers that exist throughout the experimental measurement at these low frequencies provide a frequency-dependent distribution of cluster relaxations well into the practical range of timescales that might be encountered in a real application of these materials.

Additionally, this loss tangent scaling at low frequency appears to continue upwards well above the crossover frequency into the solid regime, suggesting that the mechanism of the rearrangement of the gel over time is intimately connected to

the lifetime of the sol-like clusters that continue to exist beyond the crossover frequency, as may be expected from an understanding of the nature of the chemical bonds in the network. Interestingly, tan(δ) seems to reach a minimum and level out at a temperature dependent frequency. Estimating the characteristic time of this transition as the intersection of two least-squares power law fits, an activation energy for the tan(δ) transition of 48 kJ/mol can be calculated. Further study should reveal whether this relationship corresponds directly to the retro-Diels-Alder kinetics in a robust manner.

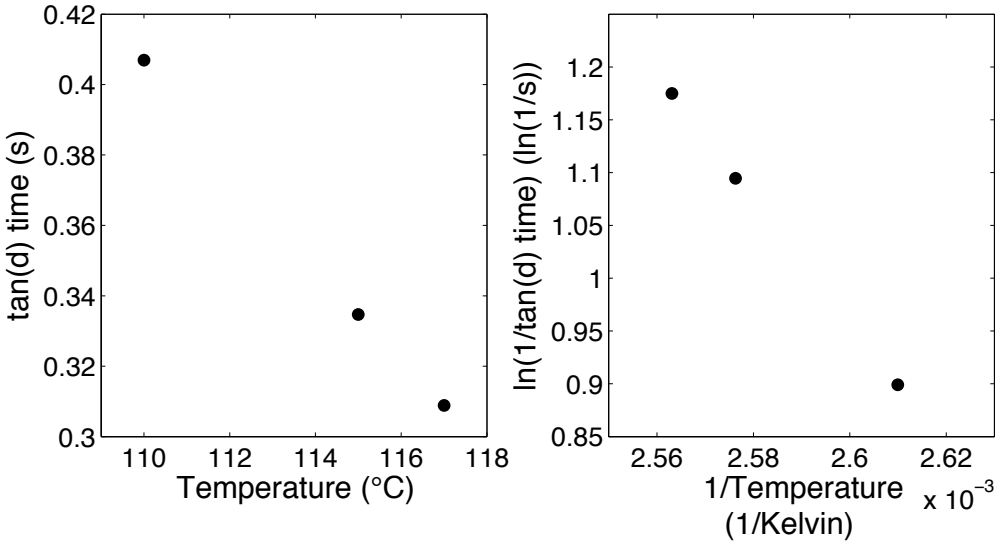

Figure 3.8: Loss tangent transition time versus temperature, plotted (left) linearly and (right) as an Arrhenius plot. The transition time is estimated by the intersection of the least-squares power law fits of the log-linear regions of the tan(δ) spectrum.

The crossover time and loss tangent minimum correspond qualitatively to features at the longest relaxation time τ_{max} and the G'' minimum time τ_2, respectively, in the work of Semenov and Rubinstein (S-R);[23] however, other features of G*(ω) have significant qualitative differences from their predictions.

Namely, the (S-R) theory predicts tan(δ) frequency scaling powers at higher and lower frequencies than the frequency of the tan(δ) transition to be 1 and -1, respectively, but our data fit scaling laws of approximately 0.25 and -0.8, respectively. Furthermore, G' never fully achieves a plateau modulus, instead trending upwards with significant slope over the entire experimental frequency range. Other predictions of the S-R theory (including whether the crossover time is indeed the longest relaxation time of the system, or whether the tan(δ) transition frequency is indeed the geometric mean of the crossover frequency and a higher frequency relaxation related to small sol clusters) are not possible to evaluate within the current experimental window, which is limited due to the unsuitability of time-temperature superposition for transient networks near the gel point.

One prediction that produces quantitative agreement between this work and the S-R theory is the relationship $\tau_{x} \sim \tau_{d} |\Delta|^{-1}$. This equation essentially states that the crossover time for a significantly post-gel transient network should be proportional to the product of the characteristic time of the transient bond and the distance (in terms of conversion) from the gel point, $\Delta = p - p_{gel}$. As with many properties associated with the distance from the gel point, the relationship is incredibly sensitive to the value of p_{gel}. By rearranging the relationship and assuming the activation energy of the retro-DA bond kinetics to be the same as previously reported[10], 88 kJ/mol, we can solve for the gel point conversion which satisfies the proportionality:

$$p_{gel} = p - \frac{\tau_{\max}}{C} e^{\frac{-E_a}{RT}} \tag{3.4}$$

Here, C is an unknown constant. Using another least squares fit to estimate C and p_{gel}, this method determines p_{gel} to be 80%, which corresponds to a gel temperature of 120.5°C, in excellent agreement with the gel point conversion range established by the F-S and W-C gel point criteria.

Conclusion

We have shown that, in a model transient network, a covalent network exists over short timescales at the conversions predicted by mean field polymerization theories. This result was indicated by the similar scaling of G' and G'', as well as the magnitude of tan(δ) and the two different frequency scaling regions apparent at each temperature beyond the gel point. Furthermore, we have demonstrated that the frequency range of the key features in the complex modulus responds strongly to temperature, even at conversions not immediately adjacent to the gel point. Finally, preliminary results indicate that the features of tan(δ) may be an effective indicator of kinetics and macromolecular structure; these relationships will be the subject of future research. The well-defined model covalent adaptable network described herein allows for direct comparison of the seminal works of Flory[24] and others[25] to the predictions of more recent works,[23, 26] and should provide insight towards the formulation of a more universal theory of transient network dynamics.

Experimental

Materials

1,1′-(Methylenedi-4,1-phenylene)bismaleimide (DPBM) (95%), triethylamine (99%), and furfuryl mercaptan (95%) were acquired from Sigma. Pentaerythritol tetraacrylate (SR295) was ordered from Sartomer. Solvents were purchased from Fisher Scientific. All reagents were used as received except furfuryl mercaptan, which was vacuum distilled to remove impurities.

Instrumentation

Rheometry was performed on a TA ARES Rheometer using a parallel plate geometry with a Peltier plate temperature controller and 18.9 cm poly(p-phenylene sulfide) (PPS) plate to minimize thermal gradients across the sample. Sample thickness was between 0.3 and 0.5 mm. Samples were mixed at room temperature, heated for 5 minutes at 160-170°C, and poured directly onto the Peltier plate, which had been pre-heated to 140°C. Samples were then pressed to an appropriate thickness and excess resin was cut from the edges with a razor blade. The samples were then brought to experimental temperature and allowed to remain in this state for 10 minutes to achieve thermal and chemical steady state behavior. Strain sweeps were performed on representative samples to ensure that frequency sweeps were performed in the linear viscoelastic regime.

Flexural dynamic mechanical analysis was performed in a TA Q800. Samples were prepared as for rheometry except the samples were instead placed into a silicone mold, allowed to cool overnight, and sanded to produce a 10.9x4.17x1.61 mm^3 rectangular prism sample.

FTIR Spectra were obtained with a Thermo-Nicolet Magna-IR 750 Series II spectrometer using a custom sample stage and temperature controller. Samples were prepared as described previously.[10]

Synthesis of multifuran monomer (SRF)

Furan-substituted monomers were produced by simple Michael addition reactions. A 100 mL round-bottom flask with a magnetic Teflon stir-bar was filled with 50 mL of methylene chloride. SR295 and furfuryl mercaptan were weighed out to 10% molar excess of mercaptan. The reagents were mixed in the flask and stirring was continued over an icewater bath. 1 wt % triethylamine was added to the chilled reaction vessel. The reaction was allowed to continue for 24 hours before a sample was taken to confirm complete reaction of the acrylate functional groups. Excess mercaptan and catalyst were removed under high vacuum at 60°C. Removal of triethylamine and furfuryl mercaptan was confirmed by ^{1}H NMR.

References

1. de Gennes, P. G., *Scaling concepts in polymer physics*. Cornell University Press: Ithaca, N.Y., 1979; p 324 p.
2. Wool, R. P.; O'Connor, K. M., A theory crack healing in polymers. *J Appl Phys* **1981,** *52* (10), 5953-5963.
3. Jud, K.; Kausch, H. H.; Williams, J. G., Fracture mechanics studies of crack healing and welding of polymers. *J Mater Sci* **1981,** *16* (1), 204-210-210.
4. Macht, M. L.; Rahm, W. E.; Paine, H. W., Injection Molding. *Industrial & Engineering Chemistry* **1941,** *33* (5), 563-567.
5. Olabisi, O., *Handbook of thermoplastics*. Marcel Dekker: New York, 1997; p xvi, 1053 p.
6. Winter, H.; Mours, M., Rheology of Polymers Near Liquid-Solid Transitions. In *Neutron Spin Echo Spectroscopy Viscoelasticity Rheology*, Springer Berlin / Heidelberg: 1997; Vol. 134, pp 165-234-234.
7. Cordier, P.; Tournilhac, F.; Soulie-Ziakovic, C.; Leibler, L., Self-healing and thermoreversible rubber from supramolecular assembly. *Nature* **2008,** *451* (7181), 977-80.

8. (a) Feldman, K. E.; Kade, M. J.; Meijer, E. W.; Hawker, C. J.; Kramer, E. J., Model Transient Networks from Strongly Hydrogen-Bonded Polymers. *Macromolecules* **2009,** *42* (22), 9072-9081; (b) Stadler, R., Transient networks by hydrogen bond interactions in polybutadiene-melts. In *Permanent and Transient Networks*, Springer Berlin / Heidelberg: 1987; Vol. 75, pp 140-145-145.
9. Brunsveld, L.; Folmer, B. J. B.; Meijer, E. W.; Sijbesma, R. P., Supramolecular Polymers. *Chemical Reviews* **2001,** *101* (12), 4071-4098.
10. Adzima, B. J.; Aguirre, H. A.; Kloxin, C. J.; Scott, T. F.; Bowman, C. N., Rheological and chemical analysis of reverse gelation in a covalently crosslinked Diels-Alder polymer network. *Macromolecules* **2008,** *41* (23), 9112-9117.
11. Kloxin, C. J.; Scott, T. F.; Adzima, B. J.; Bowman, C. N., Covalent Adaptable Networks (CANs): A Unique Paradigm in Cross-Linked Polymers. *Macromolecules* **2010,** *43* (6), 2643-2653.
12. (a) Park, H. Y.; Kloxin, C. J.; Scott, T. F.; Bowman, C. N., Stress Relaxation by Addition-Fragmentation Chain Transfer in Highly Cross-Linked Thiol-Yne Networks. *Macromolecules* **2010,** *43* (24), 10188-10190; (b) Kloxin, C. J.; Scott, T. F.; Bowman, C. N., Stress Relaxation via Addition-Fragmentation Chain Transfer in a Thiol-ene Photopolymerization. *Macromolecules* **2009,** *42* (7), 2551-2556.
13. Amamoto, Y.; Kikuchi, M.; Masunaga, H.; Sasaki, S.; Otsuka, H.; Takahara, A., Reorganizable Chemical Polymer Gels Based on Dynamic Covalent Exchange and Controlled Monomer Insertion. *Macromolecules* **2009,** *42* (22), 8733-8738.
14. Chen, X.; Dam, M. A.; Ono, K.; Mal, A.; Shen, H.; Nutt, S. R.; Sheran, K.; Wudl, F., A Thermally Re-mendable Cross-Linked Polymeric Material. *Science* **2002,** *295* (5560), 1698-1702.
15. Craven, J. M. Cross-linked Thermally Reversible Polymers Produced from Condensation Polymers with Pendant Furan Groups Cross-linked with Maleimides. 3435003, 1969.
16. Roberts, M. C.; Mahalingam, A.; Hanson, M. C.; Kiser, P. F., Chemorheology of Phenylboronate-Salicylhydroxamate Cross-Linked Hydrogel Networks with a Sulfonated Polymer Backbone. *Macromolecules* **2008,** *41* (22), 8832-8840.
17. Scott, T. F.; Draughon, R. B.; Bowman, C. N., Actuation in Crosslinked Polymers via Photoinduced Stress Relaxation. *Advanced Materials* **2006,** *18* (16), 2128-2132.
18. (a) Zhang, Y.; Broekhuis, A. A.; Picchioni, F., Thermally Self-Healing Polymeric Materials: The Next Step to Recycling Thermoset Polymers? *Macromolecules* **2009,** *42* (6), 1906-1912; (b) Chujo, Y.; Sada, K.; Saegusa, T., Reversible gelation of polyoxazoline by means of Diels-Alder reaction. *Macromolecules* **1990,** *23* (10), 2636-2641.
19. Goiti, E.; Huglin, M. B.; Rego, J. M., Some properties of networks produced by the Diels-Alder reaction between poly(styrene-co-furfuryl methacrylate) and bismaleimide. *European Polymer Journal* **2004,** *40* (2), 219-226.
20. Parker, S. F., Vibrational spectroscopy of N-phenylmaleimide. *Spectrochimica Acta Part A: Molecular and Biomolecular Spectroscopy* **2006,** *63* (3), 544-549.
21. Swanson, J. P.; Rozvadovsky, S.; Seppala, J. E.; Mackay, M. E.; Jensen, R. E.; Costanzo, P. J., Development of Polymeric Phase Change Materials On the basis of Diels-Alder Chemistry. *Macromolecules* **2010,** *43* (14), 6135-6141.

22. (a) Schetz, J. A.; Fuhs, A. E., *Fundamentals of fluid mechanics*. John Wiley: New York, 1999; p xvi, 935 p; (b) Ferry, J. D., *Viscoelastic properties of polymers*. 3rd ed. ed.; Wiley: New York, 1980; p 641.
23. Rubinstein, M.; Semenov, A. N., Thermoreversible Gelation in Solutions of Associating Polymers. 2. Linear Dynamics. *Macromolecules* **1998,** *31* (4), 1386-1397.
24. Flory, P. J., Fundamental Principles of Condensation Polymerization. *Chemical Reviews* **1946,** *39* (1), 137-197.
25. (a) Miller, D. R.; Macosko, C. W., A New Derivation of Post Gel Properties of Network Polymers. *Macromolecules* **1976,** *9* (2), 206-211; (b) Winter, H. H., Can the gel point of a cross-linking polymer be detected by the G′ – G″ crossover? *Polymer Engineering & Science* **1987,** *27* (22), 1698-1702.
26. (a) Semenov, A. N.; Rubinstein, M., Thermoreversible Gelation in Solutions of Associative Polymers. 1. Statics. *Macromolecules* **1998,** *31* (4), 1373-1385; (b) Tanaka, F., Theory of thermoreversible gelation. *Macromolecules* **1989,** *22* (4), 1988-1994.

Chapter 4: A simple relationship relating linear viscoelastic properties and chemical structure in a model Diels-Alder polymer network

Abstract

Although the gel point conversion of a thermoreversible polymer network is certainly a key parameter in determining the material properties, it is not a conventional liquid-solid transition as in common, irreversible networks. Rather, the material's viscosity is time-dependent and finite at the gel point and beyond, as bond breakage works in concert with diffusion to relax stresses imposed on the forming transient network of the material. For example, in a model Diels-Alder network with functionality 3.8 and a stoichiometric ratio of 10:6 furan:maleimide used here, a crossover frequency (0.52, 0.32, and 0.12 rad/s) was measured below the temperature corresponding to gelation (3, 5, and 10°C below, respectively.) In this work, we describe this complex process occurring in model thermoreversible networks with a simple relationship from the work of Semenov and Rubinstein on associative transient networks. This relationship provides a toolkit for the prediction of the important engineering and rheological properties of the material in the post-gel regime, such as viscosity, plateau modulus, and relaxation time, based upon the straightforward estimation of two material-dependent parameters, the gel point conversion p_{gel} and a proportionality constant C. We show key agreement between theory and experiment as the gel point conversion estimated from network dynamics matches the classical prediction of the gel point within 4% conversion. We discuss the applicability criteria of the Semenov-Rubinstein scaling relationship and

compare it to time-temperature superposition methods of describing transient network relaxation.

Introduction

Polymer networks composed of thermally reversible crosslinks – including non-covalent interactions such as hydrogen bonds[1] or pi stacking,[2] or reversible covalent reactions like the Diels-Alder,[3] boronate-diol,[4] and most recently transesterification[5] reactions – are becoming popular as mendable,[6] recyclable,[7] and smart[8] materials. The ability these various materials have to respond to an external stimulus such as exposure to light, changes in pH, or an increase in temperature with a change in material properties[8-9] makes them potentially valuable in many fields, from biomaterials to photolithography. As these materials are unified, at least in part, by common attributes of their chemical mechanism, a common structure-property relationship should be applicable to each of them.

The theoretical foundations for the behavior of "transient",[10] "thermoreversible",[11] "dynamic",[12] or "adaptable"[8] networks have been derived, most recently and completely by Semenov and Rubinstein.[13] Their theory of linear dynamics for associating polymers is suitable for many aspects and details specific to their associative network of interest; however, the derivation begins with classical polymer scaling theory that should also be widely applicable to most thermoreversible networks, as long as they can be approximated by mean-field assumptions. The crucial insight they provide is that by considering only "typical" (characteristic percolation cutoff size)[14] clusters and network chains and

"backbone"[15] transient bonds within those clusters (Figure 4.1), a scaling relationship between bond lifetime and relaxation in the sol and gel states near the gel point can be derived.

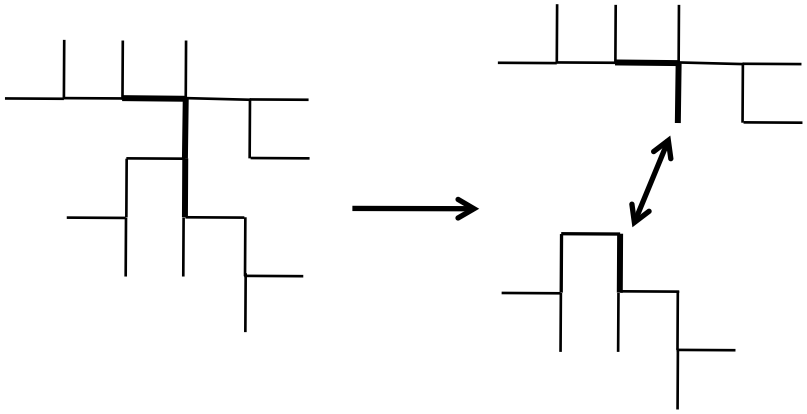

Figure 4.1: Visualization of transient cluster relaxation via backbone breakage. Bolded bonds represent critical connections which, when split, transform one transient cluster into two roughly equal parts.

$$\tau_l \propto \tau_b |\varepsilon| \tag{4.1}$$

In equation (4.1), the bond lifetime τ_b is the decay constant or the inverse of the kinetic rate constant for the thermoreversible links in the cluster, and τ_l is the rheological lifetime of the cluster as a whole. In their paper, Semenov and Rubinstein make the argument that the two timescales can be related through $\varepsilon = p - p_{gel}$, the distance from the Flory[16] gel point in terms of conversion, in the post-gel regime. If a thermoreversible network is considered as a generalized Maxwell material,[17] the longest relaxation time, τ_{max}, represents the transition timescale between viscoelastic and purely viscous behavior, and should correspond to τ_l. If we rewrite the scaling relationship as an explicit proportionality, with a material-dependent constant, C, we can algebraically rearrange it to obtain a simple equation

in terms of the most important material parameters: conversion (p), bond lifetime (τ_b), gel point conversion (p_{gel}), and the longest relaxation time in the network (τ_{max}).

$$p = C\frac{\tau_{max}}{\tau_b} + p_{gel} \tag{4.2}$$

In circumstances where a material is far above its gel point, and the lifetime of a bond is orders of magnitude longer than the time frame of interest, the viscoelastic spectrum is well predicted by classical crosslink calculations without consideration of the reversible bonds. To calculate elasticity based on conversion and the distribution of multifunctional monomers, we can employ the Miller and Macosko[18] recursive method, solving for the crosslink density, υ, numerically. This value may be converted into a "plateau" modulus via the relationship $G_p=\upsilon RT$, disregarding other potential contributions to the modulus as a first order approximation.[19] At lower temperatures, deviations would be seen as the glass transition begins to interfere with measurement of the purely rubbery behavior.[3]

Similarly, the main property of interest in the regime far away from the gel point, i.e., the viscosity, is not substantially determined by the bond breakage rate. Rather, the viscosity is largely determined by the properties of the unreacted monomers. Nearer to the gel point, a simple scaling exponent adequately[3] describes viscosity until very close to the gel point ($|p-p_{gel}| < \varepsilon_{min}$),[13b] where the largest molecular clusters are big enough that bond breakage begins to have an effect.

In this report, we aim to demonstrate the versatility of the Semenov-Rubinstein (SR) theory, particularly as expressed in equation (4.2), as an accurate

description for the viscoelastic behavior of thermoreversibly crosslinked materials, which represent an ever-increasingly important class of materials. This approach will use a chemically well-defined model Diels-Alder network to couple experiments with theory and demonstrate the validity of the theory for these materials.

Background

The Diels-Alder[20] cycloaddition reaction, often occurring between maleimide and furan functional groups (Scheme 4.1), has become a common feature of the thermoreversible networks literature, thanks to its relatively ideal and orthogonal character as an addition reaction. Polymers featuring the Diels-Alder reaction are fairly old, with a patent by Craven[21] appearing in 1969. However, thanks to work done by Wudl's group,[6] the field has seen a revitalization, with many different groups demonstrating different polymer architectures and Diels-Alder pairs.[3, 12, 22]

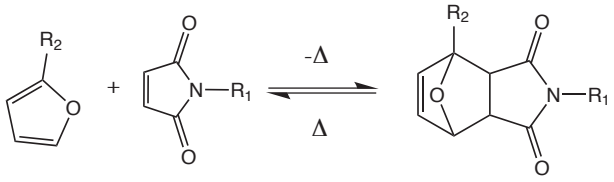

Scheme 4.1: Diels-Alder reaction between maleimide and furan. The [4+2] tricyclic adduct structure on the right generally forms at high yield at ambient temperature. At increased temperature, the adduct reversibly decouples to reform the reactant species at a rate and quantity which is determined by standard chemical equilibrium and kinetics.

Arising from an exothermic thermoreversible reaction, the equilibrium conversion of Diels-Alder functional groups is a strong function of temperature (equation 4.3). At low temperatures, the equilibrium is shifted towards the adduct state, while at elevated temperatures adducts tend to break apart into the original

furan and maleimide moieties. Multifunctional furan and maleimide monomers have been used in a number[21-22, 23] of applications to form thermoreversibly crosslinked polymers. This reaction generally follows standard chemical equilibrium behavior as in equation 4.3, which has previously been reported.[3, 24]

$$K_C(T) = \frac{x}{[L]_0(1-x)(r^{-1}-x)} = e^{\left(-\frac{\Delta H^\circ - T\Delta S^\circ}{RT}\right)} \quad (4.3)$$

Here, x is the conversion of a limiting reagent, $[L]_0$ is the initial concentration of that limiting reagent, r is the ratio of limiting to excess reagent, ΔH^0 is the heat of reaction and ΔS^0 is the entropy of the reaction. This approach describes the equilibrium constant K_C as a function of absolute temperature T with the appropriate ideal gas constant R.

For this work we use a commercially available bismaleimide and a low molecular weight, but flexible multifuran crosslinker (schemes 4.2 and 4.3). We synthesize the multifuran via the Michael addition of furfuryl mercaptan to a simple commercial tetra-acrylate, presenting several helpful features. The synthesis is straightforward and scalable, and requires only limited equipment and knowledge to perform. By limiting the reaction with a less-than-stoichiometric amount of furfuryl mercaptan, reduced functionality analogues can be produced simply by eliminating residual acrylate groups in a second Michael addition step, using a thiol inert to the Diels-Alder reaction, such as octanethiol.

The crosslink density is high enough in the fully functionalized case to form a glassy polymer at ambient temperature;[24] however, its functionality is low enough that a modest inequality of stoichiometry (in our case r=0.36 to 0.5) is sufficient to

prevent gelation, even at the equilibrium conversion of the limiting reactant at all temperatures studied. By combining the effects of these two capabilities for controlling the system, a gel point conversion and its corresponding gel temperature can be targeted during the formulation step, without any additional synthesis. We took advantage of this effect to test the Semenov and Rubinstein theory with analogous materials, but at several different conditions.

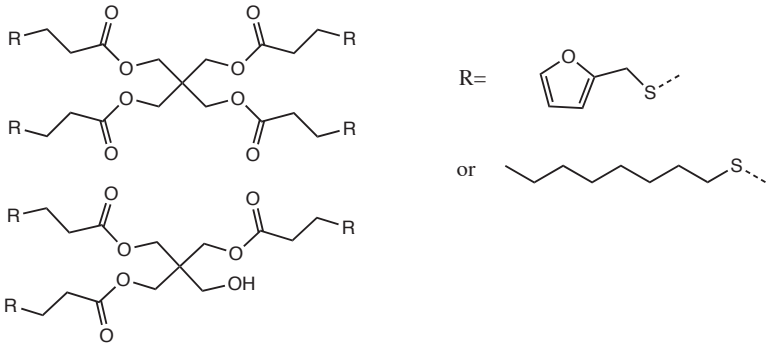

Scheme 4.2: Multifuran monomer SRF used in this study, a pentaerythritol tri-/tetraacrylate (SR295) substituted via Michael addition with furfuryl mercaptan and octanethiol. Functionality is adjusted by varying the ratio of furan to octane moieties in the reaction step. These compositions are distinguished by displaying the resultant effective functionality in parentheses, e.g. SRF(3.0).

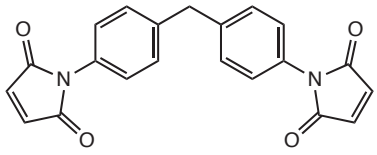

Scheme 4.3: Bismaleimide monomer DPBM used in this study (1,1′-(methylenedi-4,1-phenylene) bismaleimide). Whenever a composition's stoichiometric ratio is indicated, as in SRF(3.8) r=0.6, the ratio indicates the amount of maleimide used, as a fraction of the furan moieties used.

Experimental and Theoretical Methods

Synthesis of monomers

DPBM (1,1′-(methylenedi-4,1-phenylene) bismaleimide), triethylamine, furfuryl mercaptan and octanethiol were purchased from Sigma-Aldrich. SR295 was received from Sartomer. Dichloromethane supplied by Fisher was used as solvent.

SRF(3.8) was synthesized as reported previously.[24] Briefly, SR295 and 5% molar excess of freshly distilled furfuryl mercaptan were mixed with an equal volume of dichloromethane. This solution was stirred chilled in an ice bath, and 1 wt% triethylamine was added to catalyze the Michael addition. After 24 hours, the reaction was complete as verified by proton NMR. Excess furfuryl mercaptan and triethylamine were removed under high vacuum.

SRF(3.0) was synthesized as described above, but using 70% of the stoichiometric amount of furfuryl mercaptan, substituting ~35% octanethiol. Furfuryl mercaptan reacts much faster, as it has a lower pK_A, and no excess furfuryl mercaptan peaks were seen in proton NMR upon reaction completion, so the monomer is therefore a 30% octanethiol-substituted version of SRF(3.8).

Fourier transform infrared spectroscopy

Infrared spectra were collected on a Thermo-Nicolet Magna-IR 750 Series II instrument with a custom sample stage and temperature controller combination. Sample preparation is described in a previous publication.[3]

Rheometry

A TA ARES rheometer measured the complex modulus of the materials in this study, using a poly(p-phenylene sulfide) (PPS) 18.7 mm plate geometry with a Peltier temperature controller to minimize thermal gradients across the sample. Sample thickness was between 0.35 and 0.45 mm. Monomers were mixed at ambient temperature, heated for 4 minutes at 170°C, and poured onto the Peltier plate, which had been pre-heated to 130°C. The samples were then brought to experimental temperature and allowed to remain in this state for 15 minutes to achieve a steady thermal and chemical state. Strain sweeps were performed on representative samples to ensure that frequency sweeps were linear.

Crosslink density

The calculation of crosslink density for use in determining the theoretical plateau modulus $G_{p,theor}$ is included as supporting information.

Results and Discussion

In our experimental design, we chose compositions at representative points within the functionality/stoichiometry parameter space (See Table 4.1.) The maximum effective functionality (f_e) of 3.8 is achieved in the fully functionalized multifuran SRF(3.8) (which is a mixture of tri- and tetrafunctional molecules in a ratio of 0.2:0.8), whereas the lowest effective functionality monomer SRF(3.0) is achieved when 70% of the acrylates are reacted with furfuryl mercaptan. SRF(3.5) results when the SRF(3.8) and SRF(3.0) are mixed in equal parts by weight and the functionality of the mixture is back-calculated. (See supporting information for

details of the calculation.) Stoichiometric ratios of e.g. 6:10 maleimide:furan (r=0.6) were chosen as intermediate values that would cause a significant change in the gel point conversion and crosslink density while ensuring the ability to reach gelation with all SRF monomer mixtures in the temperature range of interest. Furthermore, the use of maleimide as the limiting reagent in the Diels-Alder reaction served to limit the amount of potential high-temperature side reactions that involve the maleimide's highly electron deficient double bond.[25] Notably absent are the "obvious" choices of the on-stoichiometry, fully-functionalized and the far-off-stoichiometry, partially-functionalized systems. These systems had important measurables, such as gel point conversion or low-temperature modulus crossover frequency, outside the operating limits needed for accurate assessment of the material behavior.

Table 4.1: Compositions and their properties

Composition name	SRF(3.8) r=0.6	SRF(3.0) r=1.0	SRF(3.0) r=0.78	SRF(3.5) r=0.91	SRF(3.5) r=0.6
Furan excess	167%	100%	128%	110%	167%
Gel point as predicted by Equation 4.5	77%	71%	80%	67%	82%
Gel point as predicted by Figure 4.6	81%	72%	81%	67%	86%

Furan excess is the amount of furan moieties available to react, as a percentage of maleimide groups present. It can be calculated via 100/r, where r is the ratio of the concentration of limiting moieties to excess moieties, because furan is always in excess in these studies.

Thermochemistry

To make use of the relationship in Equation 4.2, it is clear that equilibrium, kinetic, and structural parameters of the monomers must be combined with mechanical measurements of the polymer mixture. Estimates for the heat and

entropy of reaction, as well as Arrhenius activation energy and kinetic prefactors for forward and reverse rate constants, of the Diels-Alder reaction are available in the literature. However, for the sake of internal consistency and because of variability associated with the specific functionalization and molecular environment, we re-estimated the parameters for these specific chemical systems by evaluating temperature-dependent FTIR data for the equilibrium and time-dependent concentrations of the reactants. The maleimide ring-stretching peak at 690 cm^{-1} served as the most reliable source of conversion data. A nonlinear least-squares fit of the concentration data ([M], $[M]_0$, $[F]_0=[M]_0/r$, $[A]=[M]_0-[M]$) to a kinetic model

$$-\frac{d[A]}{dt}=\frac{d[F]}{dt}=\frac{d[M]}{dt}=k_r[A]-k_f[M][F] \qquad (4.4)$$

was used to estimate the forward and reverse rate constants k_f and k_r corresponding to each measurement, which also allowed for the calculation of the equilibrium constant K_C. A representative fit is presented in Figure 4.2.

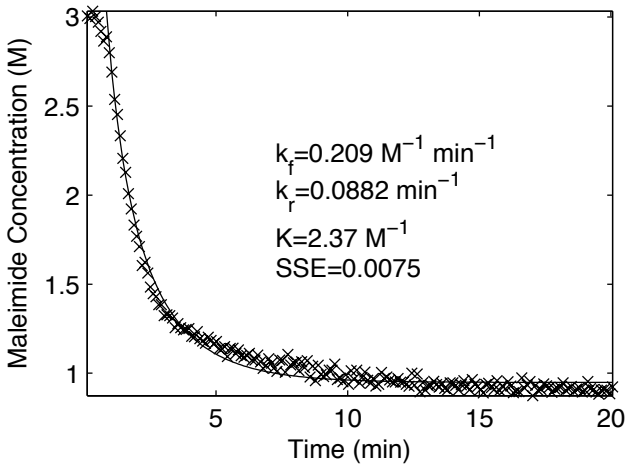

Figure 4.2: Example kinetic parameters for SRF(3.5) r=0.91 at 100°C. The parameters were obtained via nonlinear least-squares fit (solid line) to the FTIR

concentration data (x markers) obtained from measurements of the maleimide peak found at 690 cm^{-1}.

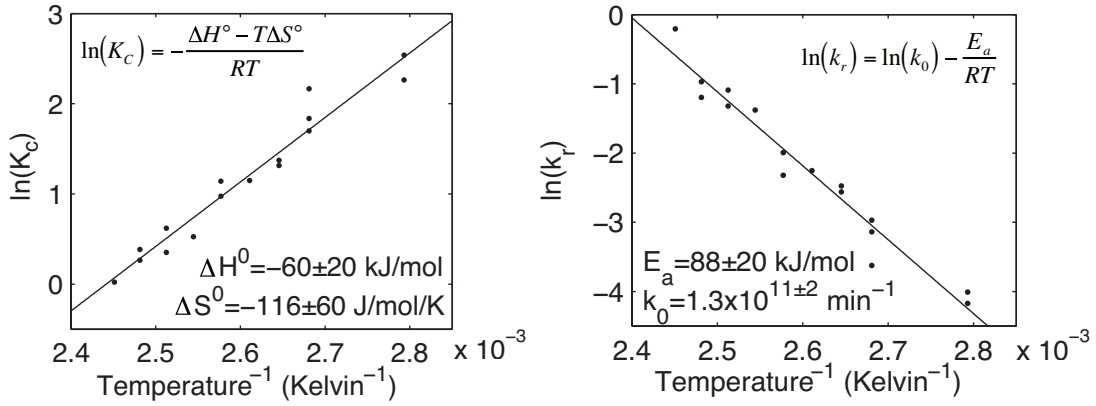

Figure 4.3: Van't Hoff and Arrhenius plots for a variety of SRF systems. ΔH^0=-60±20 kJ/mol, ΔS^0=-116±60 J/mol/K, E_a=88±20 kJ/mol, k_0=1.3x10$^{11\pm2}$ min^{-1}. Wide parameter confidence intervals were due to the relatively narrow experimental temperature range, resulting in high parameter covariance.

The main outcome of this FTIR analysis was an equilibrium temperature-conversion relationship $p(T)$ and a temperature-lifetime relationship $\tau_b(T)$=1/k_r for the Diels-Alder adducts. These parameters were consistent among the various compositions and agreed with literature values. This information allows us to rewrite (4.2) as

$$p(T) = C\frac{\tau_{max}}{\tau_b(T)} + p_{gel} \qquad (4.5)$$

leaving only the measurement of the longest relaxation time as a function of temperature before the gel point, p_{gel}, and the material-dependent proportionality constant, C, to be estimated.

Dynamic Mechanical Analysis

The viscoelastic spectra of our model networks have a number of important features predicted by SR theory that arise within this experimental window. As an example, the complex shear modulus of SRF(3.8) r=0.6 measured at 115°C is shown

in Figure 4.4, with those features marked. $G_{p,theor}=\upsilon RT$ and is the theoretical plateau modulus expected from an equivalent irreversible phantom network with crosslink density υ or, equivalently, the instantaneous number of network chains in the material, calculated according to Miller and Macosko.[18] (Description of the approach to this calculation can be found in the supporting information.) We chose the crossover frequency, ω_x, as our estimate of the longest relaxation time, τ_{max}, when converted to a characteristic timescale via the relationship $\tau_{max}=2\pi/\omega_x$. This assumption is most accurate when the crossover occurs at the maximum of a distinct final G'' peak, which is valid for our systems in the regime of interest. SR theory expects G' to scale as ω^0 over the region $2\pi/\tau_{max}$ to $2\pi/\tau_{relax}$ (the characteristic timescale of network chain and sol cluster relaxations) at the level of $G_{p,theor}$. As G' crosses over $G_{p,theor}$ in this range, the level of the complex modulus is in agreement with theoretical expectations. Likewise, G'' should scale as ω^{-1} and ω^1 over the same frequency range, with a minimum occurring at $2\pi/\tau_2$. Because τ_2 is the geometric mean of τ_{max} and τ_{relax}, and since τ_{relax} does not have a distinctive transition feature, we estimated the chain relaxation frequency as ω_2^2/ω_x and indicated it on Figure 4.4 with a dashed line. Qualitatively, then, this frequency sweep paints a picture of (from right to left) a material that settles into its network-constrained configuration in response to stress on the order of 0.3 seconds. The material exhibits a relatively elastic response to deformations persisting as long as 3-6 seconds; however, it relaxes any longer-lasting stresses as network chains disconnect and rearrange due to the retro-Diels-Alder reaction.

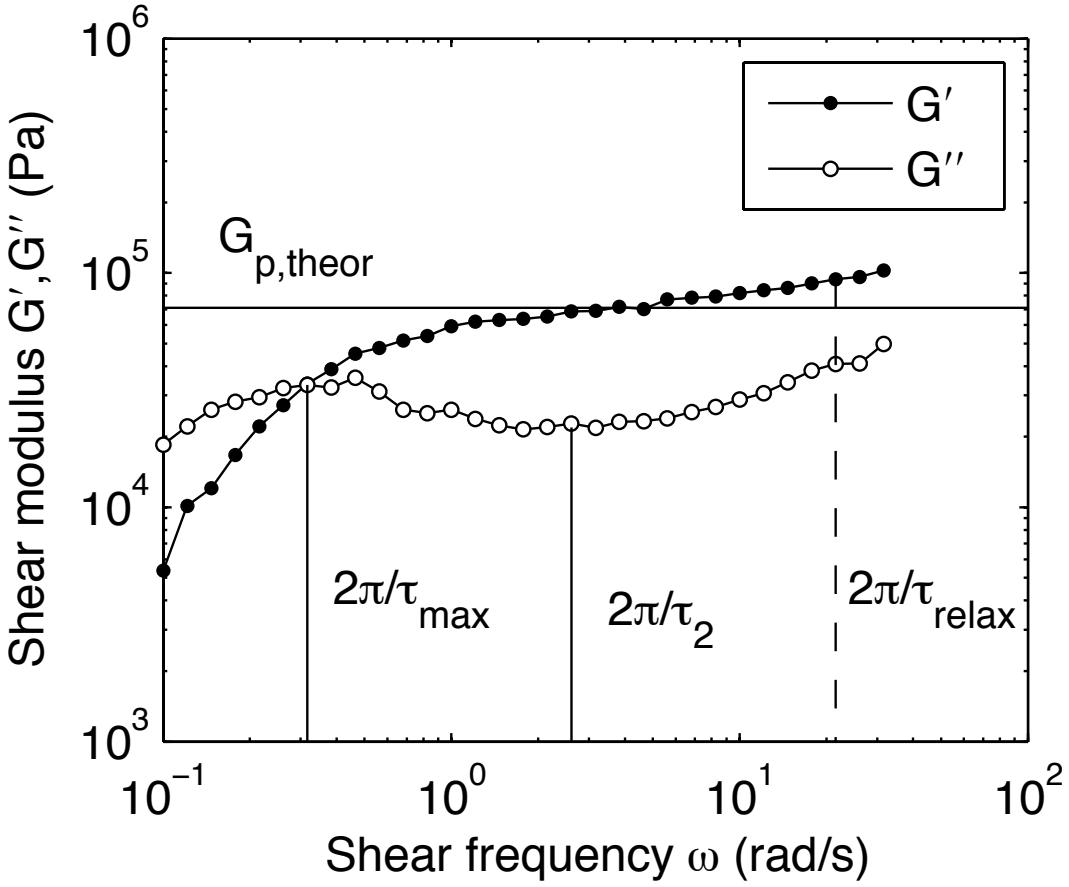

Figure 4.4: Shear modulus of SRF(3.8) r=0.6 at 115°C. $G_{p,theor}$ is the modulus corresponding to a crosslink density calculated from classical gelation theory. The crossover, G'' local minimum, and cluster relaxation frequencies (vertical solid and dashed lines) are marked as $2\pi/\tau_{max}$, $2\pi/\tau_2$, and $2\pi/\tau_{relax}$, respectively. These features are in agreement with SR theory predictions.

Figure 4.5 shows additional complex modulus curves of the SRF(3.8) r=0.6 composition, measured at two additional temperatures. The crossover frequency shifts left as temperature decreases, or equivalently as equilibrium conversion increases. As we discussed in an earlier[24] report, the apparent activation energy of this process (~260 kJ/mol according to the data of Figure 4.5) is much higher than can be explained simply by the Diels-Alder kinetics alone.

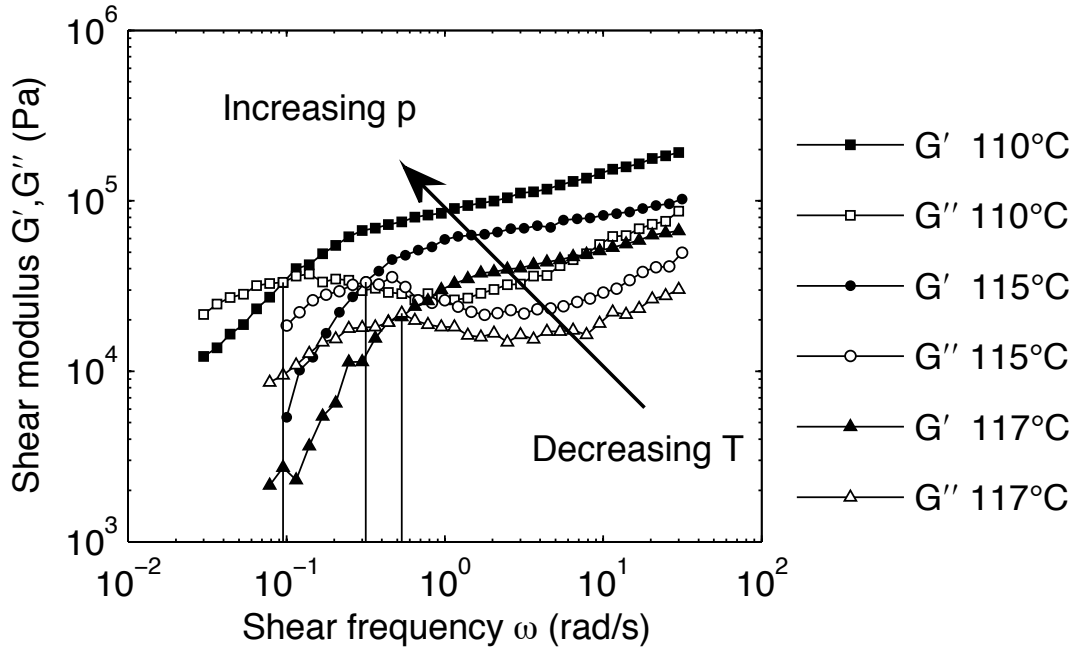

Figure 4.5: Shear modulus of SRF(3.8) r=0.6 at 110°C, 115°C, and 117°C. The crossover point (vertical solid lines) shifts up and to the left as a temperature decreases, or equivalently, as the equilibrium conversion increases.

According to the SR theory (equation 4.5), a plot of the ratio of the longest relaxation time to the adduct lifetime as a function of conversion should result in a straight line, if the material is beyond its Flory gel point conversion for an $A_n+A_{n-1}+...+A_1+B_2$ step-growth polymerization.

$$p_{gel} = \frac{1}{\sqrt{r(f_e - 1)}} \tag{4.6}$$

Figure 4.6 demonstrates that our experiments with several compositions are consistent with this expectation. An additional implication of these plots is that the rate of crosslink dissociation will be about 20X the retro-Diels-Alder rate at a distance from the gel point ε≈3%, but drops to 10X at ε≈5% in these compositions.

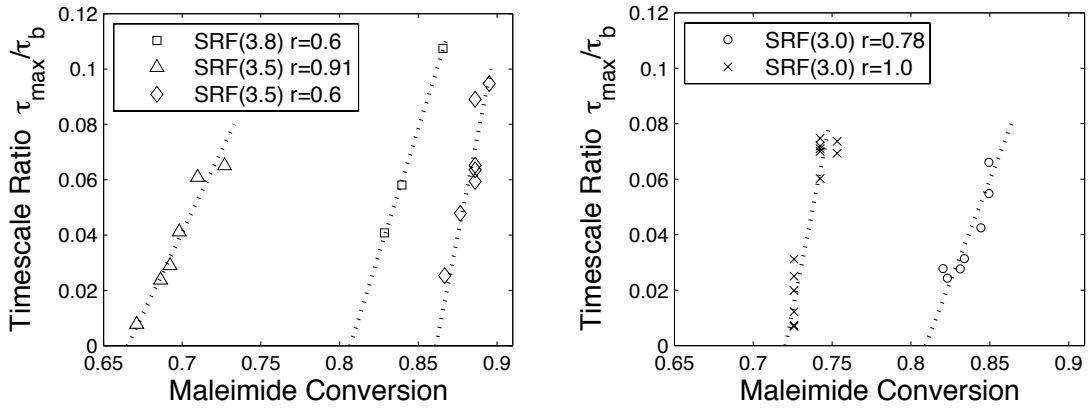

Figure 4.6: The timescale ratio τ_{max}/τ_b versus conversion, showing linear dependence on conversion beyond the gel point for various compositions. Data for τ_{max} was collected via dynamic mechanical analysis, while maleimide conversion and τ_b were calculated from the experimental temperature using the van't Hoff and Arrhenius relationships with the thermochemical parameters calculated in Figure 4.3. In fact, at any given temperature or conditions, τ_b is simply the reciprocal of the retro-Diels-Alder rate constant k_r. Comparisons of fitted intercepts to expected gel points are presented in Table 4.1.

Applicability

Although the relationship described by equation 4.2 is simple, a number of material parameters must be known before its predictive capacity becomes useful. The activation energy and (to an extent) the kinetic prefactor for the reversible bond are vital information that must be known. Attempts to estimate the retro-Diels-Alder activation energy based solely on G* and distance from the gel point showed that the estimate is highly sensitive to small errors in the gel point. A temperature-conversion relationship is required to estimate the gel point unless conversion can be measured *in situ* in the application in question. Alternatively, the analysis can be framed in terms of "temperature distance" from the "gel temperature" at equilibrium, with the assumption that change in conversion is linear with

temperature over the narrow temperature range of interest. This assumption is typically valid for the materials and conditions of this study and many others, as shown in Figure 4.7.

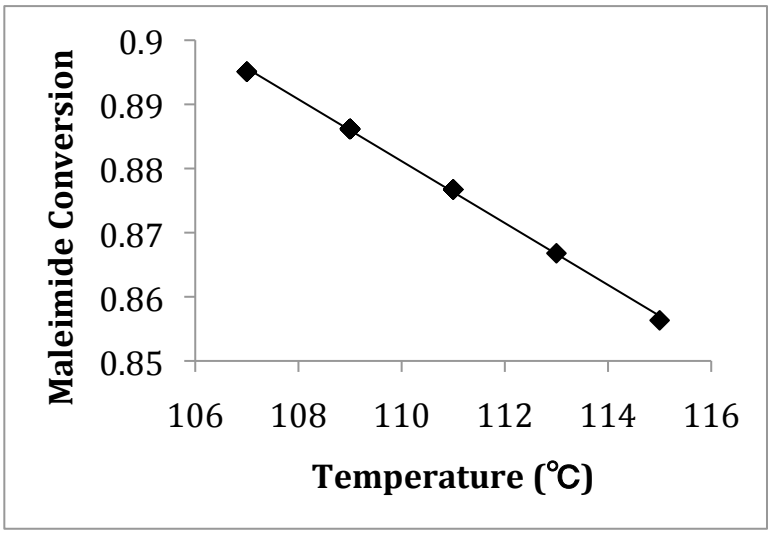

Figure 4.7: Theoretical conversion versus temperature for SRF(3.5) r=0.6 compositions in the temperature range of interest. The line is a linear fit. Although curvature in the points is apparent, the deviations from a local linear approximation are negligible.

Equation 4.2 can also be used to estimate the gel point for thermoreversible materials where the exact value is unknown, and without having to target the precise conditions of gelation. By the same token, the true effective functionality of a mixture can be calculated via the estimation of the gel point, without requiring exact knowledge of the molecular structure. Once Equation 4.2 has been used, the estimate of p_{gel} can be converted into effective functionality via the inverse of (4.6):

$$f_e = \frac{1}{rp_{gel}^2} + 1 \tag{4.7}$$

which in the case of an $A_n+A_{n-1}+\ldots+A_1+B_2$ step-growth polymerization is the effective functionality of the A components in aggregate. This approach allows structural

information to be determined from empirical dynamic mechanical tests and published thermodynamic and kinetic parameters as in Figure 4.8.

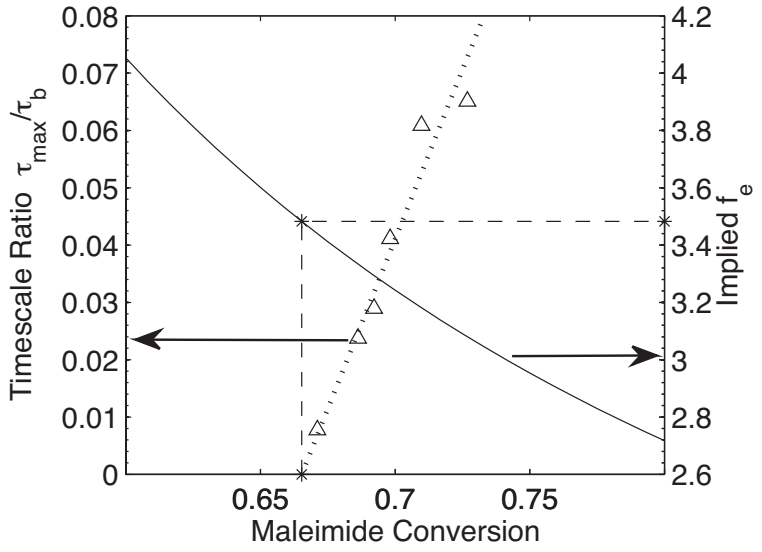

Figure 4.8: Determination of effective functionality from the intercept (implied gel point) of a timescale ratio versus conversion plot of the SRF(3.5) r=0.91 composition. By inverting the Flory-Stockmayer equation (solid line), the intercept of the linear fit (dotted line) of the data (triangles), which represents the gel point conversion, can be used to calculate (dashed lines) the overall effective functionality f_e of an unknown $A_n+A_{n-1}+...+A_1+B_2$ mixture.

Even given good estimates of p(T) and $k_r(T)$, the longest relaxation time is not a typically accessible parameter in many situations where temperature dependent properties are crucial information. To convert the relationship into a more widely applicable form, it is possible to use the relationship

$$\eta'(\omega) = G''(\omega)/\omega \tag{4.8}$$

and the assumption that the material behaves according to a generalized Maxwell model to rewrite it in terms of the steady shear viscosity and crosslink density. If the plateau modulus grows according to an appropriate scaling law $G' \sim |\varepsilon|^t$, and the

viscosity at the temperature of interest can be measured, then in the first order approximation the longest relaxation time can be written as:

$$\tau_{max} \propto \frac{T\eta_0}{|\varepsilon|^t} \tag{4.9}$$

where the absolute temperature factor normalizes the temperature dependence of rubbery elasticity. The scaling exponent t has a value of 3 according to classical theory, but may be measured for an individual system. Equation 4.2 can therefore be rewritten without any mention of characteristic times as:

$$p = C\frac{\eta_0 T}{|\varepsilon|^t} k_0 \exp\left(-\frac{E_a}{RT}\right) + p_{gel} \tag{4.10}$$

Equation 4.10 can be rearranged to produce an expression for the viscosity of the material as a function of temperature, or an even simpler expression proportional to the reverse rate constant and the distance from the gel point, as shown in equation 4.11. Note that this equation does not imply zero viscosity at the gel point, as this development only applies after a minimum distance ε_{min} beyond the gel point where breakage of network chains is the dominant relaxation mechanism.[13b]

$$\eta_0 = \frac{|\varepsilon||\varepsilon|^t}{CTk_0 \exp\left(-E_a/RT\right)} \propto \frac{\varepsilon^{t+1}}{Tk_r} \tag{4.11}$$

Relationship to time-temperature superposition

Time-temperature superposition is a staple tool of understanding the temperature dependence of properties in polymer science. Some groups[26] have used this empirical process with success on materials where bond dynamics and conversion are not strong functions of temperature, or when the crossover frequency is out of the range of measurement. Clearly, if the reversible bond is thermally responsive

within the temperature range considered, the result of conventional time-temperature superpositions will be skewed. Another superposition principle commonly used in the literature is to normalize the frequency by the crosslink reverse rate constant, as developed by Yount *et al.*[26a] This principle has been shown[1, 4, 27] to be effective in the treatment of many systems from hydrogen-bonded networks to boronate-diol systems. However, these systems are typically highly functionalized or very far from their gel point in the range of conditions studied. Several of our systems that are closer to the gel point show good overlap at the crossover frequency; however, superposition is unable to account for the G* features measured at higher frequencies. Figure 4.9 shows how G' and G'' curves shifted to match at the crossover fail to overlap at the upper range of the frequency sweeps in our materials. Indeed, the G'' curves from 2 to 100 rad/s had better overlap before the shift. This result can be interpreted as evidence that the mechanisms governing τ_{max} and τ_{relax}, namely cutoff cluster backbone breakage and small cluster diffusion, have distinct temperature dependencies. Thus, it is clear that the use of the superposition concept is inappropriate for networks with temperature dependent chemical structure.

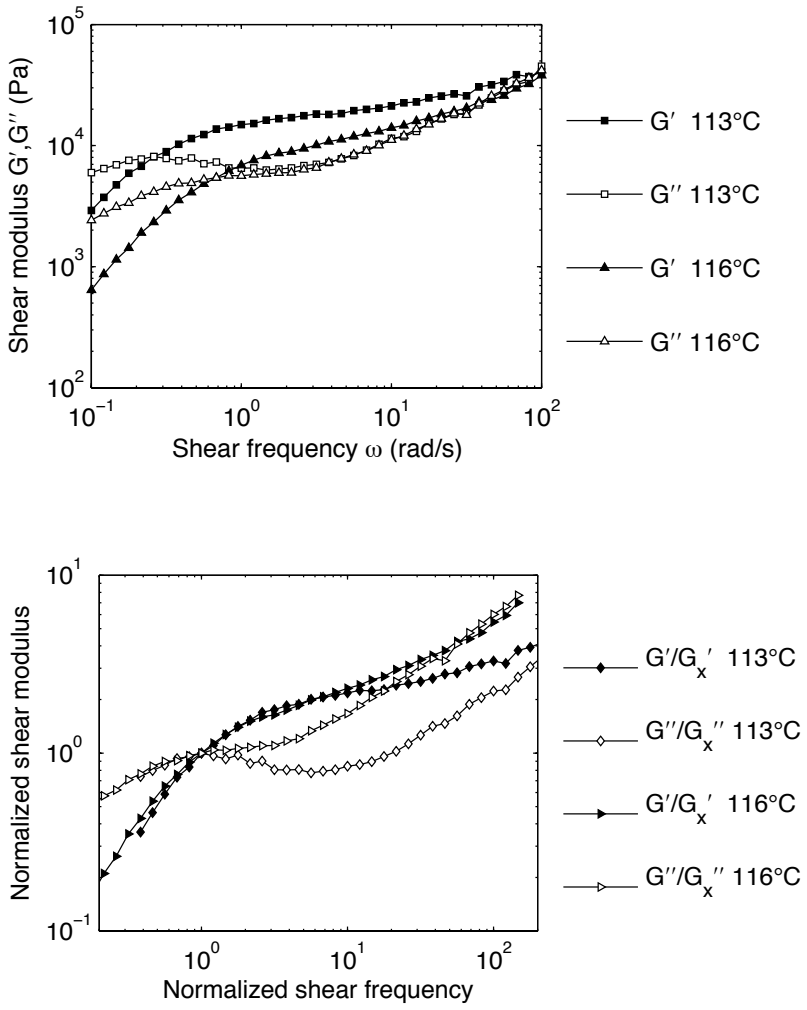

Figure 4.9. Results of attempting time-temperature superposition SRF(3.5)/DPBM model thermoreversible materials. (Top) The raw data for the material at 113°C and 116°C. (Bottom) The data are normalized to the crossover point. Low frequency behavior shows good overlap, but the high frequency behavior (of G'' especially) overlaps much better without the shift. Curves are representative of similar comparisons for multiple compositions.

Conclusion

Semenov and Rubinstein's theory of linear dynamics for reversible networks provides an appropriate description of the behavior of this model thermoreversible Diels-Alder network in a variety of situations near the gel point. Due to the simplicity of the model system, this confirmation leads us to expect that the simple

scaling relationship used here has wide applicability to reversibly bonded polymer networks, whether covalent or non-covalent. By simple measurement of the crossover time at one or two points, parameters can be obtained that enable calculation of the important material properties over a wide range of temperature, conversion, and bond breakage rate values. Furthermore, the ratio of timescales can be rewritten in terms of more accessible measurables, providing a useful qualitative description of the behavior of gelling thermoreversible materials for applications lacking sophisticated rheological equipment.

Although other groups have had success with less fundamental approaches to the description of thermoreversible network viscoelasticity, it appears that these approaches are functionally subsets of the predictions provided by equation 4.2. We believe that this further demonstrates its value as a more flexible tool for predicting the properties of transient covalent (or physical) networks in their most characteristic regime. It represents a valuable tool in the structure-property toolkit for this class of materials, filling in the gap between the limiting cases where the classic tools – crosslink density calculations, small molecule viscosity measurements, and scaling exponents – apply.

Supplemental

Miller & Macosko crosslink density

The crosslink density υ of a classical, Bethe-lattice, $A_n+A_{n-1}+\ldots+A_1+B_2$ step-growth polymer network can be calculated according to the equation

$$\upsilon = \sum_{i=3}^{f_{\max}} \frac{i-2}{2} \left[X_i \right]$$

where $[X_i]$ is the concentration of multifunctional monomers connected to the network i individual ways. The equation represents the (i-2)/2 weighted sum of all network junctions i>3. $[X_i]$ can be calculated according to the equation

$$\left[X_i \right] = \sum_{f=i}^{f_{\max}} \left[A_f \right]_0 \mathrm{P}\left(X_{i,f} \right)$$

Which simply sums the contributions of i junctions from each crosslinking, A-bearing molecular species. In this equation $[A_f]_0$ is the initial concentration of these species (molecules bearing f A moieties) and $P(X_{i,f})$ is the probability of an A_f molecule being joined to the network i times. The calculation of $P(X_{i,f})$ is straightforward given the quantity $P(F_A^{out})$, the probability that a given moiety on a crosslinker leads to a finite chain:

$$\mathrm{P}\left(X_{i,f} \right) = \binom{f}{i} \mathrm{P}\left(F_A^{out} \right)^{f-i} \left[1 - \mathrm{P}\left(F_A^{out} \right) \right]^i$$

which is the product of the relevant probabilities that i of f chains will lead to the network and the rest don't, appropriately weighted by the "n choose k" binomial coefficient function (in this case, "f choose i").

The calculation of $P(F_A^{out})$ requires a somewhat deeper conceptual leap, which is perfectly well explained in the original 1976 text of Miller and Macosko.

However, the rote calculation of it is a one-line equation of the form x=g(x), and is readily solved numerically:

$$\mathrm{P}\left(F_A^{out}\right) = p_A \sum\nolimits_j b_j \left[1 - p_B + p_B \sum\nolimits_i a_i \mathrm{P}\left(F_A^{out}\right)^{i-1}\right]^{j-1} - p_A + 1$$

In this equation, p_A is the conversion of A reactive groups, p_B is the conversion of B, and a_i and b_j are the mole fractions of A and B functional groups on i and j functional monomers, respectively.

Calculation of important quantities from crosslink mole fractions

The above method requires three material-specific vectors to describe the system, **a**, **b**, and [**A**]. Unfortunately, the general calculation of these arrays is non-trivial for our model system. A good intermediate array to calculate is the crosslinker mole-fraction arrays $\mathbf{x_A}$ and $\mathbf{x_B}$, which contain the mole fraction on a molecular basis of the various monomers present, sorted by functionality. For example, an $A_n+A_{n-1}+ \ldots +A_1+A_0$ mixture might be described as:

$$\mathbf{x_A} = \begin{bmatrix} 0 & 0 & 0 & 0.2 & 0.8 \end{bmatrix}$$

if 20% of the monomers are trifunctional and 80% are tetrafunctional. It is useful to start the index of the array at 0. For B_2 only mixtures, obviously

$$\mathbf{x_B} = \begin{bmatrix} 0 & 0 & 1 & 0 & 0 \end{bmatrix}$$

From this array, the calculation of **a** or **b** is straightforward, by weighting the components of $\mathbf{x_A}$ against the functionality each component represents:

$$a_i = ix_{A,i} \quad b_j = jx_{B,j}$$

These matrices are also usable in the direct calculation of functionality-weighted average functionality (effective functionality, f_e) via

$$f_{e,A} = \frac{\sum_i ia_i}{\sum_i a_i}$$

Crosslinker mole fraction vectors should be normalized to a magnitude of 1, by definition. However, by incorporating information about the stochiometric ratio r of functional groups, assuming [B] is limiting, we can form the vectors $\mathbf{y_A}$ and $\mathbf{y_B}$,

$$\mathbf{y_A} = \frac{1+r}{r}\frac{\mathbf{x_A}}{\sum_i a_i} \quad \mathbf{y}_B = \frac{r}{1+r}\frac{\mathbf{x_B}}{\sum_j b_j}$$

which have the useful property that, they can be combined with an average molecular concentration $[C]_0$ to calculate $[\mathbf{A}]_0$ and $[\mathbf{B}]_0$:

$$[\mathbf{A}]_0 = [C]_0 \mathbf{y_A} \quad [\mathbf{B}]_0 = [C]_0 \mathbf{y}_B$$

The $[C]_0$ quantity can be calculated by any convenient means. In our case, we had previously measured

$$[L]_0 = 2[B_2]_0$$

elsewhere as the initial maleimide concentration, so we inverted the part of the above relationship to solve for average molecular concentration.

$$[C]_0 = [B_2]_0 / y_{B,2} = [L]_0 / 2y_{B,2}$$

Calculation of crosslink mole fractions from procedure and assumptions

In our material system, we have a fully functionalized crosslinker SRF, an inert substituted crosslinker, SRFi, and mixtures of the two to make an intermediate mixture. $\mathbf{x_A}$ for any of these systems can be defined by a simple weighted sum:

$$\mathbf{x}_{\mathbf{A}} = \mathbf{x}_{\mathbf{A},SRF}\frac{n_{SRF}}{n_{SRF}+n_{SRFi}} + \mathbf{x}_{\mathbf{A},SRFi}\left(1-\frac{n_{SRF}}{n_{SRF}+n_{SRFi}}\right)$$

where n_{SRF} is the moles on a molecular basis from SRF in the mixture. The overall ratio can be determined from the mass ratio m_{SRF}/m_{SRFi}:

$$\frac{n_{SRF}}{n_{SRF}+n_{SRFi}} = \frac{n_{SRF}/n_{SRFi}}{n_{SRF}/n_{SRFi}+1} \quad \frac{n_{SRF}}{n_{SRFi}} = \frac{m_{SRF}}{m_{SRFi}}\frac{MW_{SRFi}}{MW_{SRF}}$$

The calculation of average molecular weights MW_{SRF}, MW_{SRFi} is a literal average of the molecular weights MW_q, MW_r of the expected species q, r in each mixture, weighted by their relative population x_r, x_q in the mixture:

$$MW_{SRF} = \sum_q MW_q x_q \quad MW_{SRFi} = \sum_r MW_r x_r$$

x_q is a close relative of $x_{A,i}$ but differentiating between species that may have the same number of functional groups while having different structures. We can organize x_q into a matrix $\mathbf{z_{Aq}}$ with components $z_{Aq,i,k}$, where k is an extra dimension to contain this differentiation. Doing this allows us to finally form an expression for $\mathbf{x_{A,SRF}}$ by summing over that dimension:

$$x_{A,SRF,i} = \sum_k z_{Aq,i,k} \quad x_{A,SRFi,i} = \sum_k z_{Ar,i,k}$$

$\mathbf{z_{Aq}}$ is generated straightforwardly, as the tetraacrylate precursor was measured to be, as above, 80% tetrafunctional and 20% trifunctional, and we assume complete reaction with our Diels-Alder-active thiol. Therefore, k is in this case a singleton dimension and $\mathbf{z_{Aq}}=\mathbf{x_{A,SRF}}$=[0 0 0 0.2 0.8].

$\mathbf{z_{Ar}}$ is calculated from $\mathbf{z_{Aq}}$ under the assumptions of equal reactivity of acrylate groups and complete consumption, with p=70% of the groups functionalized and 1-p=30% of the groups inert. We must generate the probability $P(f_{i,k})$ of finding an i-functional molecule among both statistically substituted populations k=3,4:

$$\mathrm{P}\left(f_{i,k}\right)=\binom{k}{i}p^{i}\left[1-p\right]^{k-i}$$

This can be multiplied against $\mathbf{z_{Aq}}$ to produce $\mathbf{z_{Ar}}$:

$$z_{\mathrm{Ar,i,k}}=\mathrm{P}\left(f_{i,k}\right)z_{Aq,i}$$

which was the last item necessary to calculate the crosslink density, and effective functionality of SRF compositions created by our statistical substitution and two-component mixing strategy.

References

1. van Beek, D. J. M.; Spiering, A. J. H.; Peters, G. W. M.; te Nijenhuis, K.; Sijbesma, R. P., Unidirectional Dimerization and Stacking of Ureidopyrimidinone End Groups in Polycaprolactone Supramolecular Polymers. *Macromolecules* **2007,** *40* (23), 8464-8475.

2. Burattini, S.; Colquhoun, H. M.; Greenland, B. W.; Hayes, W., A novel self-healing supramolecular polymer system. *Faraday Discussions* **2009,** *143*, 251-264.
3. Adzima, B. J.; Aguirre, H. A.; Kloxin, C. J.; Scott, T. F.; Bowman, C. N., Rheological and chemical analysis of reverse gelation in a covalently crosslinked Diels-Alder polymer network. *Macromolecules* **2008,** *41* (23), 9112-9117.
4. Jay, J. I.; Langheinrich, K.; Hanson, M. C.; Mahalingam, A.; Kiser, P. F., Unequal stoichiometry between crosslinking moieties affects the properties of transient networks formed by dynamic covalent crosslinks. *Soft Matter* **2011,** *7* (12), 5826-5835.
5. Montarnal, D.; Capelot, M.; Tournilhac, F. o.; Leibler, L., Silica-Like Malleable Materials from Permanent Organic Networks. *Science* **2011,** *334* (6058), 965-968.
6. Chen, X.; Dam, M. A.; Ono, K.; Mal, A.; Shen, H.; Nutt, S. R.; Sheran, K.; Wudl, F., A Thermally Re-mendable Cross-Linked Polymeric Material. *Science* **2002,** *295* (5560), 1698-1702.
7. Zhang, Y.; Broekhuis, A. A.; Picchioni, F., Thermally Self-Healing Polymeric Materials: The Next Step to Recycling Thermoset Polymers? *Macromolecules* **2009,** *42* (6), 1906-1912.
8. Kloxin, C. J.; Scott, T. F.; Adzima, B. J.; Bowman, C. N., Covalent Adaptable Networks (CANs): A Unique Paradigm in Cross-Linked Polymers. *Macromolecules* **2010,** *43* (6), 2643-2653.
9. Bowman, C. N.; Kloxin, C. J., Covalent Adaptable Networks: Reversible Bond Structures Incorporated in Polymer Networks. *Angewandte Chemie International Edition* **2012,** *51* (18), 4272-4274.
10. Stadler, R., Transient networks by hydrogen bond interactions in polybutadiene-melts. In *Permanent and Transient Networks*, Springer Berlin / Heidelberg: 1987; Vol. 75, pp 140-145-145.
11. te Nijenhuis, K., Calculation of network parameters in thermoreversible gels. *Polymer Gels and Networks* **1996,** *4* (5-6), 415-433.
12. Reutenauer, P.; Buhler, E.; Boul, P. J.; Candau, S. J.; Lehn, J. M., Room temperature dynamic polymers based on Diels-Alder chemistry. *Chemistry* **2009,** *15* (8), 1893-900.
13. (a) Semenov, A. N.; Rubinstein, M., Thermoreversible Gelation in Solutions of Associative Polymers. 1. Statics. *Macromolecules* **1998,** *31* (4), 1373-1385; (b) Rubinstein, M.; Semenov, A. N., Thermoreversible Gelation in Solutions of Associating Polymers. 2. Linear Dynamics. *Macromolecules* **1998,** *31* (4), 1386-1397.
14. Stauffer, D., Scaling theory of percolation clusters. *Physics Reports* **1979,** *54* (1), 1-74.
15. Herrmann, H. J., Geometrical cluster growth models and kinetic gelation. *Physics Reports* **1986,** *136* (3), 153-224.
16. Flory, P. J., Molecular Size Distribution in Three Dimensional Polymers. I. Gelation1. *Journal of the American Chemical Society* **1941,** *63* (11), 3083-3090.
17. Ferry, J. D., *Viscoelastic properties of polymers*. 3rd ed. ed.; Wiley: New York, 1980; p 641.
18. Miller, D. R.; Macosko, C. W., A New Derivation of Post Gel Properties of Network Polymers. *Macromolecules* **1976,** *9* (2), 206-211.

19. Dotson, N. A.; Galvan, R.; Laurence, R. L.; Tirrell, M., *Polymerization Process Modeling*. Wiley-VCH: New York, 1995.
20. Diels, O.; Alder, K., Synthesen in der hydroaromatischen Reihe. *Justus Liebigs Annalen der Chemie* **1928,** *460* (1), 98-122.
21. Craven, J. M. Cross-Linked Thermally Reversible Polymers Produced from Condensation Polymers with Pendant Furan Groups Cross-Linked with Maleimides. 3435003, 1969.
22. (a) Goiti, E.; Heatley, F.; Huglin, M. B.; Rego, J. M., Kinetic aspects of the Diels-Alder reaction between poly(styrene-co-furfuryl methacrylate) and bismaleimide. *European Polymer Journal* **2004,** *40* (7), 1451-1460; (b) Goiti, E.; Huglin, M. B.; Rego, J. M., Some properties of networks produced by the Diels-Alder reaction between poly(styrene-co-furfuryl methacrylate) and bismaleimide. *European Polymer Journal* **2004,** *40* (2), 219-226; (c) Costanzo, P. J.; Beyer, F. L., Thermoresponsive, Optically Active Films Based On Diels-Alder Chemistry. *Chemistry of Materials* **2007,** *19* (25), 6168-6173; (d) Peterson, A. M.; Jensen, R. E.; Palmese, G. R., Reversibly cross-linked polymer gels as healing agents for epoxy-amine thermosets. *ACS Appl Mater Interfaces* **2009,** *1* (5), 992-5; (e) Inglis, A. J.; Nebhani, L.; Altintas, O.; Schmidt, F. G.; Barner-Kowollik, C., Rapid Bonding/Debonding on Demand: Reversibly Cross-Linked Functional Polymers via Diels,àíAlder Chemistry. *Macromolecules* **2010,** *43* (13), 5515-5520; (f) Peterson, A. M.; Jensen, R. E.; Palmese, G. R., Room-Temperature Healing of a Thermosetting Polymer Using the Diels-Alder Reaction. *ACS Appl Mater Interfaces* **2010,** *2* (4), 1141-1149.
23. (a) Jones, J. R.; Liotta, C. L.; Collard, D. M.; Schiraldi, D. A., Cross-Linking and Modification of Poly(ethylene terephthalate-co-2,6-anthracenedicarboxylate) by Diels,àíAlder Reactions with Maleimides. *Macromolecules* **1999,** *32* (18), 5786-5792; (b) Swanson, J. P.; Rozvadovsky, S.; Seppala, J. E.; Mackay, M. E.; Jensen, R. E.; Costanzo, P. J., Development of Polymeric Phase Change Materials On the basis of Diels-Alder Chemistry. *Macromolecules* **2010,** *43* (14), 6135-6141; (c) Goussé, C.; Gandini, A., Diels–Alder polymerization of difurans with bismaleimides. *Polym Int* **1999,** *48* (8), 723-731; (d) McElhanon, J. R.; Russick, E. M.; Wheeler, D. R.; Loy, D. A.; Aubert, J. H., Removable foams based on an epoxy resin incorporating reversible Diels-Alder adducts. *Journal of Applied Polymer Science* **2002,** *85* (7), 1496-1502.
24. Sheridan, R. J.; Adzima, B. J.; Bowman, C. N., Temperature Dependent Stress Relaxation in a Model Diels-Alder Network. *Australian Journal of Chemistry* **2011,** *64* (8), 1094-1099.
25. Hopewell, J. L.; Hill, D. J. T.; Pomery, P. J., Electron spin resonance study of the homopolymerization of aromatic bismaleimides. *Polymer* **1998,** *39* (23), 5601-5607.
26. (a) Yount, W. C.; Loveless, D. M.; Craig, S. L., Small-Molecule Dynamics and Mechanisms Underlying the Macroscopic Mechanical Properties of Coordinatively Cross-Linked Polymer Networks. *Journal of the American Chemical Society* **2005,** *127* (41), 14488-14496; (b) Roberts, M. C.; Hanson, M. C.; Massey, A. P.; Karren, E. A.; Kiser, P. F., Dynamically Restructuring Hydrogel Networks Formed with Reversible Covalent Crosslinks. *Advanced Materials* **2007,** *19* (18), 2503-2507; (c) Roberts, M. C.; Mahalingam, A.; Hanson, M. C.; Kiser, P. F., Chemorheology of Phenylboronate-Salicylhydroxamate Cross-Linked Hydrogel Networks with a Sulfonated Polymer Backbone. *Macromolecules* **2008,** *41* (22), 8832-8840; (d) Cordier, P.; Tournilhac, F.;

Soulie-Ziakovic, C.; Leibler, L., Self-healing and thermoreversible rubber from supramolecular assembly. *Nature* **2008,** *451* (7181), 977-80.
27. Sijbesma, R. P.; Beijer, F. H.; Brunsveld, L.; Folmer, B. J. B.; Hirschberg, J. H. K. K.; Lange, R. F. M.; Lowe, J. K. L.; Meijer, E. W., Reversible Polymers Formed from Self-Complementary Monomers Using Quadruple Hydrogen Bonding. *Science* **1997,** *278* (5343), 1601-1604.

Chapter 5: Evaluation of Single-Molecule Fluorescence Tracking as a Rheological Technique for Transient Polymer Networks

Abstract

Model Diels-Alder polymer networks exhibit rheological characteristics that can be described using established transient network theory. However, the theory is based upon specific assumptions of the behavior of percolation clusters, such as: mean field behavior, large clusters determining the viscoelastic spectrum, or only considering bond breakage that results in splitting a cluster nearly in half. While these assumptions are certainly reasonable and make the theoretical workup tractable, they are also non-trivial to evaluate. We proposed the use of single-molecule fluorescence tracking as a method for probing the molecular scale dynamics of the model Diels-Alder material and directly test the basic assumptions of the theory. This chapter documents the motivation, techniques, and results of our evaluation of this technique.

Introduction and Background

Covalent adaptable networks (CANs) are polymer networks (crosslinked macromolecular materials) in which the connections between monomers in the network can be reversibly cleaved by application of an external stimulus.[1] CANs have the ability to: relieve stress, including polymerization-shrinkage-induced stress;[2] incorporate chemical functionality post-cure;[3] chemically bridge interfaces, including fractures;[4] undergo recycling;[5] control the diffusivity of particles via

adjustable mesh size;[6] and actuate mechanical motion.[7] These different effects are due to varying underlying chemical mechanisms; however, the fundamental nature of the phenomenon in each case is the cleavage and recombination of crosslinks. Therefore, the fundamental viscoelastic behavior should be analogous and have several common features for each of the cases.

By constructing a model CAN, using the Diels-Alder reaction between furan and maleimide groups attached to simple monomers, we have demonstrated that the bulk viscoelastic properties of neat, ideal transient networks can agree strongly with theoretical predictions from Semenov and Rubinstein's work on associative polymer networks.[8] Although the model network was chosen through a separate process from the search for a suitable theoretical framework, it became clear that the material and theory were ideally suited in terms of matching assumptions to reality in the case of independent reactivity, negligible cyclization and entanglement, and other classical polymer network properties. This helped boost our case that the experiment was a nearly direct test of the transient "modification" to classic network theory.

However, the resultant relationship of interest, $\tau_{max} \propto \tau_{bond} |\Delta|$, (i.e. mechanical relaxation time is proportional to the product of the transient bond lifetime and distance from the gel point) could conceivably arise from other molecular-scale mechanical effects rather than those listed in the 1998 papers. Specifically, they assert that:

1. Mechanical relaxation corresponds to relaxation of so-called terminal clusters,
2. Terminal clusters may relax either by diffusing a distance on the order of their own radius or breaking along their "backbone" into clusters of approximately equal size, and
3. Network chains may be described in terms of terminal clusters connected to crosslinks.

These assumptions directly lead to the proportional scaling relationship above, which we have evaluated. But passing that test is only evidence supporting the hypothesized mechanism, rather than a conclusive demonstration of it. To evaluate each of the assertions, it would be optimal to use a technique sensitive to differences in molecular behavior.

Single-fluorophore total internal reflectance fluorescence microscopy is a highly sensitive technique[9] that builds on microrheology and fluorescent particle tracking theory but scales down to the level of observing the behavior of molecules and/or particles labeled with as little as one fluorescent moiety. It has been used with great success for the elucidation of the diffusion of individual molecules at oil-water[10] and solid-liquid[9, 11] interfaces, by recording the individual steps of the signal's random walk and calculating average displacement versus time – not only over all particles, but also for a large number of individual trajectories. It is this individual tracking capability, known as MAPT (mapping using accumulated probe trajectories[11b]) which makes the technique promising for attacking these questions

of cluster mobility in transient networks. By watching an individually labeled transient cluster, it is in principle possible to observe breakage events by noting discontinuity in the slope of the squared displacement versus time curve, illustrated in figure 5.1.

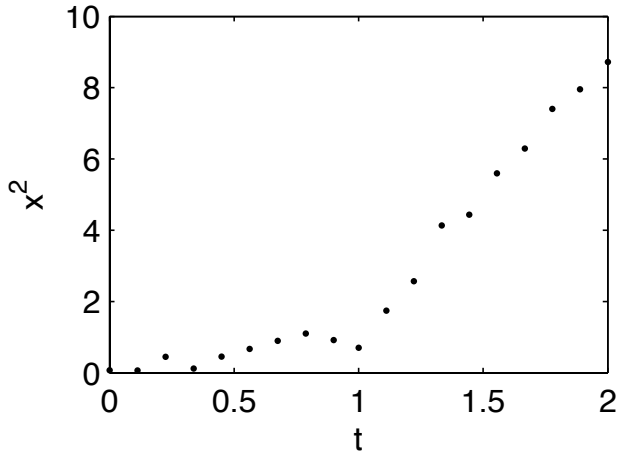

Figure 5.1: Idealized hypothetical squared displacement versus time curve potentially observed when a labeled transient cluster undergoes a significant breakage event (mass m -> m/2, hydrodynamic radius R_H -> $R_H/8$, D->8D) at time t=1.

Methods

Monomers and sample preparation

Samples were SRF(3.8) resins synthesized as previously described in Chapter 3. Typical stoichiometric ratios were between r=0.3 and r=0.4, to target the near gel point regime, as maleimide conversion tends toward 100% under these conditions. An equal mass of spectrphotometric grade DMSO was then added when required. The prepared monomers were diluted in spectrophotometric grade acetone and mixed together. An appropriate amount of AlexaFluor 647 C2 Maleimide, targeting a concentration of 10^{-11} M, was diluted and added at this step. The sample was

vortexed and cast dropwise onto a piranha/UV/Ozone/HDMS treated coverslip, then baked at 160°C for 5 minutes.

Total internal reflectance fluorescence microscopy (TIRFM) and Particle tracking and trajectory analysis

TIRFM was performed using a Nikon TE-2000 microscope with 60× objective, and a 650nm excitation laser. The setup is fully described in a number of references, as is the code for trajectory analysis, which was re-used from packages built for several other published analyses.[9-12]

Results and Discussion

Initial attempts at viewing single molecules at the glass-polymer interface were disrupted by the presence of large, bright structures that were presumed to be an insoluble impurity of some sort. As the size of these objects was on the order of tens of microns, the solution was filtered before casting the film on the slides. However, some structures larger than a micron remained even after filtration through 200nm PTFE, so we were forced to conclude that some component of the casting mixture (A) was soluble in the presence of the casting solvent and (B) crystallized at least partially as the solvent evaporated. One smaller such structure is shown in figure 5.2 amongst single fluorophore signals.

Figure 5.2: TIRFM image of a filtered SRF film on piranha treated glass. The bright spot in the middle is one of the smaller crystalline structures, and the dim signals are likely individual fluorophores.

By removing components from the mixture, we were able to determine that the crystals were associated with our bismaleimide. However, multiple purification techniques – such as filtration, recrystallization, or silica gel chromatography – failed to prevent the crystals from forming. As solubility at the temperature of interest seemed to be the main issue, we added a substantial quantity of spectrophotometric grade DMSO (equal parts resin and DMSO by weight) to prevent crystallization as the acetone evaporated. This strategy eliminated the large structures completely, even in unfiltered samples, and allowed us to begin seeing large populations of what we determined to be individual fluorophores at the glass-polymer interface. Figure 5.3 shows a typical TIRFM frame.

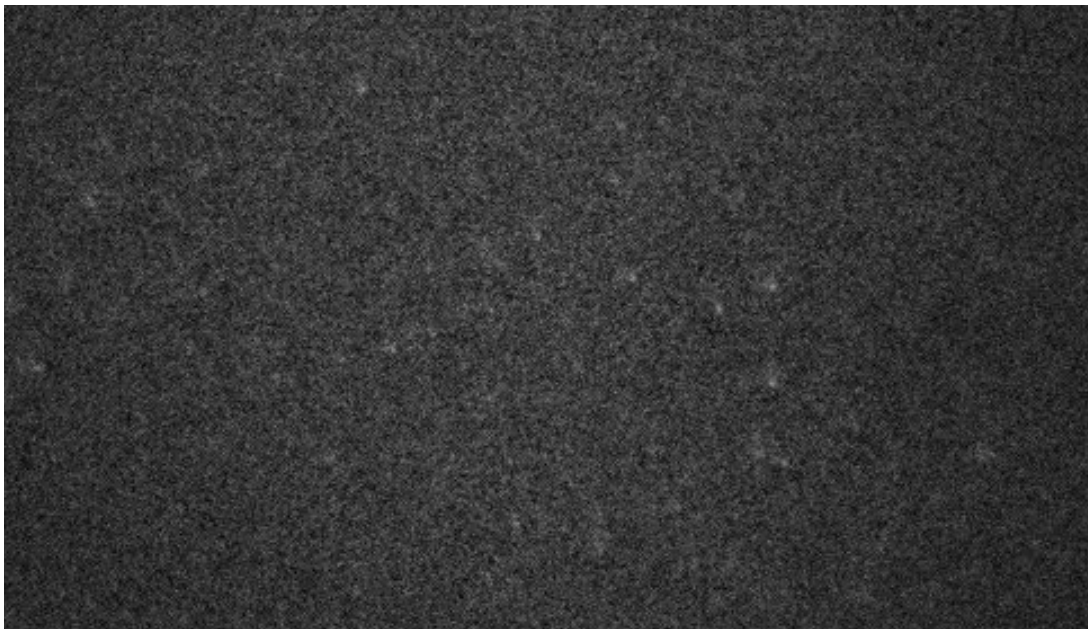

Figure 5.3: TIRFM image of a 50% DMSO SRF film on piranha treated glass. Substantially more fluorophores are visible in this frame than in figure 5.2.

In video captures of these images, the fluorophores had all the markings of typical single molecule experiments, except one: all the signals seemed, relative to oil-water or air-water interface experiments, to be stationary. While they would rapidly come into and out of the image (presumably from the bulk or z direction), all visible fluorophores remained within a few pixels of their initial location, until they vanished either due to photobleaching or moving away from the excitation zone. Because it was not unreasonable to believe that the polymer may have been extremely viscous at the conditions of interest, even after ensuring that only a minimum amount of maleimide was present and preventing gelation by working far off stoichiometry, we tracked the signals for a number of different compositions at 30 and 50°C. As shown below, the diffusion coefficients are consistent with fixed objects (0.1-1 $\mu m^2/s$), and did not have a perceptible dependence on temperature or composition (see Figure 5.4.)

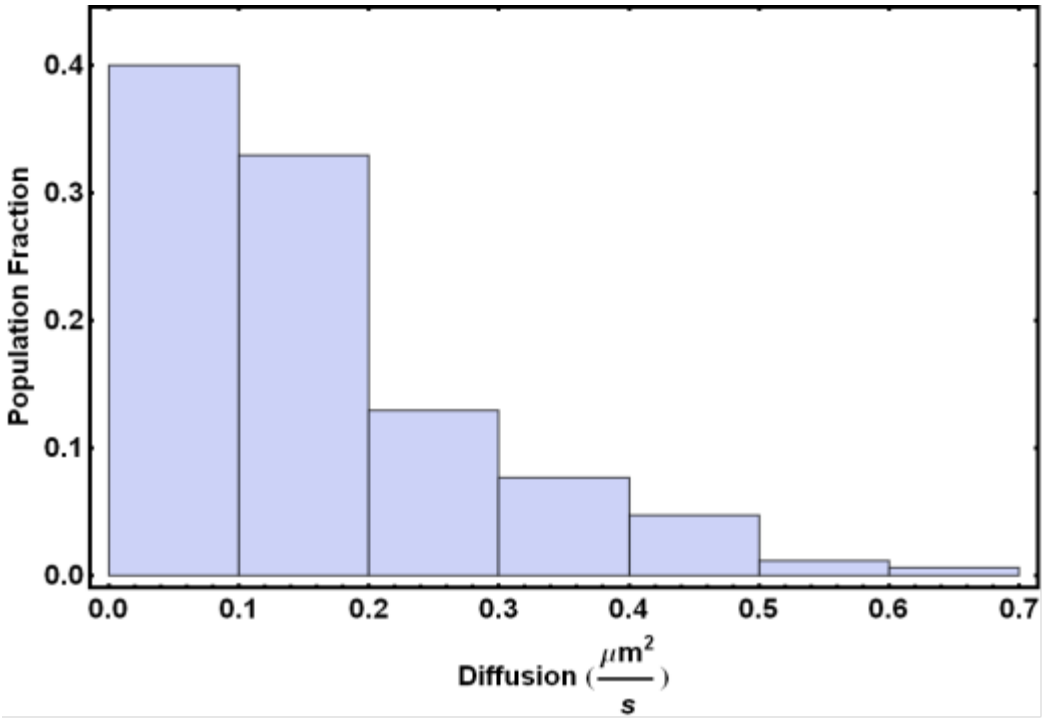

Figure 5.4: Representative diffusion histogram from trajectories of fluorophores in samples similar to figure 5.3. Typical diffusion coefficients are comparable to solid-liquid adsorbed molecules (0.1-1 $\mu m^2/s$) rather than freely diffusing molecules (10-1000 $\mu m^2/s$).

This behavior is most consistent with the idea that we were only observing stationary fluorophores adsorbed to the glass. As the fluorophore is ionically charged to provide water solubility, it is reasonable to think that a charge-hydroxy interaction would be the main cause of adsorption events. So to eliminate this, the surface of the glass was treated via vapor deposition of HMDS to react all available silica hydroxy groups into an inert trimethylsilane group. This approach had the effect of removing all discernable individual fluorophores. Some background fluorescence remained, however all attempts to remove this and attain single molecule signals by adjusting the laser, optics, fluorophore loading, composition, or

using *in situ* and external photobleaching failed to produce any visible signal above background.

Conclusion

Although TIRFM and MAPT are in principle capable of discerning microstructural mechanisms responsible for transient network relaxation, practical effects interfere with the model system of interest including low accessible temperatures, the need for extra solvent, and the background fluorescence that seems to be intrinsically attributable to one of the monomers. Future attempts at this topic should try to mitigate these issues, possibly by choosing a highly soluble, highly purified custom monomer system, and potentially avoiding completely the Diels-Alder reaction, in favor of a transient bond that does not involve such highly conjugated and likely fluorescent systems.

References

1. Kloxin, C. J.; Scott, T. F.; Adzima, B. J.; Bowman, C. N., Covalent Adaptable Networks (CANs): A Unique Paradigm in Cross-Linked Polymers. *Macromolecules* **2010,** *43* (6), 2643-2653.
2. (a) Park, H. Y.; Kloxin, C. J.; Scott, T. F.; Bowman, C. N., Stress Relaxation by Addition-Fragmentation Chain Transfer in Highly Cross-Linked Thiol-Yne Networks. *Macromolecules* **2010,** *43* (24), 10188-10190; (b) Kloxin, C. J.; Scott, T. F.; Bowman, C. N., Stress Relaxation via Addition-Fragmentation Chain Transfer in a Thiol-ene Photopolymerization. *Macromolecules* **2009,** *42* (7), 2551-2556.
3. Amamoto, Y.; Kikuchi, M.; Masunaga, H.; Sasaki, S.; Otsuka, H.; Takahara, A., Reorganizable Chemical Polymer Gels Based on Dynamic Covalent Exchange and Controlled Monomer Insertion. *Macromolecules* **2009,** *42* (22), 8733-8738.
4. (a) Chen, X.; Dam, M. A.; Ono, K.; Mal, A.; Shen, H.; Nutt, S. R.; Sheran, K.; Wudl, F., A Thermally Re-mendable Cross-Linked Polymeric Material. *Science* **2002,** *295* (5560), 1698-1702; (b) Chen, X.; Wudl, F.; Mal, A. K.; Shen, H.; Nutt, S. R., New Thermally Remendable Highly Cross-Linked Polymeric Materials. *Macromolecules* **2003,** *36* (6), 1802-1807.

5. Craven, J. M. Cross-linked Thermally Reversible Polymers Produced from Condensation Polymers with Pendant Furan Groups Cross-linked with Maleimides. 3435003, 1969.
6. Roberts, M. C.; Mahalingam, A.; Hanson, M. C.; Kiser, P. F., Chemorheology of Phenylboronate-Salicylhydroxamate Cross-Linked Hydrogel Networks with a Sulfonated Polymer Backbone. *Macromolecules* **2008,** *41* (22), 8832-8840.
7. Scott, T. F.; Draughon, R. B.; Bowman, C. N., Actuation in Crosslinked Polymers via Photoinduced Stress Relaxation. *Advanced Materials* **2006,** *18* (16), 2128-2132.
8. Rubinstein, M.; Semenov, A. N., Thermoreversible Gelation in Solutions of Associating Polymers. 2. Linear Dynamics. *Macromolecules* **1998,** *31* (4), 1386-1397.
9. Honciuc, A.; Harant, A. W.; Schwartz, D. K., Single-Molecule Observations of Surfactant Diffusion at the Solution-Solid Interface. *Langmuir* **2008,** *24* (13), 6562-6566.
10. (a) Walder, R.; Schwartz, D. K., Dynamics of protein aggregation at the oil-water interface characterized by single molecule TIRF microscopy. *Soft Matter* **2011,** *7* (17), 7616-7622; (b) Walder, R.; Schwartz, D. K., Single Molecule Observations of Multiple Protein Populations at the Oil-Water Interface. *Langmuir* **2010,** *26* (16), 13364-13367; (c) Sriram, I.; Walder, R.; Schwartz, D. K., Stokes-Einstein and desorption-mediated diffusion of protein molecules at the oil-water interface. *Soft Matter* **2012,** *8* (22), 6000-6003.
11. (a) Kastantin, M.; Schwartz, D. K., Connecting Rare DNA Conformations and Surface Dynamics Using Single-Molecule Resonance Energy Transfer. *Acs Nano* **2011,** *5* (12), 9861-9869; (b) Walder, R.; Nelson, N.; Schwartz, D. K., Super-resolution surface mapping using the trajectories of molecular probes. *Nat Commun* **2011,** *2*, 515.
12. (a) Walder, R.; Kastantin, M.; Schwartz, D. K., High throughput single molecule tracking for analysis of rare populations and events. *Analyst* **2012,** *137* (13), 2987-2996; (b) Kastantin, M.; Langdon, B. B.; Chang, E. L.; Schwartz, D. K., Single-Molecule Resolution of Interfacial Fibrinogen Behavior: Effects of Oligomer Populations and Surface Chemistry. *Journal of the American Chemical Society* **2011,** *133* (13), 4975-4983.

Chapter 6: Understanding the process of healing of thermoreversible covalent adaptable networks in self-limited hysteresis heating applications

Abstract

When Diels-Alder-based thermoreversible covalent adaptable networks (TR-CANs), are applied in fracture healing applications, the contributions of network structure tend to take a back seat to explanations based solely on the chemical behavior of the reversible bonds binding the network. However, for TR-CANs near the gel point, rheological experiments have shown that accounting for network structure via scaling relationships is necessary to understand their viscoelastic behavior. By extension, the structure of the network should have a substantial effect on fracture healing performance. In this work we demonstrate this effect in a model hysteresis heated Diels-Alder network material. The effective functionality of the monomers was varied from 3.0 to 3.5, changing the gel temperature from 106°C to 122°C. By subjecting these materials to identical healing conditions, we observed the change due to network structure while holding e.g. bond conversion and bond lifetime constant. We showed with statistical confidence that both healing time, and the interaction between healing time and composition ($p=0.016$ and $p=0.014$, respectively) are necessary to explain the observed differences in healing performance. A single-parameter model of healing was developed based on the scaling relationship that determined mechanical relaxation, and the model was

interpreted to understand how network structure and fracture healing interact in TR-CANs.

Introduction and background

Thermoreversible networks have become a prominent feature of the smart materials literature recently, with demonstrated application in biomaterials, recyclable materials, and healable materials[1]. These materials utilize the triggerable nature of the reversible bonds to exhibit transient network characteristics only when desired, thereby outperforming standard materials in similar roles. Specifically, in the field of healable[2] or mendable[3] materials, thermoreversible networks have been demonstrated to quickly and repeatedly recover strength or toughness. These thermoreversible networks often consisted of physical bonds, such as the hydrogen-bonded or pi-pi stacking supramolecular networks,[4] which demonstrated time-dependent room temperature healing, or self-recognition supramolecular networks such as those based on ureidopyrimidinone.[5] However, a number of thermoreversible covalent bonds exist, which can form what we have termed thermoreversible covalent adaptable networks (TR-CANs).[1] These materials offer potentially greater strength and chemical flexibility, and have been used in a number of materials, notably the mendable Diels-Alder networks of Chen *et al.*,[6] which spawned an entire sub field of Diels-Alder based TR-CANs.[7]

A promising trigger for TR-CANs is the use of self-limited hysteresis heating.[1, 8] By suspending ferromagnetic microparticles in a reversible network matrix, a magnetically sensitized composite is formed which heats up when exposed to a

radio-frequency, high-strength, oscillating magnetic field.[9] Depending on particle composition and geometry, Néel relaxation is the dominant contribution[10] to the heating mechanism; so, as the Curie temperature of the material is approached and the magnetic susceptibility decreases, the amount of power the particles can extract from the RF magnetic field drops until the material reaches a steady-state temperature, as diagrammed in Figure 6.1.

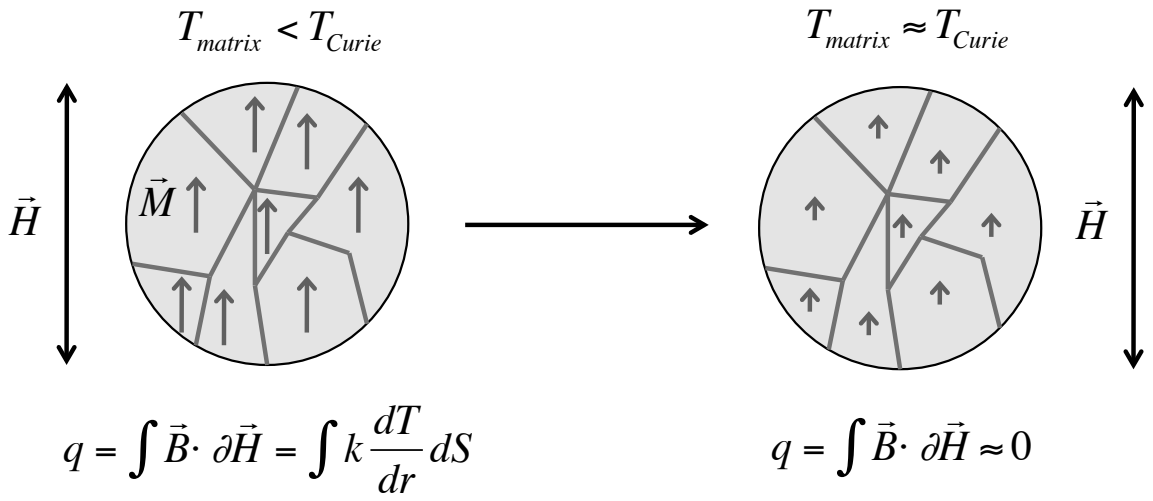

Figure 6.1: The process of hysteresis heating. When the magnetic particle such as CrO_2 is in a matrix below the Curie temperature of the material, the particle itself must be less than the Curie temperature as well due to heat transfer, so the material is coerced to a magnetization $\vec{M}$ due to the oscillating magnetic field $\left|\vec{H}\right| = H_0 \sin(2\pi ft + \varphi)$. The heat added to the matrix is equal to the hysteresis work. When the matrix approaches the Curie temperature, by the same argument, the particle must be near the Curie temperature, so the hysteresis work per cycle drops, and the heating rate approaches zero, producing a self-limiting steady final temperature.[9-10]

This steady-state temperature, related to the Curie temperature of the chromium dioxide particles, is reached within 1-2 minutes in a typical sample. Alternative particle types suffer from large contributions associated with additional heating mechanisms, such as inductive resistance and excessively high Curie

temperatures. The next lowest Curie temperature amongst common materials is 358°C for Nickel – easily hot enough to irreversibly decompose the material. Clearly, the Curie temperature of the particles is a double-edged sword, as it provides a neatly self-limited heating mechanism, but at a pre-defined temperature that is not, in principle, adjustable. Compositions must therefore be tuned to behave appropriately at the steady state temperature of the hysteresis heating process.

Our group has previously reported the use of a thermoreversible Diels-Alder resin with appropriate properties to achieve, within 2.5 minutes, total reshaping or fracture healing, over the course of as many as 15 individual heating cycles with complete recovery of the native material behavior.[8] This outcome was achieved because the resin system essentially depolymerized into oligomeric species and completely relaxed/flowed on the timescale of the experiment. Here, we demonstrate the tunable nature of these furan/maleimide-based Diels-Alder networks, modifying the composition such that different viscoelastic regimes occur at the self-limited temperature. The motif we use to achieve this tunability is to adjust the functionality of the monomer mixture to control the gel point conversion, and by extension the equilibrium temperature at that extent of reaction (i.e. the gel temperature, T_{gel}.) To achieve this aim, we synthesized CrO_2-loaded multifuran mixtures (SRFm) with a functionality-weighted average functionality (effective functionality, f_e) of 3.0 and 3.8, so that compositions of intermediate average functionality could be created via mixing. The specific composition is indicated with the final effective functionality in parentheses, e.g. SRFm(3.5). These furan monomers are then mixed in a stoichiometric ratio with a bifunctional (f_e=2)

maleimide (DPBM) to create a thermoreversible, polymerized material. Table 6.1 lists the important properties of the compositions of interest in this study, while Scheme 6.1 displays their chemical structures and reactions.

Table 6.1: Properties of the Various Compositions used in this study

Composition	SRFm(3.0)	SRFm(3.3)	SRFm(3.5)
Mass ratio (3.0:3.8)	1:0	2.08:1	1.13:1
Effective functionality	3.0	3.3	3.5
Gel Temperature (Gel Point)	106°C (71%)	117°C (65%)	122°C (63%)
Ultimate flexural strength (MPa)	13±5	12±3	17±5
Recovery of UFS after 5 min cycle	105±30%	80±20%	44±20%
Recovery of UFS after 10 min cycle	94±30%	103±10%	52±20%

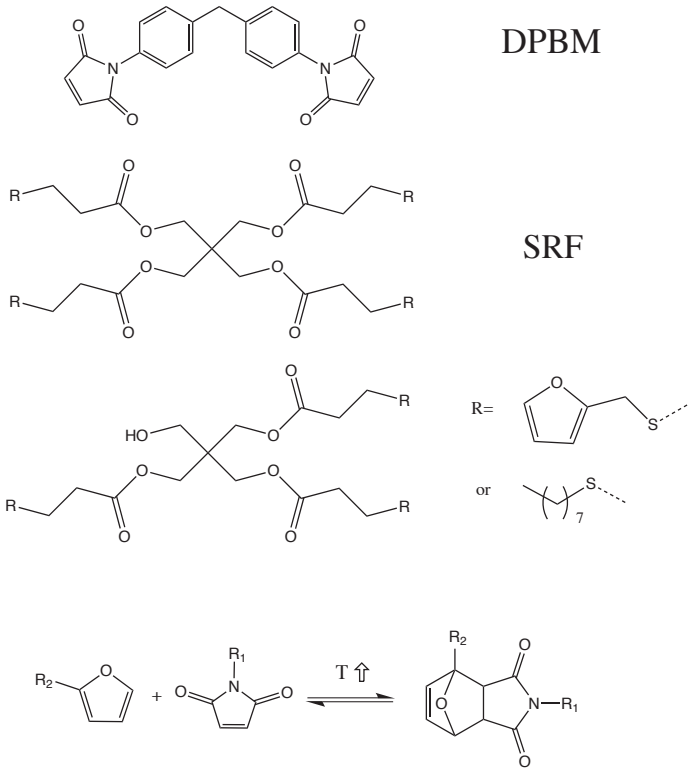

Scheme 6.1: Diels-Alder monomers used in this study – bismaleimide DPBM and multifuran SRF – and their interaction via the thermoreversible Diels-Alder cycloaddtion.

The experiment itself is a simple extension of the healing experiment in our previous report[8] (See Figure 6.2.) SRFm was cast into bar molds and allowed to cool. The bars were then removed, fractured, and returned to the same mold with the fracture interfaces aligned. The bars were then subjected to RF heating conditions for 5 or 10 minutes and immediately removed and allowed to cool (carefully controlling the cooling conditions to be comparable between bars.) These bars were finally tested to failure under a three-point bend mechanical test. Control bars were subject to the same process, skipping the fracture step only.

Figure 6.2: Healing process: (A) SRFm is cast into bar molds, (B) which are fractured and (C) returned to the mold. The bars are subjected to 5 or 10 minutes of RF heating conditions, which results in (D) the disappearance of the fracture and recovery of the flexural strength.

Results and Discussion

Our indicator of healing in this study is the ultimate flexural strength (UFS) of the bars. From Table 6.1, the general trend in UFS recovery is apparent and intuitive: the bars with higher functionality (and crosslinking, and gel temperature)

achieve less healing at a given healing time compared to lower functionality materials, and bars subjected to additional healing time experience increased fracture healing. However, the experiment is an intrinsically noisy one, so a statistical analysis of the apparent trend is necessary.

We performed an analysis of variance (ANOVA) on these data, which allows us to determine which experimental factors, if any, can explain a significant fraction of the total variability in the UFS observed at each treatment level. A fixed-effects model including three levels of functionality (F), three levels of healing (H), and their interaction (FH) explains more than a third of the total sum of squares (R^2=36%,) but the p-values for the null hypothesis of each individual effect are quite high (p_F=0.19, p_H=0.02, and p_{FH}=0.08.) Discarding the least significant parameter, the lone dependence on effective functionality, reduces the R^2 to 31% but improves the significance of the fit (p_H=0.016, p_{FH}=0.014.) The details of the ANOVA are presented in Table 6.2. This analysis allows us to have some confidence that the apparent trend in the fracture recovery from Table 6.1 is real, but doesn't directly speak to the question of the underlying mechanism.

Table 6.2: ANOVA of a fixed effects model of healing SRFm compostions

Source of Squares	Sum of Squares	Degrees of Freedom	Mean Squares	F_0 Statistic	Probability of $F>F_0$
H	111.583	2	55.79	4.56	0.016
F*H	174.000	4	43.50	3.56	0.014
Error	501.306	41	12.23		
Total	723.043	47			

The process of fracture healing in reversibly crosslinked polymer networks is generally understood to be closely bound to the chemical behavior of the reversible

bonds.[7k, 11] Fracture healing in thermoplastics has been shown to be closely related to the primary mechanical relaxation mechanism, which is in most cases reptation.[12] We have shown in previous work[7j] that the dominant relaxation mechanism, as evidenced by rheological measurement, in transient networks such as ours can be described according to a simple linear relationship between the reversible bond's lifetime τ_b and the distance from the gel point ε:

$$\tau_{relax} = C\tau_b\varepsilon \tag{6.1}$$

which connects chemical and mechanical behavior and may also apply to fracture healing behavior in this model thermoreversible network. If we assume that mechanical relaxation time is the only contributing factor to healing, a simple, idealized model of fractional UFS recovery, $H(t_H)$, after undergoing a healing cycle lasting t_H minutes might be:

$$H(t_H) = 1 - e^{-t_H/\tau_m} \tag{6.2}$$

if τ_m has a constant value over the entire healing cycle, which would be the case for a bar instantly and evenly heated to a constant temperature and bond conversion, and then immediately quenched at t_H. However, in a real healing cycle, τ_m will have significant time dependence. Therefore a more complicated integral expression is required to capture the behavior of UFS recovery for an arbitrary heating condition, $H_A(t_H)$:

$$H_A(t_H) = 1 - \exp\left(-\int_0^{t_H} \tau_m^{-1} dt\right) \tag{6.3}$$

Because Equation 6.1 provides a theoretical relationship for τ_m, we can solve the integral given the time-dependence of the component functions, τ_b and ε, which can in turn be calculated using the sample temperature as a function of time. We measured the surface temperature of several samples of each composition to use as a proxy for the actual healing condition temperature. The compositions had no significant difference in behavior, so the means of each measurement were combined and interpolated using a shape-preserving Piecewise Cubic Hermite Interpolating Polynomial (PCHIP), to maintain continuity and monotonicity.

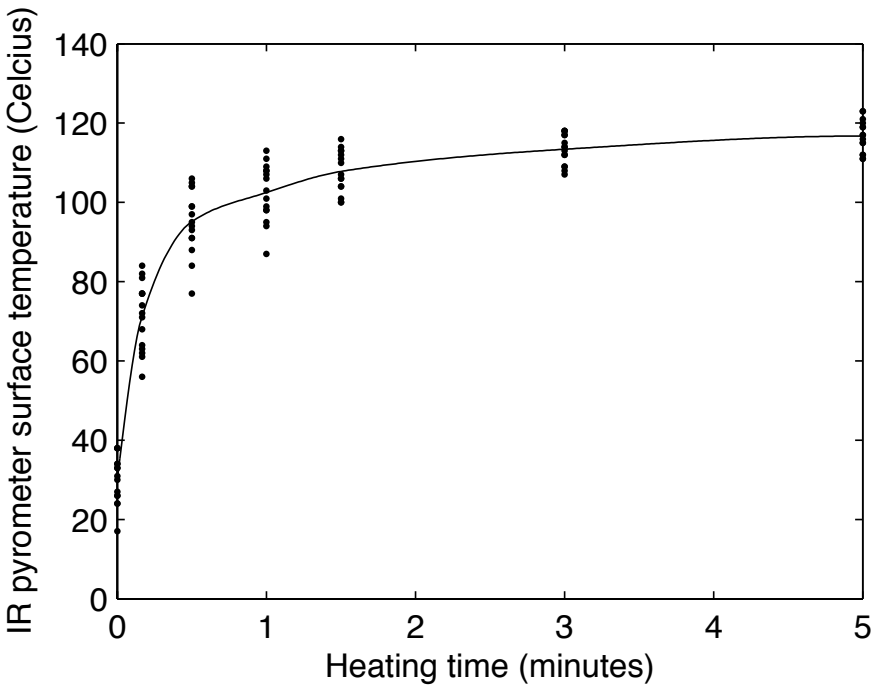

Figure 6.3: Temperature versus time in SRFm compositions in the induction heater as measured at an open sample surface using an infrared thermometer. The curve is a Piecewise Cubic Hermite Interpolating Polynomial (PCHIP) of the mean temperature at each time.

Using this relationship to model the temperature dependence, we integrated the above expression numerically (details in the supplemental section). The

resultant predicted healing curves, plotted in Figure 6.4, for each composition are qualitatively accurate. The healing rate increases with decreasing effective functionality, and different compositions are predicted to achieve different levels of healing on the 5 to 10 minute timescale, as we have observed experimentally. This model only has one free parameter from Equation 6.1, after using published thermochemical constants[7j] and sensible assumptions for initial conditions (See Methods.) This parameter, C, has a strong effect on the resulting prediction and can be fit to the fracture healing data. The best-fit value for C is found to be significantly higher than that for analogous rheological measurements (10 versus 0.6).[7j] Thus, while the same underlying bond breakage and reformation dynamics in these networks are clearly responsible for both healing and mechanical relaxation, the quantitative prediction of critical time constants for these processes indicates that healing occurs on much longer timescales.

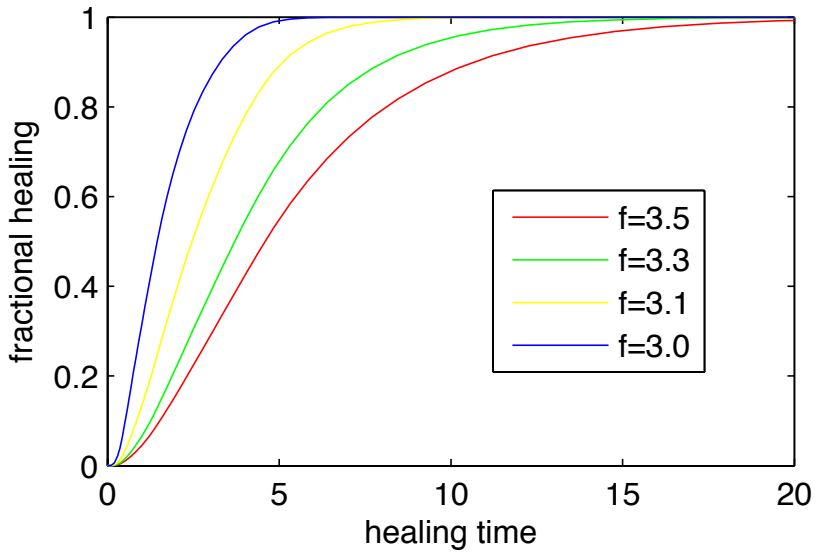

Figure 6.4: Plot of integrated healing curves $H_A(t_H)$ for SRFm compositions including a hypothetical f=3.1 material. The healing curves are qualitatively

comparable to our mechanical testing observations, using a value of 10 for the scaling parameter C from equation 6.1.

Given the similarity in the underlying chemistry and physics of mechanical relaxation and healing, and also considering that they occur over much different length scales, we propose that the healing time and mechanical relaxation time are nearly proportional, although not identical. Combining this proportionality with Equation 6.2, we derived a simple, linear relationship for the healing efficiency:

$$H_E(t_H) = 1 - e^{-t_H/\tau_{H0}} - Dt_H e^{-t_H/\tau_{H0}} \Delta T_{gel} \quad (6.4)$$

by essentially making a first-order Taylor series approximation of the simple, ideal healing model of Equation 6.2 with respect to small changes in distance from the gel point at steady healing conditions. This approach results in one lumped free parameter D (a combination of the implied scaling proportionality between characteristic healing and mechanical timescales and other constant terms) to fit the data. The difference in temperature between the steady healing condition and the gel temperature of the sample (T_{gel}-T_H=ΔT_{gel}) serves as an adequate proxy for the distance in terms of conversion from the gel point (ε=p-p_{gel}) because they are approximately proportional,[7j] and the lumped fitted parameter D absorbs this proportionality factor. The curve representing SRFm(3.3), or equivalently ΔT_{gel}=-1°C, in Figure 6.4 follows an exponential decay with a time constant of ~4 minutes at long times, which is close to the characteristic bond lifetime τ_b at 118°C. Because the gel temperature of SRFm(3.3) is ~118°C, the contribution to mechanical relaxation from the distance to the gel point trends towards zero via the retro-Diels-Alder reaction. This accelerating healing effect apparently dominates healing at this

relaxation from the distance to the gel point trends towards zero via the retro-Diels-Alder reaction. This accelerating healing effect apparently dominates healing at this critical final healing temperature. Therefore the central decay constant of the linearization need not be considered a free parameter if we fix it to the bond lifetime at the healing conditions. However, it would be necessary to vary τ_b independently of healing temperature to test this assumption directly, which is not possible with the present model system.

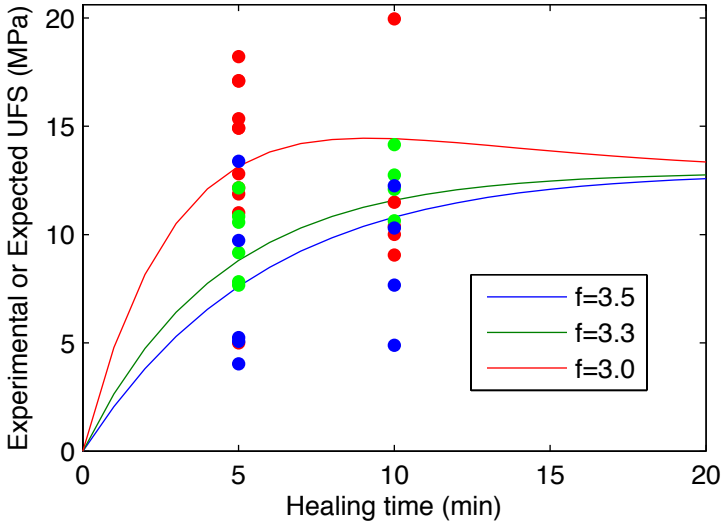

Figure 6.5: Empirical model expectations overlaid on experimental UFS results. The decrease of the f=3.0 trajectory is an artifact of the linear approximation. The curves are otherwise similar to those in Figure 6.4.

The empirical model predictions, shown in Figure 6.5, match the "full model" and remove substantial variance from the residuals, with the parameter $D=0.019\pm0.008$ K^{-1} min^{-1} and an overall R^2 of 27%, which compares favorably to the fixed effects model. Additionally, this model helps us interpret the qualitative meaning of the effects of the gel temperature on healing. Specifically,

- At long healing times, fracture healing in a transient network depends mainly on residual crosslinks breaking and forming, which is simply an exponential function of time, with a half life of $\sim \ln(2)\tau_b$.
- At intermediate healing times, fracture healing depends on the kinetics of both new crosslinks being formed, and the relaxation of the network due to chain and cluster breakage and diffusion. Compositions healing well above their gel temperature essentially receive a strength bonus as compared to those healed at or below T_{gel}.
- At short healing times, the model is too simplistic to cope with the necessary combination of non-ideal effects – such as wetting, diffusion, and initial temperature ramp-up – that may become important. This behavior is to be expected, as these conditions are also outside the range of our data set.

Conclusion

We have successfully demonstrated that a triggered healable composite will achieve varying, predictable levels of healing that are controlled by manipulating both polymer network composition and healing conditions including temperature relative to the reverse gel temperature and the amount of time allowed at that temperature. Crucially, we have demonstrated this effect while maintaining constant bond kinetics (via constant temperature experiments), which is the primary means through which other groups have controlled healing performance. To our knowledge, this is the first report of such a strategy, where temperature and bond kinetics remain invariant as the temperature of critical network behavior is manipulated by changing the network composition. This approach allowed us to

form a model of the process in which we separate chemical kinetic behavior from mechanical relaxation, using information from the expected equilibrium structure of the network. Our model is limited, in that it does not cover the case of short healing times, and simplifies a piecewise, nonlinear integral model into a one-parameter linear model. However, despite these drawbacks, this analysis should apply to other healable, reversibly bonded materials, including those networks which are intended to heal at substantially different conditions, such as at room temperature or upon exposure to a different stimulus, such as light.

Supplemental

Equation 6.3 was solved numerically using an adaptive-step Runge-Kutte 4th order integration algorithm (Matlab's ode45 built-in). The differential equation was defined as:

$$\frac{dF}{dt} + \frac{F}{\tau_m} = 0 \qquad (6.A1)$$

$$H = 1 - F \qquad (6.A2)$$

where F is a population of "flaws" that can be healed by mechanical relaxation. The lack of any other flaws or healing modes is a basis assumption of the model. Equation 6.3 results when 6.A1 is integrated by parts with the initial condition of t=0, F=1. The resulting expression for F is then substituted into 6.A2. The functional form of $\tau_m(t)$ was determined by multiplying the time dependent functions $\tau_b(t)$ and $\varepsilon(t)=p(t)-p_{gel}$ by the scaling proportionality C. Bond conversion p(t) was determined by solving the kinetic model of the Diels-Alder reaction as in previous work[7j] but

incorporating the temperature dependence (and therefore time dependence) of the kinetic parameters via the interpolation of Figure 3. $\tau_b(t)=1/k_r(t)$ was calculated in this fashion as well. Initial conditions of the kinetic model were determined by assuming a post-heating temperature decay to ambient with a time constant of 1.5 minutes (the qualitative time to vitrification for a typical induction heating experiment,) solving the kinetic model for an additional 5 minutes post-heating, and assuming the final conversion remained constant due to kinetic limitations caused by physical vitrification. This resulted in initial conversions that were ~1% greater than those predicted to occur at equilibrium at healing conditions.

Methods

SRFm monomer synthesis procedures were identical to the synthesis of SRF compositions described in previous work,[7j] with the additional step of combining the Magtrieve CrO_2 particles, according to the method of Adzima, *et al*.[8] In short, SRF(3.0) and SRF(3.8) monomers were mixed according to mass ratios, and then combined with 4 parts by volume of a suspension of Magtrieve in methanol (0.0025g/g). This was sonicated at high power for 5 minutes. The resultant material phase-separated into a dense SRF/CrO_2 rich phase and a light cloudy methanol phase, which was decanted. The residual solvent was removed by rotary evaporation and finally high vacuum (10^{-2} Torr), producing SRFm monomers.

Sample bars for flexural tests were made by mixing the stoichiometric amount of bismaleimide DPBM with the appropriate SRFm monomer and heating to 170°C in an oven for 5 minutes, a condition sufficiently hot to dissolve DPBM but for

a short enough time to avoid significant radical, [2+2] cyclo-, or other addition side reactions that can occur at these temperatures.[13] The hot liquid material was poured directly into silicone bar molds and pressed to form a uniform upper surface. Defective bar shapes were trimmed or discarded, as appropriate. Instrumentation and methods for temperature and flexural strength measurements were identical to those of Adzima *et al.*[8], except a strain rate of 1 mm/min was used instead of 10 mm/min, as the samples of this study are substantially more brittle.

References

1. Kloxin, C. J.; Scott, T. F.; Adzima, B. J.; Bowman, C. N., Covalent Adaptable Networks (CANs): A Unique Paradigm in Cross-Linked Polymers. *Macromolecules* **2010,** *43* (6), 2643-2653.
2. Wu, D.; Meure, S.; Solomon, D., Self-healing polymeric materials: A review of recent developments. *Progress in Polymer Science* **2008,** *33* (5), 479-522.
3. Bergman, S. D.; Wudl, F., Mendable polymers. *Journal of Materials Chemistry* **2008,** *18* (1), 41.
4. (a) Cordier, P.; Tournilhac, F.; Soulie-Ziakovic, C.; Leibler, L., Self-healing and thermoreversible rubber from supramolecular assembly. *Nature* **2008,** *451* (7181), 977-80; (b) Montarnal, D.; Cordier, P.; Soulié-Ziakovic, C.; Tournilhac, F.; Leibler, L., Synthesis of self-healing supramolecular rubbers from fatty acid derivatives, diethylene triamine, and urea. *Journal of Polymer Science Part A: Polymer Chemistry* **2008,** *46* (24), 7925-7936; (c) Montarnal, D.; Tournilhac, F.; Hidalgo, M.; Couturier, J. L.; Leibler, L., Versatile one-pot synthesis of supramolecular plastics and self-healing rubbers. *Journal of the American Chemical Society* **2009,** *131* (23), 7966-7; (d) Burattini, S.; Colquhoun, H. M.; Greenland, B. W.; Hayes, W., A novel self-healing supramolecular polymer system. *Faraday Discussions* **2009,** *143*, 251-264; (e) Burattini, S.; Greenland, B. W.; Hayes, W.; Mackay, M. E.; Rowan, S. J.; Colquhoun, H. M., A Supramolecular Polymer Based on Tweezer-Type pi-pi Stacking Interactions: Molecular Design for Healability and Enhanced Toughness. *Chemistry of Materials* **2010,** *23* (1), 6-8.
5. (a) Sijbesma, R. P.; Beijer, F. H.; Brunsveld, L.; Folmer, B. J. B.; Hirschberg, J. H. K. K.; Lange, R. F. M.; Lowe, J. K. L.; Meijer, E. W., Reversible Polymers Formed from Self-Complementary Monomers Using Quadruple Hydrogen Bonding. *Science* **1997,** *278* (5343), 1601-1604; (b) Brunsveld, L.; Folmer, B. J. B.; Meijer, E. W.; Sijbesma, R. P., Supramolecular Polymers. *Chemical Reviews* **2001,** *101* (12), 4071-4098; (c)

Bosman, A. W.; Sijbesma, R. P.; Meijer, E. W., Supramolecular polymers at work. *Materials Today* **2004,** *7* (4), 34-39; (d) van Beek, D. J. M.; Spiering, A. J. H.; Peters, G. W. M.; te Nijenhuis, K.; Sijbesma, R. P., Unidirectional Dimerization and Stacking of Ureidopyrimidinone End Groups in Polycaprolactone Supramolecular Polymers. *Macromolecules* **2007,** *40* (23), 8464-8475.
6. (a) Chen, X.; Dam, M. A.; Ono, K.; Mal, A.; Shen, H.; Nutt, S. R.; Sheran, K.; Wudl, F., A Thermally Re-mendable Cross-Linked Polymeric Material. *Science* **2002,** *295* (5560), 1698-1702; (b) Chen, X.; Wudl, F.; Mal, A. K.; Shen, H.; Nutt, S. R., New Thermally Remendable Highly Cross-Linked Polymeric Materials. *Macromolecules* **2003,** *36* (6), 1802-1807.
7. (a) Gotsmann, B.; Duerig, U.; Frommer, J.; Hawker, C. J., Exploiting Chemical Switching in a Diels–Alder Polymer for Nanoscale Probe Lithography and Data Storage. *Advanced Functional Materials* **2006,** *16* (11), 1499-1505; (b) Costanzo, P. J.; Beyer, F. L., Thermoresponsive, Optically Active Films Based On Diels-Alder Chemistry. *Chemistry of Materials* **2007,** *19* (25), 6168-6173; (c) Adzima, B. J.; Aguirre, H. A.; Kloxin, C. J.; Scott, T. F.; Bowman, C. N., Rheological and chemical analysis of reverse gelation in a covalently crosslinked Diels-Alder polymer network. *Macromolecules* **2008,** *41* (23), 9112-9117; (d) Peterson, A. M.; Jensen, R. E.; Palmese, G. R., Reversibly cross-linked polymer gels as healing agents for epoxy-amine thermosets. *ACS Appl Mater Interfaces* **2009,** *1* (5), 992-5; (e) Reutenauer, P.; Buhler, E.; Boul, P. J.; Candau, S. J.; Lehn, J. M., Room temperature dynamic polymers based on Diels-Alder chemistry. *Chemistry* **2009,** *15* (8), 1893-900; (f) Inglis, A. J.; Nebhani, L.; Altintas, O.; Schmidt, F. G.; Barner-Kowollik, C., Rapid Bonding/Debonding on Demand: Reversibly Cross-Linked Functional Polymers via Diels‚àíAlder Chemistry. *Macromolecules* **2010,** *43* (13), 5515-5520; (g) Peterson, A. M.; Jensen, R. E.; Palmese, G. R., Room-Temperature Healing of a Thermosetting Polymer Using the Diels-Alder Reaction. *ACS Appl Mater Interfaces* **2010,** *2* (4), 1141-1149; (h) Swanson, J. P.; Rozvadovsky, S.; Seppala, J. E.; Mackay, M. E.; Jensen, R. E.; Costanzo, P. J., Development of Polymeric Phase Change Materials On the basis of Diels-Alder Chemistry. *Macromolecules* **2010,** *43* (14), 6135-6141; (i) Sheridan, R. J.; Adzima, B. J.; Bowman, C. N., Temperature Dependent Stress Relaxation in a Model Diels-Alder Network. *Australian Journal of Chemistry* **2011,** *64* (8), 1094-1099; (j) Sheridan, R. J.; Bowman, C. N., A simple relationship relating linear viscoelastic properties and chemical structure in a model Diels-Alder polymer network. *Macromolecules* **2012,** (Accepted); (k) Murphy, E. B.; Bolanos, E.; Schaffner-Hamann, C.; Wudl, F.; Nutt, S. R.; Auad, M. L., Synthesis and Characterization of a Single-Component Thermally Remendable Polymer Network: Staudinger and Stille Revisited. *Macromolecules* **2008,** *41* (14), 5203-5209.
8. Adzima, B. J.; Kloxin, C. J.; Bowman, C. N., Externally Triggered Healing of a Thermoreversible Covalent Network via Self-Limited Hysteresis Heating. *Advanced Materials* **2010,** *22* (25), 2784-2787.
9. Ahmed, T. J.; Stavrov, D.; Bersee, H. E. N.; Beukers, A., Induction welding of thermoplastic composites-an overview. *Composites Part A: Applied Science and Manufacturing* **2006,** *37* (10), 1638-1651.
10. Bozorth, R. M., *Ferromagnetism*. 3rd ed.; IEEE Press. : Piscataway, NJ, 1993.

11. Peterson, A. M.; Jensen, R. E.; Palmese, G. R., Thermoreversible and remendable glass-polymer interface for fiber-reinforced composites. *Composites Science and Technology* **2011,** *71* (5), 586-592.
12. (a) Wool, R. P.; O'Connor, K. M., A theory crack healing in polymers. *J Appl Phys* **1981,** *52* (10), 5953-5963; (b) Wool, R. P.; O'Connor, K. M., Time dependence of crack healing. *Journal of Polymer Science: Polymer Letters Edition* **1982,** *20* (1), 7-16; (c) Jud, K.; Kausch, H. H.; Williams, J. G., Fracture mechanics studies of crack healing and welding of polymers. *J Mater Sci* **1981,** *16* (1), 204-210-210.
13. (a) Hopewell, J. L.; Hill, D. J. T.; Pomery, P. J., Electron spin resonance study of the homopolymerization of aromatic bismaleimides. *Polymer* **1998,** *39* (23), 5601-5607; (b) Hopewell, J. L.; George, G. A.; Hill, D. J. T., Quantitative analysis of bismaleimide-diamine thermosets using near infrared spectroscopy. *Polymer* **2000,** *41* (23), 8221-8229.

Chapter 7: Photothermal Nanocomposite Covalent Adaptable Networks: Optical Manipulation of a Thermally Responsive Material Containing Robust Au@SiO_2 Chromophores

Abstract

The photothermal effect observed when metal nanoparticles absorb light due to localized surface plasmon resonance (LSPR), has found use in applications that demand localized, switchable heating, such as microfluidic switching, cancer treatment, and drug release. Thermally reversible covalent adaptable networks (TR-CANs) are smart polymeric network materials that contain crosslinks that cleave in response to heat and subsequently relax stress through bond rearrangement. Photothermal nanocomposites of TR-CANs, comprised of the adaptable polymer network and specially coated gold nanoparticles that absorb 532nm light, respond to laser irradiation of sufficient intensity by locally heating and therefore relaxing stress in the beam path, representing an opportunity to demonstrate the use the photothermal effect outside of the limited set of applications in which this approach has been used to date. This approach has the surprising consequence of creating topographical features at the exposure site, which range from 200 micron high by 350 micron wide hemispheres, to 5 by 500 micron Gaussian peaks, depending on exposure conditions and sample age. We investigate these features in terms of their dependence on laser power and exposure time, as well as sample curing and aging.

Introduction

Covalent adaptable networks (CANs) are polymer networks crosslinked with reactive bonds that, in the presence of an appropriate stimulus, activate and reversibly dissociate. This triggerable rearrangement of crosslinks is the source of a number of interesting properties that these materials have been shown to exhibit, such as: stress relief, including polymerization-shrinkage-induced stress;[1] incorporation of chemical functionality post-cure;[2] chemical welding of interfaces, including fractures;[3] recyclability;[4] control of the diffusivity of particles via adjustable mesh size;[5] and actuation of mechanical motion.[6] One of the most promising classes of CANs is the photoreversible network, wherein crosslink scission is mediated via reversible addition fragmentation chain-transfer (RAFT) of radicals generated by photoinitiation. Photo-CANs have been used in stress relaxation,[7] patterned texturing,[8] and photoactuated shape memory motion.[6] Recently, even repeatable photohealing has been demonstrated via this RAFT strategy.[9] Generally, the effects observed are the result of the strong spatial and temporal control of stress relaxation afforded by the light-activated nature of the process. However, despite the name, the RAFT process is not perfectly reversible, as it is highly coupled to the notoriously irreversible processes of radical initiation and termination. Furthermore, the radicals themselves are subject to a wide variety of potential side reactions that limit reversibility.

Thermoreversible CANs represent an alternative network architecture that is in principle totally reversible. Among the possible thermoreversible reactions that are used in a network polymerization – such as the thermally reversible urea

linkages of Chan *et al*.[10] and the catalyzed ester exchange "vitrimers" of Montarnal *et al*.[11] – the Diels-Alder (DA) reaction between maleimide and furan represents one of the most ideal and orthogonal options. Our group has chemically and rheologically characterized[12] model DA networks, and has demonstrated their repeated, triggerable thermal activation.[13] Because the DA equilibrium conversion is strongly temperature dependent over a modest temperature range, one has substantial control over the material's properties, especially viscosity, despite the lack of any thermodynamic phase changes.

However, the fundamental roles of temperature and heat transfer are also natural limitations of thermoreversible networks. Typically, thermally activated (including thermoplastic) polymers are heated by ovens or hot plates, and involve using high temperatures at the external interface to drive heat into the material via thermal gradients. Using these methods, there will be an inevitable tradeoff between the desired speed, uniformity, and depth of activation. Our group has already considered one alternative heating method, the pseudo-bulk heating provided by hysteresis loss of ferromagnetic composites in an RF magnetic field.[13] This method provides fast, controlled, and relatively uniform heating, but lacks spatial control of photo-activated techniques. To move in the opposite direction, a technique providing total spatial and temporal control of temperature in a thermally activated CAN could be very useful.

In the presence of appropriate chromophores, generating heat with a high intensity light source is a straightforward method of achieving this goal. However, a

chromophore with specific characteristics is necessary to absorb the light and efficiently convert it to heat. Chemical dyes are not suitable in this application as they are subject to photochemical effects, including photobleaching at high intensity.[14] Metal ion dyes offer high stability, but a limited range of possible absorbance spectra due to the specific nature of the chemical complexation. Other highly stable absorbers, such as carbon black, have broad absorption that would limit their application. An ideal dye would have tunable absorption, thermal and chemical stability, and efficiently convert light to heat to enable local control over the heating and ultimate healing process.

The photothermal effect[15] observed when metal nanoparticles absorb light due to localized surface plasmon resonance (LSPR), has found use in applications that demand localized, switchable heating, such as microfluidic switching,[16] cancer treatment,[17] and drug release.[18] LSPR is a geometry dependent phenomenon, and is in principle tunable to absorb at many wavelengths from the visible to the infrared.[19] Noble metal nanoparticles themselves are generally stable, until extreme temperatures or light intensities are reached. However, chemisorbed capping ligands, which must approach equilibrium with the population dissolved in the surrounding matrix, are necessarily somewhat temperature sensitive.[20] To prevent irreversible aggregation and loss of LSPR, a covalently bound shell of silica can be added to the surface of the particles to form what has been termed Au@SiO_2 core/shell nanoparticles.[21] Here, the gold particles are coated with a SiO_2 shell where the gold particle at the core acts to convert light to heat efficiently and the silica shell prevents aggregation of the particles. Additionally, silica surfaces are

amenable to further functionalization to enhance compatibility with the matrix.[22] In the present work, we demonstrate the use of such Au@SiO_2 nanoparticles suspended in a DA network to produce a photothermally sensitized material with properties unlike those found elsewhere in the literature, and manipulate it on the micron to millimeter size scales using laser light.

Methods

Diels-Alder monomers

The Diels-Alder monomers, comprising a multifunctional furan and a difunctional maleimide, are identical to the SRF(3.0) r=1 composition described elsewhere.[23] Briefly, the multifuran SRF was derived from the Michael addition of furfuryl mercaptan to the commercial tetraacrylate SR295 from Sartomer. The effective functionality was adjusted to 3.0 by statistically substituting 30% of the furans with inert octanethiol. The multimaleimide used was the commercially available 1,1′-(methylenedi-4,1-phenylene) bismaleimide (DPBM). The monomers were mixed and heated to 170°C for 5 minutes to ensure that the DPBM crystals had melted and mixed with the liquid SRF. As the polymer cools, the DA reaction proceeds to high conversion and results in the formation of a glassy polymer, which maintains the capability to flow when reheated. SRF(3.0) r=1 has a reverse gel temperature of 106°C, corresponding to a gel point conversion of 71%.

Gold nanoparticles

Gold nanoparticle cores were synthesized according to the modified Frens method of Bastus and Puntes.[24] Briefly, sodium citrate was dissolved at a

concentration of 2.2 mM DI water and refluxed. 1 mL of a 25 mM solution of tetrachloroauric acid was injected into the refluxing solution, which quickly took on a brown-blue hue, then slowly transformed into a pink hue. After 10 minutes, the solution was cooled to 90°C, at which point a 2 mL aliquot was removed. Two additional growth cycles (1 mL 60 mM trisodium citrate followed by 1 mL 25 mM tetrachloroauric acid and a 30 minute reaction time) produced citrate protected 15-20 nm diameter gold-citrate (Au-Cit) nanoparticles used as cores that were subsequently silica coated. Peak absorbance was at 522 nm, as shown in Figure 7.1.

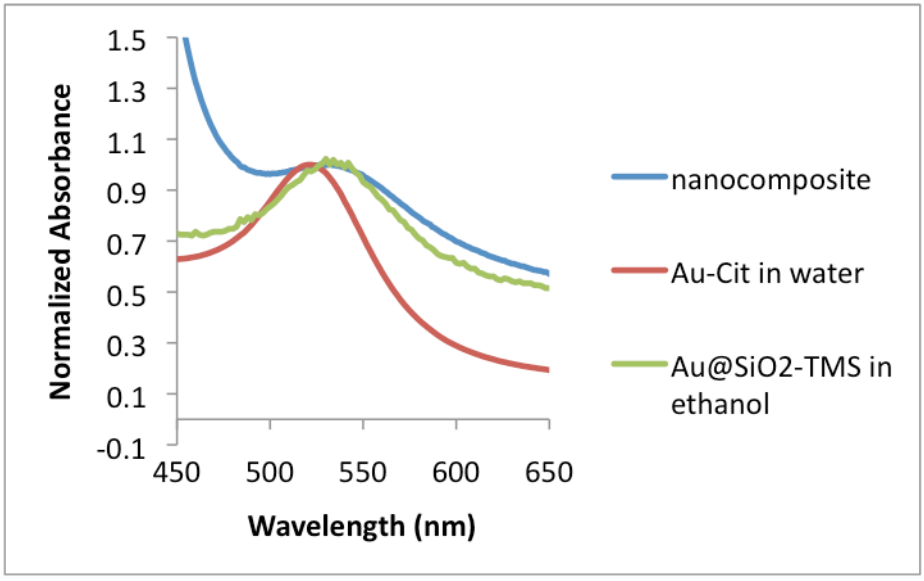

Figure 7.1: UV-Vis absorbance spectrum of gold nanoparticles in various matrices. Absorptions are normalized to the plasmon peak. The silica coating causes a redshift in the plasmon relative to Au-Cit, but compositing the Au@SiO_2 with the Diels-Alder material does not lead to a substantial shift.

Au@SiO_2

Gold citrate cores were coated with silica according to the modified biphasic Stoeber sol-gel process of Schulzendorf *et al.*[21] 20 mL of as-synthesized Au-Cit in

water was passed through a 200nm PTFE filter into a roundbottom flask, and covered with 10mL of iso-octane. The pH was titrated to >9 by the addition of 1N NaOH. This solution was stirred at 100RPM and in an oil bath at 60°C. 0.5 mL of 20 mM L-arginine solution was added to the vessel. After 10 minutes, 0.5-1 μL of mercaptopropyl trimethoxysilane was added to the octane phase and allowed to react overnight. 2-20 μL of TEOS was added and allowed to react for 24 hours. The exact amounts of the silica containing reagents were determined by direct experimentation and depended on the batch of Au-Cit cores. At this point the phases were separated and the aqueous phase was again passed through a 200nm filter. The filtered colloid was diluted with 60 mL of 190 proof ethanol and stirring was increased to 500 RPM. Finally, 4 mL of hexamethyl disilazane was added under vigorous stirring at 60°C and allowed to react overnight. The resultant Au@SiO_2 colloid was cleaned by repeated centrifugation at 11000 RPM and could be suspended in acetone, ethanol, or other organic solvents. The UV-Visible absorption spectrum is shown in Figure 7.1, and a TEM image of the composite particles is presented in Figure 7.2.

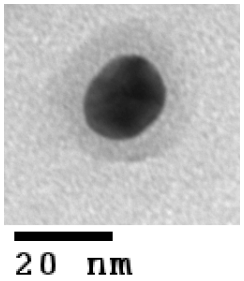

Figure 7.2: TEM micrograph of an Au@SiO2 particle, with the dark core of gold, and light shell of silica visible. Coating thickness varies but is between 5-10 nm for most particles.

Photothermal nanocomposite sample preparation

The particles from the previous step were resuspended in acetone, and then mixed with the SRF monomer mixture. The acetone was then removed by rotary evaporation. The SRF/Au@SiO_2 colloid had a stable red color, and could be handled like a non-composite material. For this work, we used a particle loading of ~10^{-4} g Au/g SRF, estimated by assuming ~50% yield of $HAuCl_4$ in the 20mL SRF/Au@SiO_2 colloid batch, suspended in 0.5g SRF. It was then mixed with DPBM and heated to 170°C in a preheated oven, then cast into silicone or butyl rubber molds of the appropriate shape. Samples were allowed to come to ambient temperature in their molds. If an alternative thermal history was desired, the bars were returned to an appropriately preheated oven for the required amount of accelerated aging.

Laser experimental setup

The naked beam of a 532nm Nd-YAG laser, with a maximum total power output of 89 mW, was used for all experiments. The beam had an approximately Gaussian profile, with a spot size of 0.51 mm, as measured by the 90-10 knife-edge technique ($X_{90\text{-}10}$=0.65mm). When appropriate, the beam intensity was attenuated using a variable reflectance disk. The beam path was quickly switched between sample exposure and a photoelectric power meter using a flip down mirror.

Surface feature profilometry

A Veeco Dektak 6M stylus profilometer was used to measure the profile of surface features developed on the nanocomposite samples. Visual inspection showed that features were generally radially symmetric. Profiles were taken from

lines that were as close as possible to the center of the feature, as determined by finding the position that produced the greatest height. Profiles were leveled manually, aiming to produce the most symmetrical profile about the maximum.

Results and Discussion

Robustness of Au@SiO_2 LSPR effect under heating

To determine whether the Au@SiO_2 composite materials indeed exhibit the desired photothermal effect in a robust manner, films of the composite were cast onto glass slides and inserted into a heated UV/Vis spectrometer. Absorbance of light by the material was monitored as a function of time at 150°C, a temperature higher than we reasonably expect to be able to generate via the photothermal effect, based on direct temperature measurements of substantially higher optical density films by Maity *et al.*[25] As can be seen in Figure 7.3, for each temperature, the plasmon absorbance remains roughly constant after initial settling of the sample, while absorbance from the matrix starts mostly in the ultraviolet, but shifts out to overwhelm the plasmon over time.

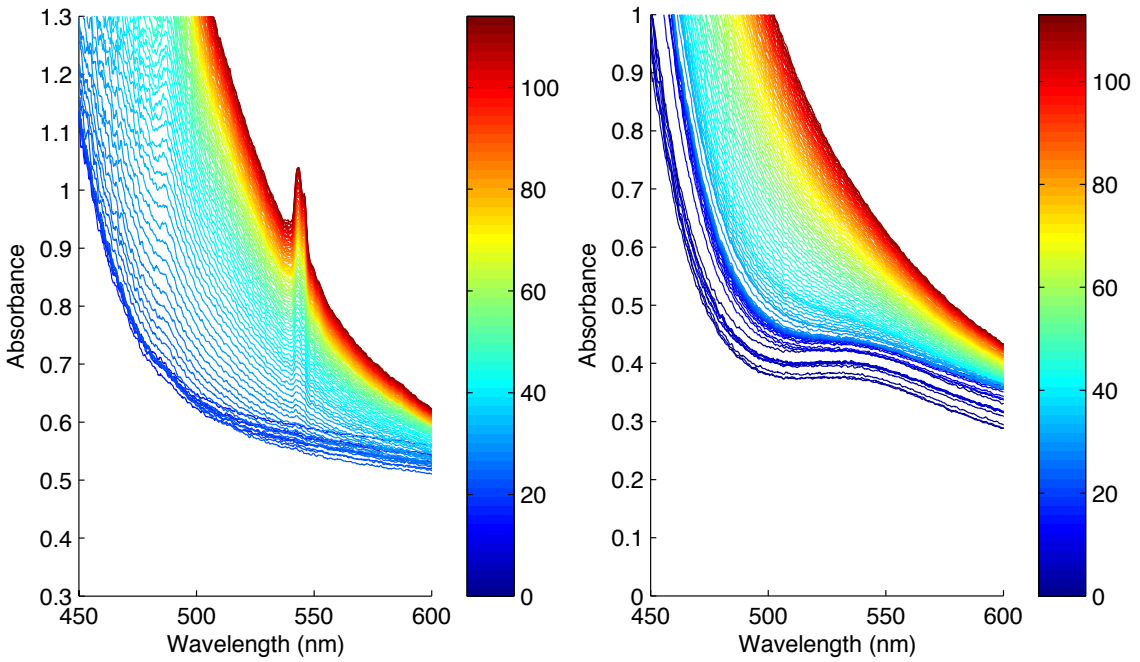

Figure 7.3: UV-Vis spectroscopy evaluation of material versus nanoparticle stability of the DA nanocomposite over 2 hours at 200°C. Time is indicated by the coloring of the line: short times are blue, whereas later times are indicated by yellow and then red. The color bar indicates the corresponding time of a specific color. Spectra were taken one minute apart. (Left) The DA material with no nanoparticle loading exhibits additional absorbance at short wavelengths over time, qualitatively "browning" due to heat. The peaks are from uncorrected ambient lighting changes. (Right) When loaded with Au@SiO_2 particles, the absorbance of the particles is initially apparent, but is slowly overwhelmed by the browning of the matrix.

The plasmon absorbance remains stable under other harsh conditions as well, including centrifugation, removal of solvent by rotary evaporation, and the high temperatures of the casting process. In comparison, alkanethiol, PEG-thiol, and other commonly used thiol protecting ligands exhibited a large redshift of the plasmon absorbance peak under otherwise identical conditions. We determined this redshift to be likely due to desorption of the ligands into the matrix, followed by reaction of the thiol with free maleimide groups. Such a condition at high

temperature quickly results in the irreversible consumption of the protective monolayer of capping ligands, followed by the irreversible aggregation of the unprotected gold nanoparticles.

Material response to laser irradiation

Having determined that we could reasonably expect extended and repeated use of the photothermal effect under our conditions of interest, sample bars (4x2x25mm) of the nanocomposite with a characteristic absorption length were cast and exposed to an 87 mW 532 nm CW laser with a spot size ($1/e^2$ radius, w_0) of 0.51 mm, corresponding to an approximate average irradiance of ~10 W/cm^2. This approach had the effect of raising smooth, lasting bumps on the bar's surface, shown in Figure 7.4. After as little as 30 seconds, a physical bump formed which remained present even after several months.

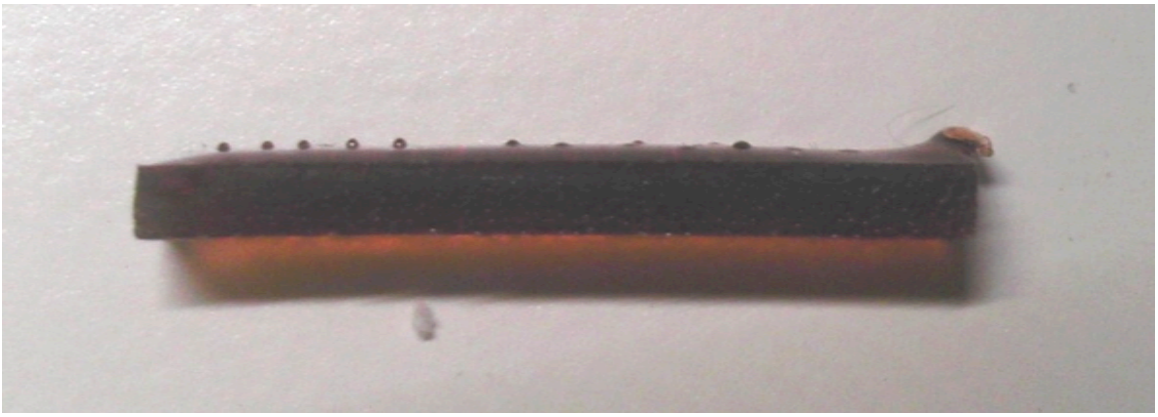

Figure 7.4: Features raised on DA-Au@SiO_2 composite bars by laser illumination from above (or downwards, relative to the photo on this page.) Features were created at a variety of laser powers and exposure times on the same bar, varying from 0.2 mm hemispheres to 0.005 mm Gaussian bumps.

Figure 7.5 shows a profile of one of the largest features. The profile appears to be hemispherical, but skewed to one side. In that and each other feature showing

skew, the direction of skew was in the direction of the pull of gravity during exposure. This occurs in a sample irradiated with 87 mW of laser power for three minutes, which had been annealed at ambient conditions for 8 days. A sample with a different thermal history, 48 hours of annealing at 80°C, produced smaller, quasi-Gaussian features at a similar laser power.

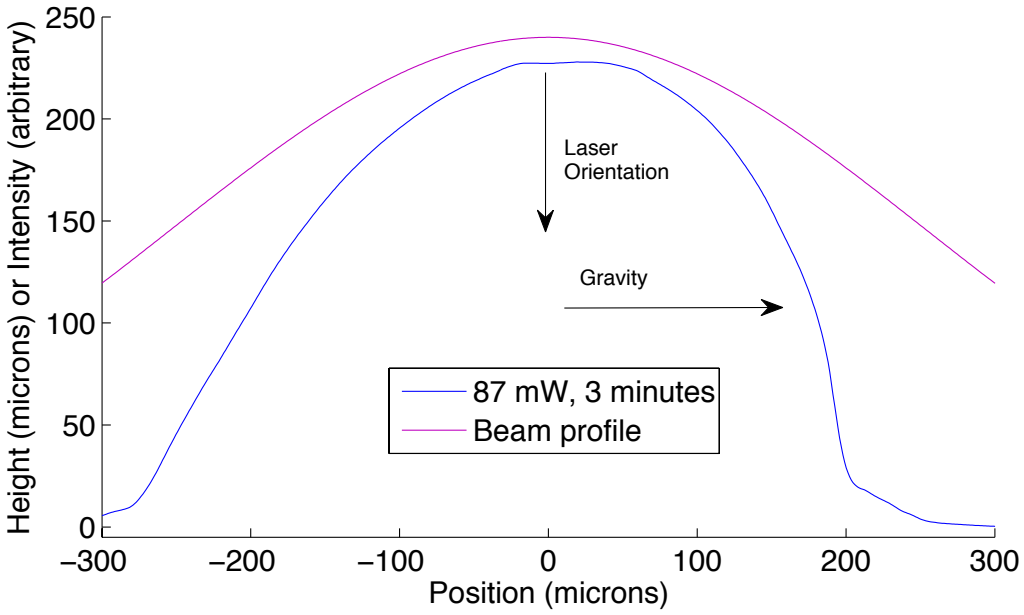

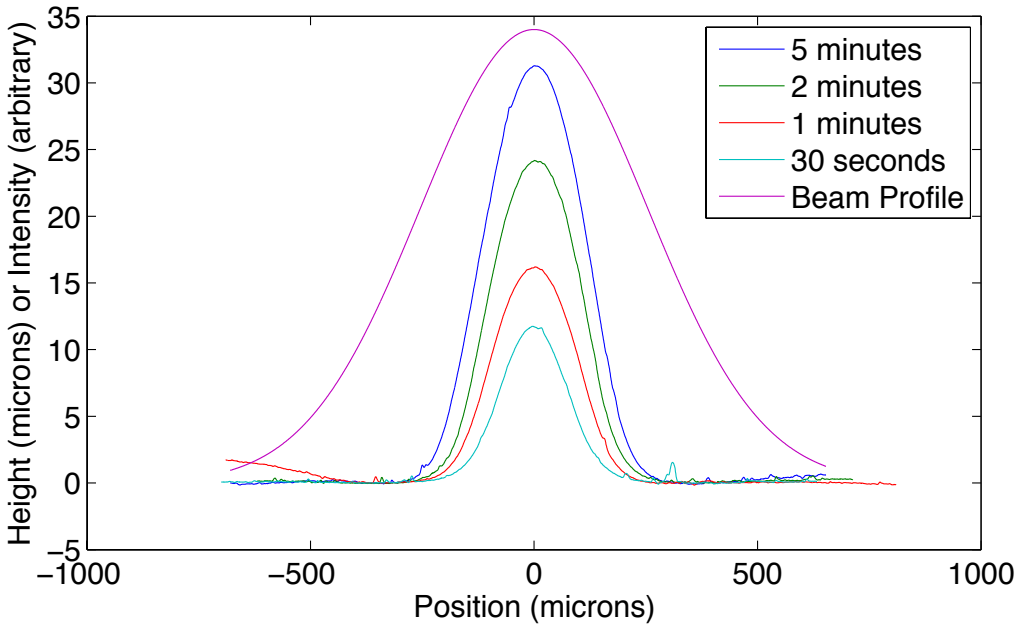

Figure 7.5: (Top) Profile of a feature raised on a DA-Au@SiO_2 composite, overlaid with the incident laser beam intensity profile. This profile was the result of a three minute exposure to a 87 mW laser 8 days after casting the substrate. Skew is in the direction of the force of gravity during exposure. (Bottom) Profiles of the 80 mW experiments at various exposure times in a sample aged for 48 hours at 80°C. Peaks are roughly Gaussian, and are not skewed in the direction of the pull of gravity during irradiation. The beam intensity profile is overlaid, demonstrating that the region of activation is significantly narrower than the beam.

Such features have, to our knowledge, not been reported in any composition in the literature to date. These data thus suggest that the effect is a unique property of our composite or process. To gain insight into the nature of the phenomenon, a systematic study of the various controllable parameters was undertaken. The same bar as above was subjected (15 days later) to exposures of the beam at powers of 87, 74, and 60mW, for 5 minutes, at unique locations. Additionally, for the 87 and 60 mW cases, the duration of the exposure was varied to 0.5 and 1 minute in the former case, and 3 and 15 minutes in the latter. These data are presented in Figure 7.6.

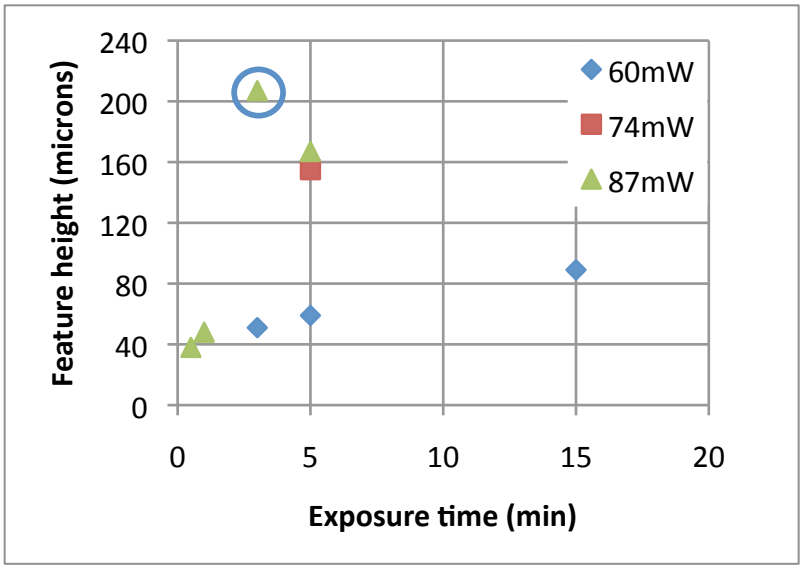

Figure 7.6: Heights of features raised by 0.5 - 15 minute irradiation of DA-Au@SiO_2 at total laser powers of 87, 74, and 60 mW. All measurements were on the same physical sample, but the circled feature was created and measured 15 days before the rest. Feature height has a linear dependence on exposure time, but nonlinear dependence on laser power.

This result reveals several trends. Over the range studied, the feature height seems to be a linear function of time (after some initial short-time effects) though the slope of this line seems to be a nonlinear function of laser power, as the 74 mW exposure resulted in a feature that more closely tracks the 87 mW measurement than the 60 mW measurement, despite being a midpoint temperature. Finally, the initial 3 minute, 87 mW exposure does not fall on the same line as the rest of the exposure times for the same power. This value was collected two weeks earlier than all the other points, implying that vitrification and physical aging may play a substantial role in determining the outcome of a given exposure condition. Indeed, when plotting comparable exposures on the same bar (stored at ambient conditions), there is a distinct downward trend over time (Figure 7.7).

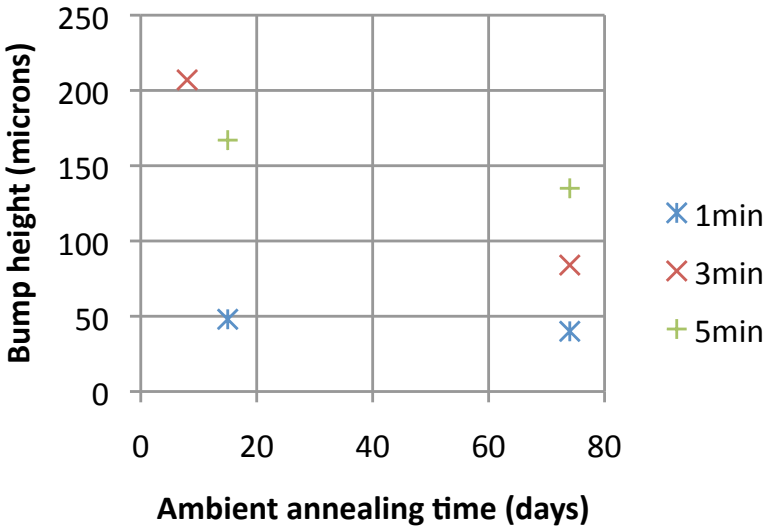

Figure 7.7: The effect of physical aging or annealing at ambient conditions, prior to exposure, on the height of bumps raised in DA-Au@SiO_2 with laser light. (80 mW total power, except for the top left measurement, which was 87 mW.) Achievable feature height tended downwards over time.

To probe the effect of vitrification, accelerated aging experiments were performed where a separate bar identical to the previous experiment was split into three parts, aged at 3 separate temperatures (78°C, 92°C, and 101°C) for 21 hours. Notably, during this aging process, the bar sections maintained their geometry except for the one aged at the highest temperature, which flowed into a globular shape. These were exposed to 80mW of laser power for 1 minute each, which was then compared to the 1 minute exposure as depicted in Figure 7.6 (Results in Figure 7.8). There is a distinct trend in which aging reduces the feature height achieved in that time, which is consistent with the reduction due to aging over two weeks at ambient temperature. Extrapolating, one might expect sufficient ambient temperature aging to reduce the achievable feature height to as little as 10 microns in 1 minute.

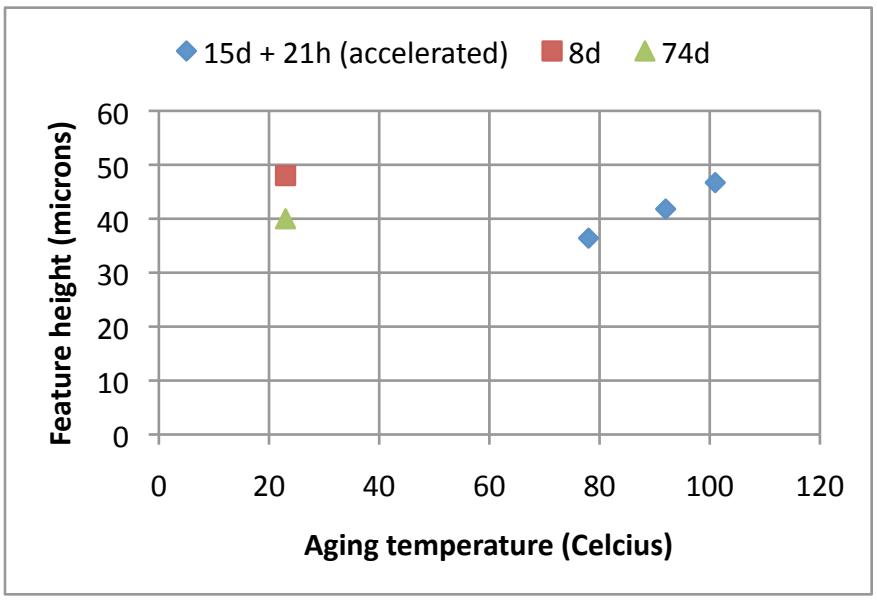

Figure 7.8: Effect of accelerated aging on the height of bumps raised in DA-Au@SiO_2 with 80mW of laser light for one minute. If we assume the accelerated aging samples reach their corresponding equilibrium free volume with no stress at that temperature, the graph indicates that samples aged at lower temperature have less stress available to form features.

These experiments point to one particular interpretation of the causes of the formation of the bumps in terms of molecular mobility. Of course, we must conserve mass, so therefore we expect the effect is largely due to a volumetric expansion or contraction of some component of the polymer composite. When the Diels-Alder network is mixed, heated to 170°C, and cooled to ambient to cure and vitrify, a stress is built into the material, essentially resulting from a combination of densification associated with the polymerization and that associated with thermal expansion (or contraction). This results in the bulk essentially squeezing any given volumetric element. This shrinkage is observed in other circumstances, such as when cooling (composite or non-composite) Diels-Alder materials are constrained at a rigid surface like silica glass: residual films on glass vials from the bar casting

process tend to fracture spontaneously, and allowing entire vials full of Diels-Alder material to cool can result in delamination, fracture, or even the glass vial itself fracturing.

When exposed to heat from the photothermal effect, the illuminated volume gains enough thermal energy to relax that stress, and any additional stress due to thermal expansion or depolymerization, via transient network viscoelasticity. Because the cylindrical edge of the beam remains glassy, only the top surface (and bottom, if sufficient heating occurs) represents a free interface for the volume to flow into, and bumps are produced. These bumps cool and vitrify quickly as the laser is switched off, and remain static on glassy timescales. Aging, whether accelerated or at ambient conditions, results in overall stress relaxation, and with less intrinsic stress the material requires reduced strain to relieve it, i.e. smaller bumps. Following this line of reasoning, an aged sample would not only exhibit reduced bump height, but also a reduced maximum bump height. This effect was seen in the sample aged for 48 hours at 80°C, as shown in Figure 7.9.

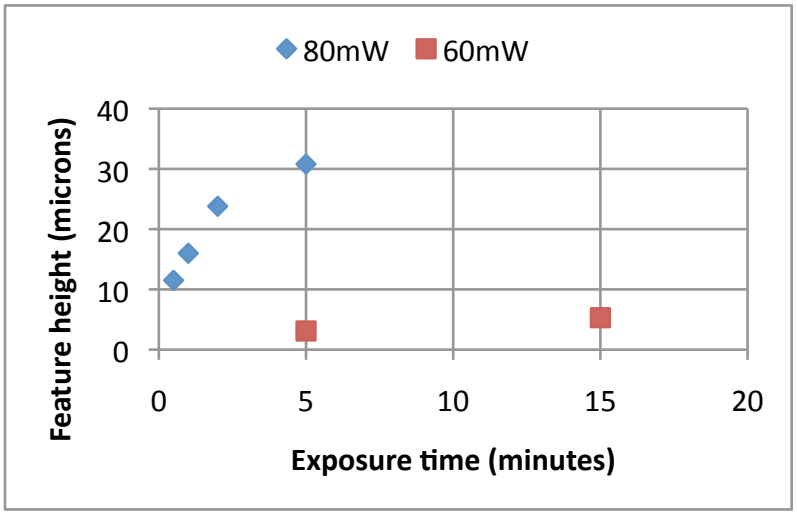

Figure 7.9: Additional (48 hours total) aging at 80°C leads to non-linear time dependence of bump height at 80 mW laser power. 60 mW exposures on the same sample raised extremely small bumps.

Conclusion

In this study we have demonstrated a thermoreversible covalent adaptable network nanocomposite material, showing a photothermal response to irradiation with laser light of sufficient intensity. Though much work has been focused on either biomedical hypothermia applications of the photothermal effect or the switchable lower critical solution temperature of poly(N-isopropylacrylamide) (pNIPAAm), relatively little has been studied about the potential to use the effect to trigger responses in other thermally responsive materials, particularly polymer networks and actuating materials. This report shows that a judicious combination of nanoparticle and matrix can result in interesting and unusual phenomena. The observed response, although unexpected, is explicable in terms of standard polymer materials concepts such as vitrification, thermal expansion, and shrinkage. Presently, we have attributed the behavior to the presence of a residual stress, which is likely related to the ongoing Diels-Alder reaction volume change outpacing mechanical relaxation during vitrification. However, our results so far cannot definitively differentiate between this working hypothesis and any other. Despite these limitations, we believe this CAN nanocomposite presents a promising platform for the creation of a series of photoactivatable smart materials, with application in diverse fields such as mechanophotopatterning, optical materials, metamaterials, and healable materials.

References

1. (a) Park, H. Y.; Kloxin, C. J.; Scott, T. F.; Bowman, C. N., Stress Relaxation by Addition-Fragmentation Chain Transfer in Highly Cross-Linked Thiol-Yne Networks. *Macromolecules* **2010,** *43* (24), 10188-10190; (b) Kloxin, C. J.; Scott, T. F.; Bowman, C. N., Stress Relaxation via Addition-Fragmentation Chain Transfer in a Thiol-ene Photopolymerization. *Macromolecules* **2009,** *42* (7), 2551-2556.
2. Amamoto, Y.; Kikuchi, M.; Masunaga, H.; Sasaki, S.; Otsuka, H.; Takahara, A., Reorganizable Chemical Polymer Gels Based on Dynamic Covalent Exchange and Controlled Monomer Insertion. *Macromolecules* **2009,** *42* (22), 8733-8738.
3. (a) Chen, X.; Dam, M. A.; Ono, K.; Mal, A.; Shen, H.; Nutt, S. R.; Sheran, K.; Wudl, F., A Thermally Re-mendable Cross-Linked Polymeric Material. *Science* **2002,** *295* (5560), 1698-1702; (b) Chen, X.; Wudl, F.; Mal, A. K.; Shen, H.; Nutt, S. R., New Thermally Remendable Highly Cross-Linked Polymeric Materials. *Macromolecules* **2003,** *36* (6), 1802-1807.
4. Craven, J. M. Cross-linked Thermally Reversible Polymers Produced from Condensation Polymers with Pendant Furan Groups Cross-linked with Maleimides. 3435003, 1969.
5. Roberts, M. C.; Mahalingam, A.; Hanson, M. C.; Kiser, P. F., Chemorheology of Phenylboronate-Salicylhydroxamate Cross-Linked Hydrogel Networks with a Sulfonated Polymer Backbone. *Macromolecules* **2008,** *41* (22), 8832-8840.
6. Scott, T. F.; Draughon, R. B.; Bowman, C. N., Actuation in Crosslinked Polymers via Photoinduced Stress Relaxation. *Advanced Materials* **2006,** *18* (16), 2128-2132.
7. Scott, T. F.; Schneider, A. D.; Cook, W. D.; Bowman, C. N., Photoinduced Plasticity in Cross-Linked Polymers. *Science* **2005,** *308* (5728), 1615-1617.
8. Kloxin, C. J.; Scott, T. F.; Park, H. Y.; Bowman, C. N., Mechanophotopatterning on a Photoresponsive Elastomer. *Advanced Materials* **2011,** *23* (17), 1977-1981.
9. Amamoto, Y.; Kamada, J.; Otsuka, H.; Takahara, A.; Matyjaszewski, K., Repeatable Photoinduced Self-Healing of Covalently Cross-Linked Polymers through Reshuffling of Trithiocarbonate Units. *Angewandte Chemie* **2011,** *123* (7), 1698-1701.
10. Chang, J. Y.; Do, S. K.; Han, M. J., A sol-gel reaction of vinyl polymers based on thermally reversible urea linkages. *Polymer* **2001,** *42* (18), 7589-7594.
11. Montarnal, D.; Capelot, M.; Tournilhac, F. o.; Leibler, L., Silica-Like Malleable Materials from Permanent Organic Networks. *Science* **2011,** *334* (6058), 965-968.
12. (a) Kloxin, C. J.; Scott, T. F.; Adzima, B. J.; Bowman, C. N., Covalent Adaptable Networks (CANs): A Unique Paradigm in Cross-Linked Polymers. *Macromolecules* **2010,** *43* (6), 2643-2653; (b) Adzima, B. J.; Aguirre, H. A.; Kloxin, C. J.; Scott, T. F.; Bowman, C. N., Rheological and chemical analysis of reverse gelation in a covalently crosslinked Diels-Alder polymer network. *Macromolecules* **2008,** *41* (23), 9112-9117; (c) Sheridan, R. J.; Adzima, B. J.; Bowman, C. N., Temperature Dependent Stress Relaxation in a Model Diels-Alder Network. *Australian Journal of Chemistry* **2011,** *64* (8), 1094-1099.

13. Adzima, B. J.; Kloxin, C. J.; Bowman, C. N., Externally Triggered Healing of a Thermoreversible Covalent Network via Self-Limited Hysteresis Heating. *Advanced Materials* **2010,** *22* (25), 2784-2787.
14. Meyvis, T.; De Smedt, S.; Van Oostveldt, P.; Demeester, J., Fluorescence Recovery After Photobleaching: A Versatile Tool for Mobility and Interaction Measurements in Pharmaceutical Research. *Pharmaceutical Research* **1999,** *16* (8), 1153-1162.
15. Govorov, A.; Richardson, H., Generating heat with metal nanoparticles. *Nano Today* **2007,** *2* (1), 30-38.
16. Sershen, S. R.; Mensing, G. A.; Ng, M.; Halas, N. J.; Beebe, D. J.; West, J. L., Independent Optical Control of Microfluidic Valves Formed from Optomechanically Responsive Nanocomposite Hydrogels. *Advanced Materials* **2005,** *17* (11), 1366-1368.
17. (a) Huang, X.; El-Sayed, I. H.; Qian, W.; El-Sayed, M. A., Cancer cell imaging and photothermal therapy in the near-infrared region by using gold nanorods. *Journal of the American Chemical Society* **2006,** *128* (6), 2115-20; (b) El-Sayed, I. H.; Huang, X.; El-Sayed, M. A., Selective laser photo-thermal therapy of epithelial carcinoma using anti-EGFR antibody conjugated gold nanoparticles. *Cancer Lett* **2006,** *239* (1), 129-35.
18. Skirtach, A. G.; Dejugnat, C.; Braun, D.; Susha, A. S.; Rogach, A. L.; Parak, W. J.; M√∂hwald, H.; Sukhorukov, G. B., The Role of Metal Nanoparticles in Remote Release of Encapsulated Materials. *Nano Lett* **2005,** *5* (7), 1371-1377.
19. (a) Hu, K. W.; Liu, T. M.; Chung, K. Y.; Huang, K. S.; Hsieh, C. T.; Sun, C. K.; Yeh, C. S., Efficient near-IR hyperthermia and intense nonlinear optical imaging contrast on the gold nanorod-in-shell nanostructures. *Journal of the American Chemical Society* **2009,** *131* (40), 14186-7; (b) Sardar, R.; Funston, A. M.; Mulvaney, P.; Murray, R. W., Gold nanoparticles: past, present, and future. *Langmuir* **2009,** *25* (24), 13840-51; (c) Palpant, B.; Pr; eacute; vel, B.; Lerm; J.; Cottancin, E.; Pellarin, M.; Treilleux, M.; Perez, A.; Vialle, J. L.; Broyer, M., Optical properties of gold clusters in the size range 2–4 nm. *Phys Rev B* **1998,** *57* (3), 1963; (d) Link, S.; El-Sayed, M. A., Shape and size dependence of radiative, non-radiative and photothermal properties of gold nanocrystals. *International Reviews in Physical Chemistry* **2000,** *19* (3), 409-453; (e) Link, S.; El-Sayed, M. A., Size and Temperature Dependence of the Plasmon Absorption of Colloidal Gold Nanoparticles. *The Journal of Physical Chemistry B* **1999,** *103* (21), 4212-4217.
20. Kim, S. Y.; Zukoski, C. F., Particle Restabilization in Silica/PEG/Ethanol Suspensions: How Strongly do Polymers Need To Adsorb To Stabilize Against Aggregation? *Langmuir* **2011**, null-null.
21. Schulzendorf, M.; Cavelius, C.; Born, P.; Murray, E.; Kraus, T., Biphasic synthesis of Au@SiO2 core-shell particles with stepwise ligand exchange. *Langmuir* **2011,** *27* (2), 727-32.
22. Badley, R. D.; Ford, W. T.; McEnroe, F. J.; Assink, R. A., Surface modification of colloidal silica. *Langmuir* **1990,** *6* (4), 792-801.
23. Sheridan, R. J.; Bowman, C. N., A simple relationship relating linear viscoelastic properties and chemical structure in a model Diels-Alder polymer network. *Macromolecules* **2012,** (Accepted).

24. Bastus, N. G.; Comenge, J.; Puntes, V., Kinetically Controlled Seeded Growth Synthesis of Citrate-Stabilized Gold Nanoparticles of up to 200 nm: Size Focusing versus Ostwald Ripening. *Langmuir* **2011**, null-null.
25. Maity, S.; Bochinski, J. R.; Clarke, L. I., Metal Nanoparticles Acting as Light-Activated Heating Elements within Composite Materials. *Advanced Functional Materials* **2012**, n/a-n/a.

Chapter 8: Conclusions and recommendation of future directions

This project has approached the question of the fundamental causes of the viscoelastic and mechanical behavior of thermoreversible networks, in order to better understand their complex response to activation in standard and novel applications, from reshaping via bulk heating to local laser heating. By choosing a facile model monomer system, we could creatively vary the parameters implied by established chemistry and materials science theory to directly test their predictions. After finding and verifying the necessary tools to describe the unusual transient network regime, we applied them to describe the processes of fracture healing by hysteresis heating, and photothermal activation by laser irradiation. It is our hope that this toolkit will provide the necessary understanding to advance the field of thermoreversible network materials, to develop new technology based on them, and to use them to solve known and as-yet-undiscovered problems.

Rheology of CANs

In Chapter 3, we have shown that, in a model transient network, a covalent network exists over short timescales at the conversions predicted by mean field polymerization theories. This result was indicated via measurements of G* by the similar scaling of G' and G'', as well as the magnitude of tan(δ) and the two different frequency scaling regions that were apparent at each temperature beyond the gel point. Furthermore, we have demonstrated that the frequency range of the key features in the complex modulus are strongly temperature dependent, even at

conversions not immediately adjacent to the gel point. The well-defined model covalent adaptable network allows for direct comparison to theory, and should provide insight towards the formulation of a more universal theory of transient network dynamics.

Semenov and Rubinstein's theory of linear dynamics for reversible networks was found to provide an appropriate description of the behavior of this model thermoreversible Diels-Alder network in a variety of situations near the gel point. Due to the simplicity of the model experimental system, this confirmation leads us to expect that the simple scaling relationship used in Chapter 4 has wide applicability to reversibly bonded polymer networks, whether covalent or non-covalent. By simple measurement of G(t) or G*(ω), the relaxation time or crossover time can be measured at one or two conditions, and parameters can be obtained that enable calculation of the important material properties over a wide range of temperature, conversion, and bond breakage rate values. Furthermore, the ratio of timescales is rewritten in terms of more accessible measurables, providing a useful qualitative description of the behavior of gelling thermoreversible materials for applications lacking sophisticated rheological equipment. Demonstration of the effectiveness of the rewritten relationships would be a sensible next step for this research.

Although other groups have had success with less fundamental approaches to the description of thermoreversible network viscoelasticity, it appears that these approaches are functionally subsets of the predictions provided by Semenov and

Rubinstein's work. We believe that this further demonstrates its value as a more flexible tool for predicting the properties of transient covalent (or physical) networks in their most characteristic regime. It represents a valuable tool in the structure-property toolkit for this class of materials, filling in the gap between the limiting cases where the classic tools – crosslink density calculations, small molecule viscosity measurements, and scaling exponents – apply.

The scaling relationship of Chapter 4 is in principle applicable to any transient network material satisfying the basic theoretical assumptions. A promising direction to continue this line of inquiry would be to attempt to apply the relationship to materials that push the boundaries of these assumptions. It should be possible to design materials that are analogous to those studied so far, except far from the gel point, highly cyclized, inhomogeneous, containing multiple types of reversible bonds, or containing reversible bonds which are not strongly temperature dependent. Such materials would allow probing of the limits of the theory on an assumption-by-assumption basis. Transient materials that contain breakable crosslinks, such as RAFT photoadaptable networks, that do not directly correspond to the paradigm of the transient networks considered by Semenov and Rubinstein may still be analyzed in terms of the timescale ratio, if a suitable first order crosslink chemical lifetime can be derived. An analysis of RAFT mechanics in terms of transient network theory could provide valuable insight into directions for new monomers and material compositions.

In Chapter 5, we determined that although TIRFM and MAPT are in principle capable of discerning microstructural mechanisms responsible for transient network relaxation, practical effects interfere with the model system of interest including operating temperature range, the need for extra solvent, and the background fluorescence that seems to be intrinsically attributable to one of the monomers. Future attempts on single-molecule microrheology should try to mitigate these issues, possibly by choosing a highly soluble, highly purified custom monomer system, and potentially avoiding completely the Diels-Alder reaction, in favor of a transient bond that does not involve such highly conjugated and likely fluorescent systems.

Modeling fracture healing using CrO_2 composites

In Chapter 6, we have successfully demonstrated that a triggered healable composite will achieve varying levels of healing depending on both healing conditions and, for the first time, network structure. Crucially, we have demonstrated this effect while maintaining constant bond kinetics (via constant temperature experiments), which is the primary variable with which other groups have controlled healing performance. To our knowledge, this is the first report of such a strategy. This approach allowed us to form a model of the process in which we completely isolate the mechanical relaxation from any changes in the temperature dependent chemical kinetic behavior, using information from the expected equilibrium structure of the network. This analysis should apply to other healable, reversibly bonded materials, including those networks which are intended

to heal at substantially different conditions, such as at room temperature or upon exposure to a different stimulus, such as light.

However, the experiments completed so far do leave some open questions, which could be the foundation for future work on the topic. By collecting more data at shorter and longer times, we can probe the range of applicability of the empirical, simplified healing model. With sufficient additional data or reduction in experimental variance, it may be possible to study the validity of the comprehensive theoretical model from which the empirical healing model was derived. An important factor in the complete model, the time-dependent temperature, was intentionally kept constant as other factors were studied. However, it is certainly possible to vary this curve in a controlled manner by adjusting parameters such as induction heater power or particle loading, as demonstrated in previous work in our group. Studying the interaction between the temperature ramp and effective functionality of a composition could provide additional insight into the validity of both the empirical and theoretical healing models described in Chapter 6.

Photothermal nanocomposite CANs

In Chapter 7 we have demonstrated a thermoreversible covalent adaptable network nanocomposite material, showing a photothermal response to irradiation with laser light of sufficient intensity. The observed response, although unexpected, is potentially explicable in terms of standard polymer materials concepts such as vitrification, thermal expansion and shrinkage. Presently, we have assumed the presence of residual shrinkage stress and excess free volume. This stress is likely

related to the ongoing Diels-Alder reaction volume change outpacing mechanical relaxation during vitrification. However, our results so far cannot differentiate between this working hypothesis and any other, so this should be an area of future investigation, along with studies varying material optical density and laser spot geometry, including interferogram and hologram patterning. Despite these limitations, we believe this CAN nanocomposite presents a promising platform for the creation of a series of photoactivatable smart materials, with application in diverse fields such as mechanophotopatterning, optical materials and metamaterials, or remotely healable materials.

Bibliography

Adzima, B. J.; Aguirre, H. A.; Kloxin, C. J.; Scott, T. F.; Bowman, C. N. Rheological and chemical analysis of reverse gelation in a covalently crosslinked Diels-Alder polymer network, *Macromolecules* **2008**, *41*, 9112.

Adzima, B. J.; Kloxin, C. J.; Bowman, C. N. Externally Triggered Healing of a Thermoreversible Covalent Network via Self-Limited Hysteresis Heating, *Advanced Materials* **2010**, *22*, 2784.

Ahmed, T. J.; Stavrov, D.; Bersee, H. E. N.; Beukers, A. Induction welding of thermoplastic composites-an overview, *Composites Part A: Applied Science and Manufacturing* **2006**, *37*, 1638.

Amamoto, Y.; Kamada, J.; Otsuka, H.; Takahara, A.; Matyjaszewski, K. Repeatable Photoinduced Self-Healing of Covalently Cross-Linked Polymers through Reshuffling of Trithiocarbonate Units, *Angewandte Chemie* **2011**, *123*, 1698.

Amamoto, Y.; Kikuchi, M.; Masunaga, H.; Sasaki, S.; Otsuka, H.; Takahara, A. Reorganizable Chemical Polymer Gels Based on Dynamic Covalent Exchange and Controlled Monomer Insertion, *Macromolecules* **2009**, *42*, 8733.

Badley, R. D.; Ford, W. T.; McEnroe, F. J.; Assink, R. A. Surface modification of colloidal silica, *Langmuir* **1990**, *6*, 792.

Bastus, N. G.; Comenge, J.; Puntes, V. Kinetically Controlled Seeded Growth Synthesis of Citrate-Stabilized Gold Nanoparticles of up to 200 nm: Size Focusing versus Ostwald Ripening, *Langmuir* **2011**, null.

Bergman, S. D.; Wudl, F. Mendable polymers, *Journal of Materials Chemistry* **2008**, *18*, 41.

Bosman, A. W.; Sijbesma, R. P.; Meijer, E. W. Supramolecular polymers at work, *Materials Today* **2004**, *7*, 34.

Bowman, C. N.; Kloxin, C. J. Covalent Adaptable Networks: Reversible Bond Structures Incorporated in Polymer Networks, *Angewandte Chemie International Edition* **2012**, *51*, 4272.

Bozorth, R. M. *Ferromagnetism*; 3rd ed.; IEEE Press. : Piscataway, NJ, 1993.

Brunsveld, L.; Folmer, B. J. B.; Meijer, E. W.; Sijbesma, R. P. Supramolecular

Polymers, *Chemical Reviews* **2001**, *101*, 4071.

Burattini, S.; Colquhoun, H. M.; Greenland, B. W.; Hayes, W. A novel self-healing supramolecular polymer system, *Faraday Discussions* **2009**, *143*, 251.

Burattini, S.; Greenland, B. W.; Hayes, W.; Mackay, M. E.; Rowan, S. J.; Colquhoun, H. M. A Supramolecular Polymer Based on Tweezer-Type pi-pi Stacking Interactions: Molecular Design for Healability and Enhanced Toughness, *Chemistry of Materials* **2010**, *23*, 6.

Chang, J. Y.; Do, S. K.; Han, M. J. A sol-gel reaction of vinyl polymers based on thermally reversible urea linkages, *Polymer* **2001**, *42*, 7589.

Chen, X.; Dam, M. A.; Ono, K.; Mal, A.; Shen, H.; Nutt, S. R.; Sheran, K.; Wudl, F. A Thermally Re-mendable Cross-Linked Polymeric Material, *Science* **2002**, *295*, 1698.

Chen, X.; Wudl, F.; Mal, A. K.; Shen, H.; Nutt, S. R. New Thermally Remendable Highly Cross-Linked Polymeric Materials, *Macromolecules* **2003**, *36*, 1802.

Chujo, Y.; Sada, K.; Saegusa, T. Reversible gelation of polyoxazoline by means of Diels-Alder reaction, *Macromolecules* **1990**, *23*, 2636.

Cordier, P.; Tournilhac, F.; Soulie-Ziakovic, C.; Leibler, L. Self-healing and thermoreversible rubber from supramolecular assembly, *Nature* **2008**, *451*, 977.

Costanzo, P. J.; Beyer, F. L. Thermoresponsive, Optically Active Films Based On Diels-Alder Chemistry, *Chemistry of Materials* **2007**, *19*, 6168.

Craven, J. M. 1969.

de Gennes, P. G. *Scaling concepts in polymer physics*; Cornell University Press: Ithaca, N.Y., 1979.

Diels, O.; Alder, K. Synthesen in der hydroaromatischen Reihe, *Justus Liebigs Annalen der Chemie* **1928**, *460*, 98.

Dotson, N. A.; Galvan, R.; Laurence, R. L.; Tirrell, M. *Polymerization Process Modeling*; Wiley-VCH: New York, 1995.

El-Sayed, I. H.; Huang, X.; El-Sayed, M. A. Selective laser photo-thermal therapy of epithelial carcinoma using anti-EGFR antibody conjugated gold nanoparticles, *Cancer Lett* **2006**, *239*, 129.

Feldman, K. E.; Kade, M. J.; Meijer, E. W.; Hawker, C. J.; Kramer, E. J. Model Transient Networks from Strongly Hydrogen-Bonded Polymers,

Macromolecules **2009**, *42*, 9072.

Ferry, J. D. *Viscoelastic properties of polymers*; 3rd ed. ed.; Wiley: New York, 1980.

Flory, P. J. Molecular Size Distribution in Three Dimensional Polymers. I. Gelation1, *J Am Chem Soc* **1941**, *63*, 3083.

Flory, P. J. Fundamental Principles of Condensation Polymerization, *Chemical Reviews* **1946**, *39*, 137.

Goiti, E.; Heatley, F.; Huglin, M. B.; Rego, J. M. Kinetic aspects of the Diels-Alder reaction between poly(styrene-co-furfuryl methacrylate) and bismaleimide, *European Polymer Journal* **2004**, *40*, 1451.

Goiti, E.; Huglin, M. B.; Rego, J. M. Some properties of networks produced by the Diels-Alder reaction between poly(styrene-co-furfuryl methacrylate) and bismaleimide, *European Polymer Journal* **2004**, *40*, 219.

Gotsmann, B.; Duerig, U.; Frommer, J.; Hawker, C. J. Exploiting Chemical Switching in a Diels–Alder Polymer for Nanoscale Probe Lithography and Data Storage, *Advanced Functional Materials* **2006**, *16*, 1499.

Goussé, C.; Gandini, A. Diels–Alder polymerization of difurans with bismaleimides, *Polymer International* **1999**, *48*, 723.

Govorov, A.; Richardson, H. Generating heat with metal nanoparticles, *Nano Today* **2007**, *2*, 30.

Herrmann, H. J. Geometrical cluster growth models and kinetic gelation, *Physics Reports* **1986**, *136*, 153.

Honciuc, A.; Harant, A. W.; Schwartz, D. K. Single-Molecule Observations of Surfactant Diffusion at the Solution-Solid Interface, *Langmuir* **2008**, *24*, 6562.

Hopewell, J. L.; Hill, D. J. T.; Pomery, P. J. Electron spin resonance study of the homopolymerization of aromatic bismaleimides, *Polymer* **1998**, *39*, 5601.

Hu, K. W.; Liu, T. M.; Chung, K. Y.; Huang, K. S.; Hsieh, C. T.; Sun, C. K.; Yeh, C. S. Efficient near-IR hyperthermia and intense nonlinear optical imaging contrast on the gold nanorod-in-shell nanostructures, *J Am Chem Soc* **2009**, *131*, 14186.

Huang, X.; El-Sayed, I. H.; Qian, W.; El-Sayed, M. A. Cancer cell imaging and photothermal therapy in the near-infrared region by using gold nanorods, *J Am Chem Soc* **2006**, *128*, 2115.

Inglis, A. J.; Nebhani, L.; Altintas, O.; Schmidt, F. G.; Barner-Kowollik, C. Rapid Bonding/Debonding on Demand: Reversibly Cross-Linked Functional Polymers via Diels,àíAlder Chemistry, *Macromolecules* **2010**, *43*, 5515.

Jay, J. I.; Langheinrich, K.; Hanson, M. C.; Mahalingam, A.; Kiser, P. F. Unequal stoichiometry between crosslinking moieties affects the properties of transient networks formed by dynamic covalent crosslinks, *Soft Matter* **2011**, *7*, 5826.

Jones, J. R.; Liotta, C. L.; Collard, D. M.; Schiraldi, D. A. Cross-Linking and Modification of Poly(ethylene terephthalate-co-2,6-anthracenedicarboxylate) by Diels,àíAlder Reactions with Maleimides, *Macromolecules* **1999**, *32*, 5786.

Jud, K.; Kausch, H. H.; Williams, J. G. Fracture mechanics studies of crack healing and welding of polymers, *Journal of Materials Science* **1981**, *16*, 204.

Kastantin, M.; Langdon, B. B.; Chang, E. L.; Schwartz, D. K. Single-Molecule Resolution of Interfacial Fibrinogen Behavior: Effects of Oligomer Populations and Surface Chemistry, *J Am Chem Soc* **2011**, *133*, 4975.

Kastantin, M.; Schwartz, D. K. Connecting Rare DNA Conformations and Surface Dynamics Using Single-Molecule Resonance Energy Transfer, *Acs Nano* **2011**, *5*, 9861.

Kim, S. Y.; Zukoski, C. F. Particle Restabilization in Silica/PEG/Ethanol Suspensions: How Strongly do Polymers Need To Adsorb To Stabilize Against Aggregation?, *Langmuir* **2011**, null.

Kloxin, C. J.; Scott, T. F.; Adzima, B. J.; Bowman, C. N. Covalent Adaptable Networks (CANs): A Unique Paradigm in Cross-Linked Polymers, *Macromolecules* **2010**, *43*, 2643.

Kloxin, C. J.; Scott, T. F.; Bowman, C. N. Stress Relaxation via Addition-Fragmentation Chain Transfer in a Thiol-ene Photopolymerization, *Macromolecules* **2009**, *42*, 2551.

Kloxin, C. J.; Scott, T. F.; Park, H. Y.; Bowman, C. N. Mechanophotopatterning on a Photoresponsive Elastomer, *Advanced Materials* **2011**, *23*, 1977.

Link, S.; El-Sayed, M. A. Size and Temperature Dependence of the Plasmon Absorption of Colloidal Gold Nanoparticles, *The Journal of Physical Chemistry B* **1999**, *103*, 4212.

Link, S.; El-Sayed, M. A. Shape and size dependence of radiative, non-radiative

and photothermal properties of gold nanocrystals, *International Reviews in Physical Chemistry* **2000**, *19*, 409.

Macht, M. L.; Rahm, W. E.; Paine, H. W. Injection Molding, *Industrial & Engineering Chemistry* **1941**, *33*, 563.

Maity, S.; Bochinski, J. R.; Clarke, L. I. Metal Nanoparticles Acting as Light-Activated Heating Elements within Composite Materials, *Advanced Functional Materials* **2012**, n/a.

McElhanon, J. R.; Russick, E. M.; Wheeler, D. R.; Loy, D. A.; Aubert, J. H. Removable foams based on an epoxy resin incorporating reversible Diels-Alder adducts, *Journal of Applied Polymer Science* **2002**, *85*, 1496.

Meyvis, T.; De Smedt, S.; Van Oostveldt, P.; Demeester, J. Fluorescence Recovery After Photobleaching: A Versatile Tool for Mobility and Interaction Measurements in Pharmaceutical Research, *Pharmaceutical Research* **1999**, *16*, 1153.

Miller, D. R.; Macosko, C. W. A New Derivation of Post Gel Properties of Network Polymers, *Macromolecules* **1976**, *9*, 206.

Montarnal, D.; Capelot, M.; Tournilhac, F. o.; Leibler, L. Silica-Like Malleable Materials from Permanent Organic Networks, *Science* **2011**, *334*, 965.

Montarnal, D.; Cordier, P.; Soulié-Ziakovic, C.; Tournilhac, F.; Leibler, L. Synthesis of self-healing supramolecular rubbers from fatty acid derivatives, diethylene triamine, and urea, *Journal of Polymer Science Part A: Polymer Chemistry* **2008**, *46*, 7925.

Montarnal, D.; Tournilhac, F.; Hidalgo, M.; Couturier, J. L.; Leibler, L. Versatile one-pot synthesis of supramolecular plastics and self-healing rubbers, *J Am Chem Soc* **2009**, *131*, 7966.

Murphy, E. B.; Bolanos, E.; Schaffner-Hamann, C.; Wudl, F.; Nutt, S. R.; Auad, M. L. Synthesis and Characterization of a Single-Component Thermally Remendable Polymer Network: Staudinger and Stille Revisited, *Macromolecules* **2008**, *41*, 5203.

Olabisi, O. *Handbook of thermoplastics*; Marcel Dekker: New York, 1997.

Palpant, B.; Cottancin, E.; Pellarin, M.; Treilleux, M.; Perez, A.; Vialle, J. L.; Broyer, M. Optical properties of gold clusters in the size range 2- 4 nm, *Physical Review B* **1998**, *57*, 1963.

Park, H. Y.; Kloxin, C. J.; Scott, T. F.; Bowman, C. N. Stress Relaxation by

Addition-Fragmentation Chain Transfer in Highly Cross-Linked Thiol-Yne Networks, *Macromolecules* **2010**, *43*, 10188.

Parker, S. F. Vibrational spectroscopy of N-phenylmaleimide, *Spectrochimica Acta Part A: Molecular and Biomolecular Spectroscopy* **2006**, *63*, 544.

Peterson, A. M.; Jensen, R. E.; Palmese, G. R. Reversibly cross-linked polymer gels as healing agents for epoxy-amine thermosets, *ACS Appl Mater Interfaces* **2009**, *1*, 992.

Peterson, A. M.; Jensen, R. E.; Palmese, G. R. Room-Temperature Healing of a Thermosetting Polymer Using the Diels-Alder Reaction, *ACS Appl Mater Interfaces* **2010**, *2*, 1141.

Peterson, A. M.; Jensen, R. E.; Palmese, G. R. Thermoreversible and remendable glass-polymer interface for fiber-reinforced composites, *Composites Science and Technology* **2011**, *71*, 586.

Reutenauer, P.; Buhler, E.; Boul, P. J.; Candau, S. J.; Lehn, J. M. Room temperature dynamic polymers based on Diels-Alder chemistry, *Chemistry* **2009**, *15*, 1893.

Roberts, M. C.; Hanson, M. C.; Massey, A. P.; Karren, E. A.; Kiser, P. F. Dynamically Restructuring Hydrogel Networks Formed with Reversible Covalent Crosslinks, *Advanced Materials* **2007**, *19*, 2503.

Roberts, M. C.; Mahalingam, A.; Hanson, M. C.; Kiser, P. F. Chemorheology of Phenylboronate-Salicylhydroxamate Cross-Linked Hydrogel Networks with a Sulfonated Polymer Backbone, *Macromolecules* **2008**, *41*, 8832.

Rubinstein, M.; Semenov, A. N. Thermoreversible Gelation in Solutions of Associating Polymers. 2. Linear Dynamics, *Macromolecules* **1998**, *31*, 1386.

Sardar, R.; Funston, A. M.; Mulvaney, P.; Murray, R. W. Gold nanoparticles: past, present, and future, *Langmuir* **2009**, *25*, 13840.

Schetz, J. A.; Fuhs, A. E. *Fundamentals of fluid mechanics*; John Wiley: New York, 1999.

Schulzendorf, M.; Cavelius, C.; Born, P.; Murray, E.; Kraus, T. Biphasic synthesis of Au@SiO2 core-shell particles with stepwise ligand exchange, *Langmuir* **2011**, *27*, 727.

Scott, T. F.; Draughon, R. B.; Bowman, C. N. Actuation in Crosslinked Polymers via Photoinduced Stress Relaxation, *Advanced Materials* **2006**, *18*, 2128.

Scott, T. F.; Schneider, A. D.; Cook, W. D.; Bowman, C. N. Photoinduced Plasticity in Cross-Linked Polymers, *Science* **2005**, *308*, 1615.

Semenov, A. N.; Rubinstein, M. Thermoreversible Gelation in Solutions of Associative Polymers. 1. Statics, *Macromolecules* **1998**, *31*, 1373.

Sershen, S. R.; Mensing, G. A.; Ng, M.; Halas, N. J.; Beebe, D. J.; West, J. L. Independent Optical Control of Microfluidic Valves Formed from Optomechanically Responsive Nanocomposite Hydrogels, *Advanced Materials* **2005**, *17*, 1366.

Sheridan, R. J.; Adzima, B. J.; Bowman, C. N. Temperature Dependent Stress Relaxation in a Model Diels-Alder Network, *Australian Journal of Chemistry* **2011**, *64*, 1094.

Sheridan, R. J.; Bowman, C. N. A simple relationship relating linear viscoelastic properties and chemical structure in a model Diels-Alder polymer network, *Macromolecules* **2012**.

Sijbesma, R. P.; Beijer, F. H.; Brunsveld, L.; Folmer, B. J. B.; Hirschberg, J. H. K. K.; Lange, R. F. M.; Lowe, J. K. L.; Meijer, E. W. Reversible Polymers Formed from Self-Complementary Monomers Using Quadruple Hydrogen Bonding, *Science* **1997**, *278*, 1601.

Skirtach, A. G.; Dejugnat, C.; Braun, D.; Susha, A. S.; Rogach, A. L.; Parak, W. J.; M√∂hwald, H.; Sukhorukov, G. B. The Role of Metal Nanoparticles in Remote Release of Encapsulated Materials, *Nano letters* **2005**, *5*, 1371.

Sriram, I.; Walder, R.; Schwartz, D. K. Stokes-Einstein and desorption-mediated diffusion of protein molecules at the oil-water interface, *Soft Matter* **2012**, *8*, 6000.

Stadler, R. In *Permanent and Transient Networks*; Springer Berlin / Heidelberg: 1987; Vol. 75, p 140.

Stauffer, D. Scaling theory of percolation clusters, *Physics Reports* **1979**, *54*, 1.

Swanson, J. P.; Rozvadovsky, S.; Seppala, J. E.; Mackay, M. E.; Jensen, R. E.; Costanzo, P. J. Development of Polymeric Phase Change Materials On the basis of Diels-Alder Chemistry, *Macromolecules* **2010**, *43*, 6135.

Tanaka, F. Theory of thermoreversible gelation, *Macromolecules* **1989**, *22*, 1988.

te Nijenhuis, K. Calculation of network parameters in thermoreversible gels, *Polymer Gels and Networks* **1996**, *4*, 415.

van Beek, D. J. M.; Spiering, A. J. H.; Peters, G. W. M.; te Nijenhuis, K.;

Sijbesma, R. P. Unidirectional Dimerization and Stacking of Ureidopyrimidinone End Groups in Polycaprolactone Supramolecular Polymers, *Macromolecules* **2007**, *40*, 8464.

Walder, R.; Kastantin, M.; Schwartz, D. K. High throughput single molecule tracking for analysis of rare populations and events, *Analyst* **2012**, *137*, 2987.

Walder, R.; Nelson, N.; Schwartz, D. K. Super-resolution surface mapping using the trajectories of molecular probes, *Nat Commun* **2011**, *2*, 515.

Walder, R.; Schwartz, D. K. Single Molecule Observations of Multiple Protein Populations at the Oil-Water Interface, *Langmuir* **2010**, *26*, 13364.

Walder, R.; Schwartz, D. K. Dynamics of protein aggregation at the oil-water interface characterized by single molecule TIRF microscopy, *Soft Matter* **2011**, *7*, 7616.

Winter, H.; Mours, M. In *Neutron Spin Echo Spectroscopy Viscoelasticity Rheology*; Springer Berlin / Heidelberg: 1997; Vol. 134, p 165.

Winter, H. H. Can the gel point of a cross-linking polymer be detected by the G′ – G″ crossover?, *Polymer Engineering & Science* **1987**, *27*, 1698.

Wool, R. P.; O'Connor, K. M. A theory crack healing in polymers, *Journal of Applied Physics* **1981**, *52*, 5953.

Wool, R. P.; O'Connor, K. M. Time dependence of crack healing, *Journal of Polymer Science: Polymer Letters Edition* **1982**, *20*, 7.

Wu, D.; Meure, S.; Solomon, D. Self-healing polymeric materials: A review of recent developments, *Progress in Polymer Science* **2008**, *33*, 479.

Yount, W. C.; Loveless, D. M.; Craig, S. L. Small-Molecule Dynamics and Mechanisms Underlying the Macroscopic Mechanical Properties of Coordinatively Cross-Linked Polymer Networks, *J Am Chem Soc* **2005**, *127*, 14488.

Zhang, Y.; Broekhuis, A. A.; Picchioni, F. Thermally Self-Healing Polymeric Materials: The Next Step to Recycling Thermoset Polymers?, *Macromolecules* **2009**, *42*, 1906.